Spin Systems and Boundary Conditions on Random Planar Graphs

Aravinth Kulanthaivelu

Merton College

University of Oxford

A thesis submitted for the degree of

Doctor of Philosophy

Trinity 2020

Statement of Originality

This thesis contains a record of the work conducted by myself and in collaboration with my supervisor. It is written wholly by myself, except as indicated in the following text. Chapters 1 and 2 are authored by myself and contain an introduction and background material respectively. Chapters 3 and 4 are based on an article written in collaboration with John F. Wheater. Chapter 5 is based on unpublished work and written by myself, and Chapter 6 presents my conclusions which are also written by myself. Appendix A is based on an article written by myself.

This thesis contains no material that has already been accepted, or is currently being submitted, for any degree or diploma or certificate or other qualification at the University of Oxford or another institution. To the best of my knowledge and belief this thesis contains no material previously published or written by another person, except where due reference is made in the text.

Acknowledgements

This thesis would not have been possible without an uncountable mix of interactions had with many people over the past four years. It would be right to acknowledge all of them, but I can only endeavour to thank a subset of particular importance.

First and foremost, I would like to express my gratitude to my supervisor, John F. Wheater, for introducing me to the world of 2D quantum gravity and random matrices, and for all his help, support, and encouragement during my DPhil studies. Many of the results described in this thesis would not have been possible without his insight and helpful suggestions, shared during our weekly meetings, after extended periods of time staring at blackboards. His enthusiasm and passion for physics were a powerful motivating force, that kept me calculating during difficult times. I would also like to thank him for so carefully reading and correcting the $n \to \infty$ drafts of this thesis.

Much of my time spent in Oxford was made fun and meaningful by the many friends I had the privilege of making. I am grateful to my friends at Merton: Laura Hankins, Edwin Lock, Valerian Hall-Chen, Jakob Jonnerby, Divya Sridhar, and many more. I am fortunate to have shared an office with Emma Slade and Augustinas Malinauskas. They were the best office-mates one could have hoped for, and I hope to never forget the dazzling array of strange and interesting conversations throughout.

Last but not least, I owe very special thanks to my family. I thank my mother and father for relentlessly and unconditionally supporting me, and my elder sisters, Sharmini and Roshini, for always looking out for me. Finally, thanks to Gayatri, for being my perfect companion in all things.

My DPhil was funded by the STFC studentship ST/N504233/1, for which I am extremely grateful. I also thank Merton College for financial support.

Abstract

In this thesis we discuss the multi-matrix integral formulation of spin systems on random planar graphs, as a discretised model of 2D Euclidean quantum gravity coupled to matter.

We begin by extending a recent analysis of the q-states Potts model with $p \leqslant q$ allowed, equally weighted spins on a random lattice with a connected boundary. We explore the $(q < 4, p \leqslant q)$ parameter space of the model, classify solutions in (q, p) that yield finite-sheeted resolvents, and derive the associated critical exponents. For the particular case of $q = 3$ we find a new solution with $p = 3/2$, which we conjecture to be the random lattice analogue of the New boundary condition.

Following this we study the Kramers-Wannier dual of the 3-state Potts model on the random lattice. We explicitly construct the known boundary conditions and show that the mixed boundary condition is dual to the New boundary condition, in accordance with the fixed lattice identification. However, we find that the mixed boundary condition of the dual theory, and the corresponding New boundary condition are not described by conventional resolvents.

Finally, we formalise a combinatorial method for calculating the partition function of the 3-states Potts model on a random planar lattice with various boundary conditions imposed. We determine the $p = 1, 2$ and 3 boundary conditions via this technique, and discuss other types of boundary condition that may be calculated, before turning our attention to the dilute Ising and dilute Potts models, where we compute the $p = 1$ boundary condition.

Contents

Appendices

List of Figures

Chapter 1

Introduction

The field that this thesis falls into is quantum gravity, the study of potential quantum descriptions of the gravitational field that would apply at high energies, where such quantum effects cannot be ignored. Such a theory would be unnecessary to describe most terrestrial phenomena, so why concern ourselves with it?

The twentieth century saw the advent of two revolutionary theories, quantum mechanics and general relativity. Relativity transformed our understanding of space and time, unifying them in the single concept of spacetime. In this framework, spacetime can curve, and the effect of this curvature on particles is to be interpreted as the force of gravity. Moreover, spacetime geometry is dynamic, being sourced by, and responding to, matter via the Einstein field equations. All things considered, general relativity is a classical theory that describes gravitational phenomena at large scales, and has been vindicated many times over through successful experimental and observational predictions.

Quantum mechanics, however, presides over the behaviour of microscopic particles, and is a fundamentally probabilistic theory, contrary to the deterministic laws of classical physics. Even though one may know the initial state of a system, one can only compute the probability that the system ends up in a given final state. Nevertheless, the framework has been remarkably successful at giving us a firm and reliable understanding of atomic processes. By applying the principles of quantum mechanics to fields, it was found that one could construct theories compatible with Einstein's special theory of relativity, a subset of general relativity

in which the laws of physics are invariant under Lorentz transformations, as long as gravitational interactions can be ignored. Within the framework of quantum field theory the Standard Model of particle physics was constructed, which itself has withstood decades of experimental scrutiny.

Each of these theories has its own domain of validity, where we believe them to be fundamentally correct, but they seem to be incompatible. In general relativity, matter is treated classically and the rules are deterministic, whereas in quantum field theory particles obey probabilistic laws whilst the spacetime background is fixed. However, we know that each of these frameworks are flawed. Under general initial conditions, general relativity appears to break down, with singularities inevitably forming in the form of black holes or the initial big bang singularity. At such instances, one expects quantum mechanics to have an important effect. Furthermore, the electromagnetic, weak and strong interactions have received a unified description in the Standard Model, yet does not include gravity.

An early attempt at combining these two frameworks, called quantum field theory in curved spacetime, tried to describe gravitational effects on matter by treating matter quantum mechanically whilst keeping the background geometry classical. The hope was that it might form an appropriate semi-classical regime for the full theory, much like how, in the early days of quantum theory, calculations were performed coupling matter to a classical electromagnetic field, and yielded results in accordance with the full theory of quantum electrodynamics. However, the discovery of Hawking radiation from black holes, perhaps the fundamental achievement of the field, highlights the inconsistency between general relativity and quantum mechanics by challenging the postulate of unitarity in quantum mechanics.

Unifying quantum mechanics and general relativity is a major challenge, but since all particles interact gravitationally and obey the laws of quantum mechanics, one expects a coherent framework which encompasses these. The search for this framework is the main goal of quantum gravity research.

Quantum mechanics offers a procedure for constructing a quantum field theory given a classical field theory, and so a natural first guess at constructing a quantum

theory of gravity is to quantise general relativity. However, to do so, one must first determine which underlying degrees of freedom are to be quantised. At this stage, one can adopt several attitudes, leading to the many different areas of ongoing research. It could be the case that the degrees of freedom observed in general relativity are merely an effective description of a more fundamental set that can be resolved at the microscopic scale. This is the position adopted by string theory, where the fundamental degrees of freedom are extended objects, as opposed to point-like particles. Another point of view is to adhere to the spacetime geometric picture and try to quantise metric fluctuations. It has long been known that quantum gravity in four dimensions is perturbatively non-renormalisable [1], and one needs an infinite number of counterterms to remove divergences. This does not preclude the asymptotic safety scenario, in which there exists an ultra-violet (UV) fixed point, such that the theory is non-perturbatively renormalisable.

In this thesis, we will adopt an approach which sits somewhere in the middle of these perspectives, and study the dynamical triangulation approach to two-dimensional Euclidean quantum gravity coupled to matter systems. Dynamical triangulations have the interpretation of a lattice regularisation of the gravitational path integral, are inherently non-perturbative in nature, and admit powerful computational tools in two-dimensions [2]. The hope is that, whilst the full four-dimensional theory is still out of reach, one may be able to observe phenomena in lower dimensions that could offer some insight into how the higher-dimensional theory would operate. One could also consider dynamical triangulations as a regularisation of the bosonic string embedded in a (potentially complicated) target space defined by the matter model endowed upon it, which we now call minimal string theory. We will be particularly interested in the study of boundary conditions of matter systems when coupled to quantum gravity on surfaces with the topology of a disc, since these, from a mathematical point of view, are the simplest geometries which support such analysis. Another way of phrasing this would be that we will be interested in studying disc amplitudes with a diverse array of implementable boundary conditions.

This thesis will be organised as follows. In Chapter 2 we will review the dynamical triangulation approach, introduce the machinery of random matrix models, and the connection to the continuum physics of conformal field theory. In Chapter 3 we will introduce the q-states Potts model on random planar geometries. We will construct the general solution for boundary conditions that can be employed in the random matrix model using the saddle-point approximation, and explore the scaling behaviour of the theory. Following this, in Chapter 4 we will turn our attention to Kramers-Wannier duality. We will formulate the observables that describe geometries with prescribed boundary conditions in both the dual and original theory, and establish that they are in accordance with expected behaviour. Finally, in Chapter 5 we will develop and employ the combinatorial method of loop equations to compute the loop functions representing boundary conditions in both the 3-states Potts model, and the dilute Potts model, before summarising the key results of our investigation in Chapter 6.

Chapter 2

Review

2.1 2D Quantum Gravity

We begin by introducing the quantum gravity path integral. Let $\mathcal{M}$ be a two-dimensional, closed, compact and connected orientable manifold of genus h. Then we formally write the partition function of two-dimensional Euclidean quantum gravity as the following functional integral,

$$\mathcal{Z} = \sum_h \int \frac{\mathcal{D}g_{\mu\nu}\mathcal{D}X}{\mathrm{Vol}(\mathrm{Diff}_{\mathcal{M}})} e^{-S_{\mathrm{EH}}[g;G,\Lambda]-S_M[g;X]}. \tag{2.1}$$

The Einstein-Hilbert action is given by

$$S_{\mathrm{EH}} = \Lambda \int d^2\xi\sqrt{g} - \frac{1}{4\pi G}\int d^2\xi\sqrt{g}R, \tag{2.2}$$

where Λ is the cosmological constant, G the gravitational (Newton) constant, $g_{\mu\nu}$ the metric and g its associated determinant, R is the Ricci scalar, and we integrate over the manifold $\mathcal{M}$. The matter sector, which we do not specify at this moment, is represented by a set of fields X, and governed by the action $S_M[g;X]$. The measure denotes integration over all geometries by integrating over all equivalence classes of metrics under diffeomorphisms. This is formally indicated through the quotient by the volume of the group of diffeomorphisms of $\mathcal{M}$ to counter the overcounting of diffeomorphic geometries.

We note that from the outset we have chosen to work with a Euclidean partition function, as opposed to a more phenomenologically relevant Lorentzian model. The origin of this is the scenario where one tries to remedy the rapidly oscillating

exponential phase of the Lorentzian Einstein-Hilbert action through a rotation to Euclidean geometries where one can compute observables, in a similar manner to the Wick rotation of quantum field theory. Whether, and how, one can perform the analogous inverse Wick rotation is a non-trivial question which we will not touch upon in this thesis. Instead, we regard the Euclidean path integral as a statistical theory of geometries from the outset.

According to the Gauss-Bonnet theorem, we can express the last term in (2.2) in terms of a topological invariant, the Euler characteristic of $\mathcal{M}$,

$$\chi(h) = \frac{1}{4\pi}\int_{\mathcal{M}} d^2\xi\sqrt{g}R = 2 - 2h. \tag{2.3}$$

We may also identify the first term in (2.2) as the area of $\mathcal{M}$,

$$A = \int_{\mathcal{M}} d^2\xi\sqrt{g}. \tag{2.4}$$

Hence the partition function (2.1) for fixed topology is governed by the matter action and the area of manifolds that are integrated over. To make sense of this integral in the continuum perspective, one must properly define the measure and gauge fix the functional integral, which we will postpone until the end of the chapter.

For geometries with b boundaries we supplement the Einstein-Hilbert action with the following boundary action,

$$S_b = \sum_{i=1}^{b} \lambda_i \int d\zeta_i - \frac{1}{2\pi G}\int d\zeta_i\sqrt{h_i}k_i, \tag{2.5}$$

where λ_i denotes the boundary cosmological constant, h_i the determinant of the induced metric, and k_i the geodesic curvature associated with the i^{th} boundary component which we integrate over. The former terms can be identified with the length of the i^{th} boundary component, while the latter can be interpreted as Gibbons-Hawking-York boundary terms. Together with the last term in (2.2) these terms may be expressed, using the Gauss-Bonnet theorem, in terms of the Euler characteristic for genus h manifolds with b boundaries

$$\chi(h, b) = 2 - 2h - b. \tag{2.6}$$

There are a number of observables that have been studied in the literature, such as correlation functions of local operators and the dimension of spacetime [2]. In this thesis, we will focus on the Hartle-Hawking wave functionals, dictated by the modified Einstein-Hilbert action given by the sum of (2.2) and (2.5)[1],

$$S_{\mathrm{EH},b} = \Lambda A - \chi(h,b)/G + \sum_{i=1}^{b} \lambda_i L_i, \tag{2.7}$$

which describes two-dimensional universes with b boundaries, where L_i denotes the length of the i^{th} boundary component. In the simplest case with $b = 1$, this essentially represents the sum over geometries with disc topology, and so at various times we will call this observable the disc-function or the loop function. In the rest of this chapter we will outline a means of computing these observables using the technique of dynamical triangulations. We first review the triangulation of manifolds using Regge calculus, followed by the combinatorial solution to the one-loop function. We will then introduce random matrix models, as a convenient means of capturing the combinatorics of summing over triangulations, and we discuss two methods of solution, the saddle-point method and the loop equation method, in the context of the one- and two-matrix models. We describe how one can endow discrete geometries with spin systems using multi-matrix models, and how to describe the various boundary conditions that one can employ. We then review 2D conformal field theory, with emphasis on the boundary physics of systems that describe the continuum physics of these discretised models, and we outline how they emerge from gauge fixing the quantum gravity path integral.

2.2 Dynamical Triangulations

2.2.1 Discretisation

To regularise (2.1) we must first construct a discrete lattice picture of the geometries and express the action in a suitable form. This is captured by Regge calculus, which provides a prescription for defining curvature on manifolds that discretises the

[1]It is possible to consider higher derivative terms in the action. This is not necessary in two-dimensions as the Einstein-Hilbert action yields a finite and renormalisable theory.

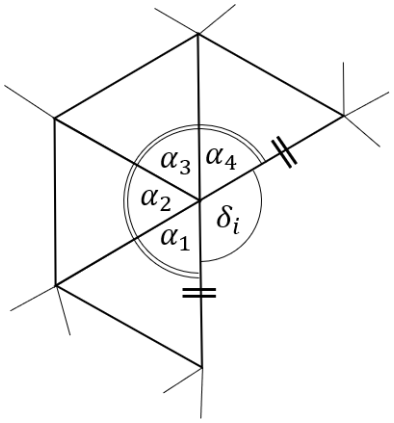

Figure 2.1: Curvature generated by a number of triangles meeting at a vertex.

notion of parallel transport in a natural way [3]. The proposal originally envisioned by Regge involved attempting to approximate and study specific manifolds via discretisation, whereas we will be attempting a summation over all geometries.

We define a two-dimensional piecewise linear manifold as a simplicial complex constructed from points, links, and triangles (equivalently 0-, 1- and 2-simplices) such that the neighbourhood of each point is homeomorphic to a disc. Intuitively, each simplicial complex is constructed by gluing together a collection of triangles along their edges, and we can represent a given geometry by a suitable triangulation. Such piecewise linear manifolds will serve as a discretisation of continuous manifolds. Defining v, l, n as the number of vertices, links and triangles respectively, we can express the Euler characteristic associated to each triangulation, T, as

$$\chi(h) = n - l + v, \tag{2.8}$$

where h is the genus of the triangulation.

We can endow piecewise linear manifolds with a metric structure by assigning lengths to the links, regarding triangles as flat in their interior. Therefore geodesics between points are shortest distance paths along the edges in units of the assigned link length. This metric is Euclidean within each triangle, and must be continuous as one traverses the edge to an adjoining triangle. Since curvature is an intrinsic quantity of the manifold, bending around an edge should not generate curvature. Therefore curvature must reside at the vertices of the manifold. Referring to Fig.2.1,

one can construct a discretised curvature invariant by understanding the notion of deficit angles in the piecewise structure,

$$\delta_i = 2\pi - \sum_{t \in T_i} \alpha_t, \tag{2.9}$$

where i denotes a vertex in the triangulation, T_i denotes the collection of triangles meeting at i, and α_t are the corresponding angles at i. In triangulations of a Euclidean space, the sum of angles meeting at a given vertex is 2π, so the deficit angle measures deviations from the flat geometry. The corresponding quantity for continuous manifolds can be constructed by considering the parallel transport of a vector about a point in the manifold. In this case the vector will undergo a rotation through an angle given by,

$$\delta = \frac{1}{2} \int_{T'} dA\, R, \tag{2.10}$$

where T' denotes a geodesic triangle on the two-dimensional surface. This motivates the following discretised definition of the Ricci scalar

$$R_i = 2\frac{\delta_i}{\delta A_i}, \tag{2.11}$$

with the area of each triangle distributed equally among its three vertices, such that each vertex is assigned an area

$$\delta A_i = \frac{1}{3} \sum_{t \in T_i} A_t. \tag{2.12}$$

Hence, one can make the following identification between the continuous and discretised descriptions

$$\int dA \to \sum_{i=1}^{v} \delta A_i, \quad \int dAR \to \sum_{i=1}^{v} R_i \delta A_i. \tag{2.13}$$

We now fix the triangle edge lengths to be given by a, which serves as the cutoff for the theory, such that we are now dealing with triangulations by equilateral triangles. The formulae (2.11), (2.12) become

$$\delta A_i = \frac{\sqrt{3}}{12} a^2 n_i, \quad R_i \delta A_i = \frac{2\pi}{3}(6 - n_i), \tag{2.14}$$

where n_i is the order of the vertex i. By rescaling a we have

$$\sum_{i=1}^{v} \delta A_i = n, \quad \sum_{i=1}^{v} \delta A_i R_i = 4\pi\chi. \tag{2.15}$$

Therefore, we can write down a discretisation for the action (2.2),

$$S_T(\mu, G) = \mu n - \chi(h)/G, \tag{2.16}$$

where μ is an appropriately scaled bare cosmological constant.

Now that we have constructed a discretisation of the action, we must consider the measure. The measure must describe summation over different equivalence classes of metric structure. These equivalence classes are realised in the discrete picture as triangulations that are non-isomorphic. For example, given two triangulations that cannot be mapped onto each other by a relabelling of its constituent vertices, one observes different local curvature assignments, and thus different metric structures. Given a fixed topology and cutoff scale, the combinatorially non-isomorphic triangulations are expected to form a grid of points in the space of equivalence classes of metrics, and the hope is that this will become uniformly dense when $a \to 0$, realising the continuum measure. Thus, we can write down the discretised partition function as follows,

$$Z = \sum_h \sum_{T \in \mathcal{T}} \frac{1}{|\mathrm{Aut}(T)|} e^{-S_T(\mu,G)} Z_M(T), \tag{2.17}$$

where $\mathcal{T}$ is a suitable class of abstract triangulations, $\mathrm{Aut}(T)$ is the set of automorphisms of T, and $Z_M(T)$ is the appropriate discretised matter partition function defined on the fixed triangulation T. This can be further refined as follows

$$Z = \sum_h e^{\chi(h)/G} Z_h, \quad Z_h = \sum_{n=0}^{\infty} e^{-\mu n} \mathcal{N}(h, n), \tag{2.18}$$

where $\mathcal{N}(h, n)$ is the number of non-isomorphic triangulations of genus h consisting of n triangles. The benefit of organising the summation in this way is that, ignoring matter contributions for the moment, the sum over triangulations of fixed topology is exponentially bounded as a function of n, whereas the number of inequivalent

triangulations of arbitrary topology grows factorially [4]. This is important when it comes to discussing the continuum limit.

We can easily generalise this to determine regularised versions of the Hartle-Hawking wave functionals:

$$W(\mu, \lambda_1, ..., \lambda_b) = \sum_h e^{\chi(h,b)/G} \sum_{l_1,\cdots,l_b} \sum_n e^{-\mu n - \sum_i \lambda_i l_i} \mathcal{N}(h; n; l_1, \cdots, l_b), \qquad (2.19)$$

where $\mathcal{N}(h; n; l_1, \cdots, l_b)$ denotes the number of triangulations of topology h composed of n triangles with b boundaries, where the length of the i^{th} boundary is l_i, again suppressing matter contributions. Restricting to the single boundary case and triangulations of S^2, the disc function can be expressed as

$$W_0(z, g) = \sum_{n,l} \mathcal{N}(n; l) g^n z^{-(l+1)}, \qquad (2.20)$$

where we have made the identifications

$$g = e^{-\mu}, \quad z = e^{\lambda}. \qquad (2.21)$$

This is a convenient form for what follows, where we will determine the one-loop function combinatorially, and then using matrix model techniques.

2.2.2 Combinatorial solution

As we have seen, the problem of evaluating the gravitational path integral can be replaced by the combinatorial problem of calculating the number of non-isomorphic triangulations of fixed topology with a given number of triangles. So far we have not specified what abstract class of triangulations we should use. For example, one could consider the class of so-called regular triangulations, which are constrained such that no two vertices in the same boundary component can be connected by an interior link, single links cannot form a loop, and closed connected paths of links of length one and two are excluded. This excludes a number of quite singular structures, examples of which are presented in Fig.2.2.

We will instead choose a quite different set, the class of unrestricted triangulations. These are the set of simplicial complexes, homeomorphic to surfaces with a given

Figure 2.2: Examples of singular triangulations. Dashed lines indicate the identification of vertices in the triangulation.

topology and number of holes, that can be obtained by successively gluing together a collection of triangles and a collection of double links, where the links and triangles can be glued onto the boundary of a complex at both vertices and along links respectively. This is a much larger class of triangulations, and intuitively does not seem to agree with the piecewise linear manifold structure we wish to simulate. However, the presence of degenerate structures should not be important in the continuum scaling limit, since these structures occur at the level of the cutoff. Indeed, it can be shown that it does not matter whether one selects unrestricted or regular triangulations, so long as they provide an identification of the topology of the piecewise linear manifold they are meant to represent, as the same results are obtained in the scaling limit [2].

In this section, we will study the genus zero disc function (2.20), interpreted as the generating function for two-dimensional universes with a single boundary. Strictly speaking, we will compute the marked disc function, which is given by the first derivative of the disc function with respect to z, and counts triangulations with a marked point on the boundary. This leads to an overcount of the the number of triangulations by distinguishing triangulations that are otherwise isomorphic under rotations of the boundary. Henceforth, by an abuse of notation, we will identify the marked disc function with (2.20).

To compute this object, we follow the prescription developed by Tutte [5] and derive recursion relations for the number of triangulations, which leads to a recursion relation for the one-loop function. Starting from a given triangulation with n triangles and a k length boundary we remove a marked edge, resulting in a

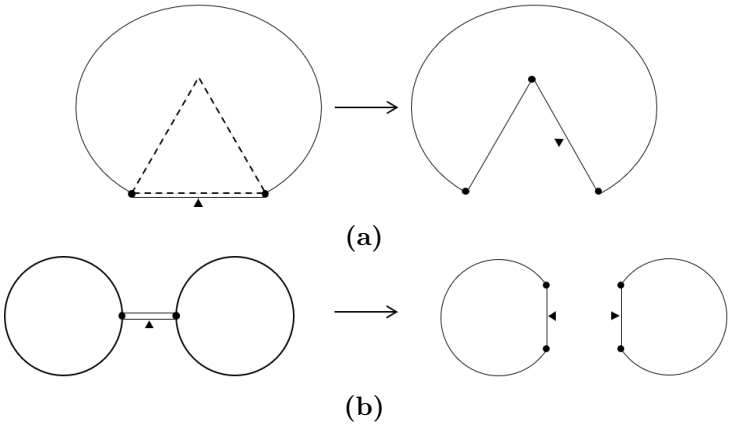

Figure 2.3: The two decomposition outcomes from removing a marked edge.

number of smaller triangulations. The marked edge of the original triangulation can be connected in one of two ways:

(i) to a triangle on the boundary. In this case removing the marked edge results in a new triangulation which has one fewer triangles and one more boundary edge.

(ii) to another boundary edge. In this case removing the marked edge removes the other edge as well, and the triangulation is split into two triangulations with the same number of triangles but two fewer boundary edges.

To make these moves precise, a convention should be adopted regarding the resulting marked edge. We follow the convention adopted in [6]: in case (i), once the original edge is removed we mark the edge oriented counterclockwise to the original removed edge; and in case (ii) we mark the two edges adjacent to those which were removed. This is illustrated in Fig.2.3. The recursion relation for the number of marked triangulations is then given by

$$\mathcal{N}(k;n) = \mathcal{N}(k+1;n-1) + \sum_{l=0}^{k-2}\sum_{m=0}^{n} \mathcal{N}(l;m)\mathcal{N}(k-2-l;n-m). \qquad (2.22)$$

The first term on the right hand side corresponds to case (i), where we have one fewer triangles and one more boundary edge, and the second term corresponds to case (ii), where we sum over two triangulations with n triangles and $k-2$ boundary edges between them. To completely determine the number of triangulations this

recursion relation needs to be supplemented with a boundary condition, which we take to be $\mathcal{N}(0;n) = \delta_{n,0}$, i.e. that there is only one trivial triangulation.

We can connect this to the one-loop function by simply performing the sum in (2.20). The final expression is given by

$$(z - gz^2)W_0(z,g) - 1 + g(p_1(g) + z) = W_0^2(z,g), \tag{2.23}$$

where $p_1(g)$ is the sum over geometries with a single link boundary, and coefficient of z^{-2} in the large z expansion of $W_0(z)$. Therefore we find that the genus zero one-loop function, as a function of z, satisfies an algebraic equation with one undetermined constant. This is an observation that repeats itself for the systems studied in this thesis, where we will attempt to find the algebraic curve that suitable one-loop functions satisfy. From now on we will call this the spectral curve.

The coefficient $p_1(g)$ is fixed by the imposition of the algebraic genus zero condition on the spectral curve. In this case, where $W_0(z,g)$ has two sheets when regarded as a multivalued complex function in z, this condition is equivalent to requiring that $W_0(z,g)$ has only two branch points. This is the one-cut assumption. In practice, we can arrange this by demanding $W_0(z,g)$ has the following form,

$$W_0(z,g) = \frac{1}{2}\left(z - gz^2 + \left(gz - 1 - \frac{g}{2}(a+b)\right)\sqrt{(z-a)(z-b)}\right). \tag{2.24}$$

There are now two branch points located at a and b, and without loss of generality we take $b > a$. These points may be determined by requiring $\lim_{z\to\infty} zW_0(z,g) = 1$, which yields [4]

$$g^2(b-a)^2 = 8S(1-S),\ S = \frac{g}{2}(a+b),\ S - 3S^2 + 2S^3 = 2g^2. \tag{2.25}$$

There is more than one solution to these equations; this is fixed by demanding $b > a$ and requiring consistency with the $g = 0$ solution where $b = -a = 2$.

2.2.3 Continuum limit

As we noted in Section 2.2.1, the sum of non-isomorphic triangulations of fixed topology is exponentially bounded. For spherical topology, one can show [5]

$$Z_0 = \sum_{n=1}^{\infty} e^{-(\mu-\mu_c)n} n^{\gamma_s - 3}(1 + \mathcal{O}(1/n)). \tag{2.26}$$

where $\gamma_s = -1/2$ for pure gravity. For $\mu < \mu_c$ the sum is dominated by contributions with large numbers of triangles, n, and will not converge, while for $\mu > \mu_c$ large n contributions are heavily suppressed. Therefore we see that the critical cosmological constant μ_c is the minimal value for which the sum is convergent.

The higher order moments of the area may be computed by taking derivatives of Z_0 with respect to the cosmological constant, and these behave as follows:

$$\langle A^m \rangle = \frac{(-1)^m}{Z_0} \frac{d^m Z_0}{d\mu^m} \sim \frac{1}{(\mu - \mu_c)^{\gamma_s - 2 + m}}. \tag{2.27}$$

These moments diverge as $\mu \to \mu_c$ for $m > 3$, indicating that large area surfaces will dominate, and the onset of a continuous phase transition. We therefore introduce a scaling parameter ε such that the physical area is given by $A_{\text{phys.}} = n\varepsilon^2$, and we define the scaling limit as

$$\mu \to \mu_c, \quad \varepsilon \to 0, \quad \tilde{\mu} = (\mu - \mu_c)/\varepsilon^2 \text{ fixed}, \tag{2.28}$$

where $\tilde{\mu}$ is a renormalised bulk cosmological constant. The exponent γ_s, called the string susceptibility, is a universal constant independent of the discretisation procedure chosen, be it triangulations or general polygonulations. Hence it may be used as a way of determining which universality class the continuum theory resides in.

To check whether this is the correct prescription for taking the continuum limit, and that this generates a reparameterisation invariant theory, we should compare these results with continuum calculations. We will discuss the continuum theory at the end of this chapter, where we will demonstrate that the scaling of the discrete partition function is consistent with the continuum. In anticipation of

this, we note that near the critical point the fixed area partition function, given by a Laplace transform of (2.26), scales as

$$Z_0(A) \sim A^{\gamma_s - 3}. \tag{2.29}$$

For general observables with boundaries, we assume the contribution of a finite length loop or finite area surface should always be analytic in the associated fugacities. Therefore nonanalytic contributions must arise from loops and surfaces whose perimeter and area are infinite in lattice units. We turn this reasoning on its head and determine the continuum limit more generally by isolating the nonanalytic dependence of these observables. Continuum quantities are then calculated as scaling functions in the limit (2.28).

For example, consider once more the pure gravity one-loop function (2.24). We may identify the critical coupling g_c by studying the functions $p_l(g)$, obtained from the coefficient of $z^{-(l+1)}$ in the large z expansion of $W_0(z, g)$. By computing their branch points one may determine the radius of convergence, and hence g_c. In practice these objects are polynomials in a, b, and therefore S, and so it suffices to compute the radius of convergence of these simpler quantities as a function of g, giving $g_c = \frac{1}{2}3^{-3/4}$.

The relation (2.28) tells us that we should compute continuum quantities by taking $g = g_c e^{-\varepsilon^2 \tilde{\mu}}$, and taking $\varepsilon \to 0$. However, this would yield geometries with finite length boundaries in lattice units, which then become infinitesimal. We have an extra fugacity for the boundary links, given by the boundary cosmological constant, which should be tuned to its critical value in order to obtain continuous geometries with a finite length macroscopic boundary. In analogy with (2.28) this is achieved through the scaling $z = z_c e^{\varepsilon \tilde{z}}$, where $\tilde{z}$ is represents the renormalised boundary cosmological constant. z_c will be given by the radius of convergence of $W_0(z, g)$, which may be identified with the branch point $b(g_c)$. Inserting these

relations into (2.24) gives

$$W_0(\tilde{z},\tilde{\mu}) = \frac{1}{2}3^{-1/4} - \frac{2}{3^{3/4}}\tilde{\mu}^{1/2}\zeta\varepsilon + \varepsilon^{3/2}\frac{\sqrt{2}}{3}\tilde{\mu}^{3/4}\left(\left(\zeta+\sqrt{\zeta^2-1}\right)^{3/2} + \left(\zeta-\sqrt{\zeta^2-1}\right)^{3/2}\right), \quad (2.30)$$

where we have introduced $\zeta = 4\sqrt{\tilde{\mu}}\tilde{z}/(3+\sqrt{3})$.

We define the scaling one-loop function to be the leading nonanalytic term as $\varepsilon \to 0$. This we take to correspond to the continuum marked disc partition function, and it is universal, independent of discretisation chosen. Motivated by this, we conjecture that in general the continuum disc function $\tilde{W}_0(\tilde{z})$ is obtained through an expansion of the form

$$W_0(z) = W_0(z_c) + c_1\varepsilon\tilde{z} + \varepsilon^{1-\gamma_s}c_2\tilde{W}_0(\tilde{z}) + \cdots, \quad (2.31)$$

where c_1 and c_2 are non-universal constants.

2.3 Matrix Models

2.3.1 Basic notions

In the preceding section we demonstrated how one could determine the discretised pure gravity partition function using combinatorial methods. Here we introduce matrix models, which serve as a convenient means of implementing the counting of unrestricted triangulations.

The random matrix models we consider furnish examples of the simplest form of quantum field theory. Namely, they are zero-dimensional quantum field theories where the fundamental degrees of freedom are $N \times N$ Hermitian matrices. As an example, take the following one-matrix model path integral:

$$Z = \int [dX] e^{-N\mathrm{Tr}V(X)}, \quad V(z) = \frac{1}{2}z^2 - \frac{g}{3}z^3, \quad (2.32)$$

where X is an $N \times N$ Hermitian matrix, and $[dX]$ denotes component-wise integration

$$[dX] = \prod_{1\leqslant a,b\leqslant N} d\mathrm{Re}(X_i)^a{}_b \prod_{1\leqslant a,b\leqslant N} d\mathrm{Im}(X_i)^a{}_b. \quad (2.33)$$

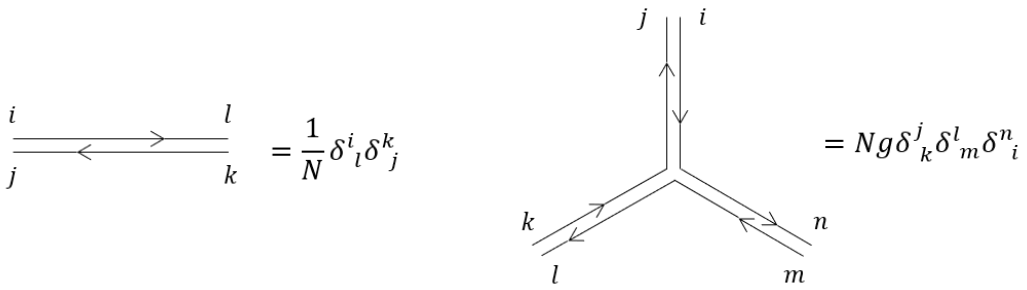

Figure 2.4: The Feynman rules of the one-matrix model (2.32).

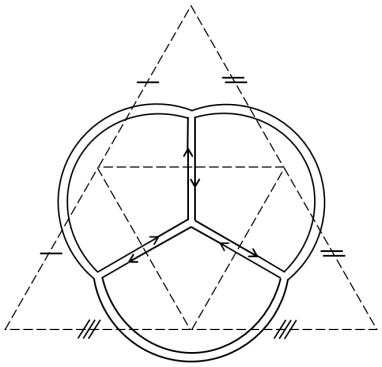

Figure 2.5: An example triangulation with the topology of the sphere.

We may interpret the terms of the perturbative expansion in the coupling constant g about the Gaussian point with a Feynman graph expansion. The Feynman rules are given in Fig.2.4, where the presence of upper and lower matrix indices are represented by double lines. The subsequent Feynman graph expansion of the free energy about the Gaussian point is thus given by a series of closed ribbon graphs, which possess enough structure to associate with unrestricted triangulations. This is seen by studying the dual graph expansion, which is obtained by associating triangles to trivalent vertices, with sides identified when connected by a propagator, as shown in Fig.2.5. Each dual graph T, with l links and n triangles comes with a weight given by

$$\frac{N^{2-2h}}{|\mathrm{Aut}(T)|}g^n. \tag{2.34}$$

Comparing with (2.18), it is clear, with the identification

$$e^{1/G} = N, \quad g = e^{-\mu}, \tag{2.35}$$

that the free energy of the partition function reproduces the discretised quantum gravity partition function. Moreover, we note that we can organise the dual graph expansion in a topological expansion, and in the limit $N \to \infty$ the leading order contribution to the free energy is dominated by $h = 0$ graphs, i.e. planar surfaces. This limit is therefore called the planar limit.

The explicit choice of a cubic potential in (2.32) led to triangulated surfaces. We could instead consider discretisation by squares or higher order polygons by considering potentials that are polynomials of the corresponding order. One may be interested in considering general polygonulations in order to simplify calculations by, for example, considering even potentials, for which correlators of odd numbers of matrices vanish. As we shall discuss in the context of multi-matrix models, another motivation for considering more general potentials may be to uncover multi-critical behaviour in the continuum limit, beyond the critical point which corresponds to pure gravity.

The technology of matrix models is particularly convenient when it comes to the description of boundaries, as this is encoded in a natural observable of interest, the resolvent function

$$W(z) = \frac{1}{N} \left\langle \mathrm{Tr} \frac{1}{z - X} \right\rangle . \tag{2.36}$$

We can express the large z expansion as

$$W(z) = \frac{1}{N} \sum_{n=0}^{\infty} z^{-(n+1)} \left\langle \mathrm{Tr}\, X^n \right\rangle . \tag{2.37}$$

Considering the dual Feynman graph expansion of a given moment, say $\langle \mathrm{Tr}\, X^n \rangle$, it is straightforward to see that it is given by a sum over surfaces with a length n boundary. Hence the resolvent is the generating function for triangulations of surfaces with a connected boundary, with a fugacity z associated to each boundary link. In fact this observable coincides with the one-loop function (2.20) in the planar limit.

Similarly, we can write down matrix model expressions for the other Hartle-Hawking wave functionals (2.19),

$$W(z_1, \cdots, z_b) = N^{b-2} \left\langle \mathrm{Tr} \frac{1}{z_1 - X} \cdots \mathrm{Tr} \frac{1}{z_b - X} \right\rangle_{\mathrm{conn.}} , \tag{2.38}$$

where the subscript indicates the connected part of the expectation value. The two expressions are related through the identifications (2.21) and (2.35), where each z_i denotes the boundary cosmological component associated with the i^{th} component. With a general potential,

$$V(z) = \frac{1}{2}z^2 - \sum_{j=1}^{\infty} \frac{t_j}{j} z^j, \tag{2.39}$$

these can be obtained through repeated action of the loop insertion operator [2] on the single boundary resolvent,

$$\frac{d}{dV(z)} = \sum_{j=1}^{\infty} \frac{j}{z^{j+1}} \frac{d}{dt_j}. \tag{2.40}$$

For (2.32) the only non-zero coefficient is $t_3 = g$. In the power series expansion of $W(z)$, the operator $d/dV(z')$ will act on the term g^k to give $3kg^{k-1}/z'^4$. This may be interpreted as removing a triangle from the random graph it operates on, and introducing a new boundary of length 3, with a new boundary cosmological constant z'. The factor of k is a combinatorial factor representing the possibility of replacing any of the k triangles on the random graph, and the factor of 3 is introduced to count the possibilities of choosing the new marked link.

In the planar limit, (2.36) can be expressed as the Stieltjes transform of the eigenvalue density distribution of X,

$$W_0(z) = \lim_{N\to\infty} W(z) = \int_{\text{supp}\rho_X} d\lambda \frac{\rho(\lambda)}{z-\lambda}, \quad z \in \mathbb{C}\backslash\text{supp}\rho_X, \tag{2.41}$$

where $\rho(\lambda)$ is defined by

$$\rho(\lambda) = \frac{1}{N}\left\langle \sum_{i=1}^{N} \delta(\lambda - \lambda_i) \right\rangle, \tag{2.42}$$

and $\{\lambda_i\}_{i=1}^N$ denotes the N eigenvalues of X. With this one can compute the set of correlators

$$\lim_{N\to\infty} \frac{1}{N}\langle \text{Tr} X^n \rangle = \int_{-\infty}^{+\infty} \rho(\lambda)\lambda^n. \tag{2.43}$$

Hence, in random matrix theory, determining the resolvent allows one to extract a wealth of information through the correlators of the theory. Moreover, the planar resolvent forms one of the primary ingredients in computing higher order terms in the topological expansion of the full loop function [7].

2.3.2 Saddle-point method

To determine the resolvent, we can exploit the invariance of the path integral (2.32) under the adjoint action of the unitary group,

$$X^i{}_j \to \tilde{X}^i{}_j = U^i{}_k X^k{}_l (U_j{}^l)^*, \quad U \in U(N). \tag{2.44}$$

We use this to choose a parameterisation where X is diagonal. The measure factorises into the product of the Haar measure for unitary matrices and an integration measure for the eigenvalues. Performing the integral over the unitary matrices, we are left with the following integral over the eigenvalues of X,

$$Z = \int \prod_{i=1}^{N} d\lambda_i \Delta^2(\lambda) e^{-N \sum_{i=1}^{N} V(\lambda_i)}, \tag{2.45}$$

where $\Delta(\lambda) = \det_{i,j} \lambda_i^{j-1}$ is the Vandermonde determinant.

In the large N limit, the eigenvalue configurations that dominate the path integral are those which minimise the effective potential. We can easily determine these by varying an eigenvalue, resulting in the following set of saddle-point equations,

$$\frac{2}{N} \sum_{j \neq i} \frac{1}{\lambda_i - \lambda_j} = V'(\lambda_i). \tag{2.46}$$

Multiplying (2.46) by $1/(\lambda_i - z)$ and summing over i, we recover (2.23), from which one can compute the eigenvalue density distribution.

2.3.3 Loop equations

The method of loop equations involves exploiting the reparameterisation invariance of the matrix model to generate constraints on the loop functions. They essentially represent the Schwinger-Dyson equations of quantum field theory.

Consider an infinitesimal variation of the type

$$X \to \tilde{X} = X + \epsilon f(X). \tag{2.47}$$

To order ϵ, this reparameterisation results in the following,

$$\int [dX](1 + \epsilon J(X) + \mathcal{O}(\epsilon^2))\, e^{-N \mathrm{Tr} V(X) - \epsilon K(X) + \mathcal{O}(\epsilon^2)}, \tag{2.48}$$

where $J(X)$ is the first order contribution from the Jacobian under the change of variables, and $K(X)$ is the first order contribution from the variation of the potential. The constraint is achieved by demanding that the total variation of the matrix integral vanishes to order ϵ, giving

$$\langle J \rangle = \langle K \rangle. \tag{2.49}$$

The reparameterisations chosen are typically taken to be the loop function, hence the term 'loop equations'. Moreover, there is a one-to-one correspondence[2] between loop equations of the matrix model and the combinatorial recursion relations previously described in Section 2.2.2.

The variation of the potential can always be computed in a straightforward manner, but the variation of the Jacobian requires some care. One can prove [8] that for reparameterisations of the form

$$f(X) = A(X)\frac{1}{z-X}B(X), \tag{2.50}$$

the variation of the measure is given by

$$J(X) = \mathrm{Tr}\left(A(X)\frac{1}{z-X}\right)\mathrm{Tr}\left(\frac{1}{z-X}B(X)\right) + \text{contributions from } A,\ B. \tag{2.51}$$

The trace therefore splits into two traces containing the loop operator whenever the reparameterisation involves a loop function that is not traced over. We call this the 'split' rule. Furthermore, for reparameterisations of the form

$$f(X) = A(X)\mathrm{Tr}\left(B(X)\frac{1}{z-X}\right), \tag{2.52}$$

the variation of the measure is given by

$$J(X) = \mathrm{Tr}\left(A(X)\frac{1}{z-X}B(X)\frac{1}{z-X}\right) + \text{contributions from } A,B. \tag{2.53}$$

Hence, we call this the 'merge' rule.

[2]This statement is not entirely obvious for general multi-matrix models. However this is the case for the systems considered in this thesis. In particular we will derive the loop equations of the 3-state Potts model in Chapter 5, and present the combinatorial recursion relations in Appendix A.

By taking $f(X) = 1/(z - X)$, and using the split rule, we find

$$J = \mathrm{Tr}\frac{1}{z-X}\mathrm{Tr}\frac{1}{z-X}, \tag{2.54}$$

and

$$K = N\mathrm{Tr}\left(V'(X)\frac{1}{z-X}\right). \tag{2.55}$$

Using (2.49) the loop equation is then given by

$$\frac{1}{N^2}\left\langle \mathrm{Tr}\frac{1}{z-X}\mathrm{Tr}\frac{1}{z-X}\right\rangle = \frac{V'(z)}{N}\left\langle \mathrm{Tr}\frac{1}{z-X}\right\rangle - Q(z), \tag{2.56}$$

where $Q(z) = \frac{1}{N}\langle\frac{V'(z)-V'(X)}{z-X}\rangle$ is a polynomial in z. We can separate the left hand side into contributions from connected and disconnected Feynman diagrams using the prescription $\langle \mathrm{Tr}A\mathrm{Tr}B\rangle = \langle \mathrm{Tr}A\rangle\langle \mathrm{Tr}B\rangle + \langle \mathrm{Tr}A\mathrm{Tr}B\rangle_{\mathrm{conn.}}$, giving

$$W^2(z) + \frac{1}{N^2}W(z,z) = V'(z)W(z) - Q(z), \tag{2.57}$$

where the second term on the left hand side represents the Hartle-Hawking wave functional for universes with two boundaries (or two-loop function). Utilising the topological expansion for both the one-loop function and the two-loop function (2.19), we can take the large N limit of (2.57). The contribution of the two-loop function is then suppressed, and we recover the spectral curve (2.23).

2.3.4 Adding matter to surfaces

The coupling of any matter fields to two-dimensional quantum gravity at the discretised level is straightforward in principle - adopt a fixed lattice statistical model representation of the matter partition function in (2.17). We will now consider a simple example, the Ising model spin system.

The partition function is given by

$$Z_M(T) = \sum_{\{\sigma_i\}} e^{\beta(\sum_{\langle i,j\rangle}\sigma_i\sigma_j - 1)}, \tag{2.58}$$

where the spin degrees of freedom, σ_i, can take values in $\{+1, -1\}$, and reside at the centre of triangles, labelled by i, j, in the triangulation T on which the

model is defined. The angle brackets indicate that the sum is taken over nearest neighbour pairs of spins.

It is possible to realise this partition function on random graphs by mapping it onto the following two-matrix model,

$$Z = \int [dX_1][dX_2] e^{-N\mathrm{Tr}S(X_1,X_2)}, \tag{2.59}$$

where the action is of the form

$$S(X_1, X_2) = V_1(X_1) + V_2(X_2) - X_1 X_2, \tag{2.60}$$

with potentials

$$V_1(z) = -\frac{1}{2}z^2 + \sum_{k=2}^{d_1+1} \frac{t_k}{k} z^k, \quad V_2(z) = -\frac{1}{2}z^2 + \sum_{k=2}^{d_2+1} \frac{t'_k}{k} z^k. \tag{2.61}$$

The potentials may be kept arbitrary, corresponding to any generic polygonulation of two-dimensional manifolds.

Consider the case $V_1 = V_2$, with $t_m = 0, m > 3$. As in the case of the one-matrix model, we can write down the Feynman rules and evaluate the free energy as a dual graph expansion. We have two trivalent vertices corresponding to X_1 and X_2, and hence any given triangulation in the dual graph expansion is composed of two different types of triangle. Identifying each type of triangle with a distinct spin, placed at the centre of the triangle in either the up or down orientation, we endow a given triangulation with the spin system. The weighting for nearest neighbour spins is realised by the quadratic part of the action, giving the propagator

$$\begin{pmatrix} 1 & c(t_2) \\ c(t_2) & 1 \end{pmatrix} \delta_{\alpha_1,\beta_1}\delta_{\alpha_2,\beta_2}, \tag{2.62}$$

where c is a function of t_2, and the Kronecker delta operate on matrix indices, while the 2×2 matrix refers to the spin indices, i.e. the matrices X_1 and X_2. Therefore equivalent triangles are glued together with weight 1, whilst inequivalent triangles are glued together with weight $e^{-2\beta} \coloneqq c$, giving the Boltzmann factor one obtains on the fixed lattice (2.58).

The machinery of matrix models is particularly convenient for studying boundary conditions of the Ising spin system. In this case the two integrable boundary

conditions [9] are 'fixed', where spins are aligned at the boundary, and 'free', where the spins are completely unconstrained. We can represent these through the following two resolvents:

$$W_{X_1}(z) = \frac{1}{N}\left\langle \mathrm{Tr}\frac{1}{z-X_1}\right\rangle, \quad W_{X_1+X_2}(z) = \frac{1}{N}\left\langle \mathrm{Tr}\,\frac{1}{z-(X_1+X_2)}\right\rangle, \tag{2.63}$$

where the connection with the 'fixed' and 'free' boundary conditions, respectively, is observed through the dual graph expansion. The resolvent

$$W_{X_1-X_2}(z) = \frac{1}{N}\left\langle \mathrm{Tr}\,\frac{1}{z-(X_1-X_2)}\right\rangle, \tag{2.64}$$

does not represent a physical boundary condition. This is further discussed in Chapter 4.

The two functions (2.63), can be evaluated, in the planar limit, using the saddle-point approach [10] and the method of loop equations [6]. The one-loop function with fixed boundary conditions has been derived by a number of means [11–13]. The loop equation method devised in [12] is particularly powerful as it provides a recursive procedure through which subleading terms in the topological expansion of the one-loop function may be determined, and it may be derived independent of the particular structure of the potentials $V_1(x), V_2(y)$. In this approach one considers two infinitesimal reparameterisations:

$$\delta X_2 = \frac{1}{x-X_1}, \qquad \delta X_1 = \frac{V_2'(y)-V_2'(X_2)}{y-X_2}\frac{1}{x-X_1}, \tag{2.65}$$

which yields the two loop equations

$$xW(x) - 1 = \frac{1}{N}\left\langle \mathrm{Tr}\frac{1}{x-X_1}V_2'(X_2)\right\rangle, \tag{2.66}$$

$$\left\langle \mathrm{Tr}\frac{1}{x-X_1}\mathrm{Tr}\frac{1}{x-X_1}\frac{V_2'(y)-V_2'(X_2)}{y-X_2}\right\rangle = N\left\langle \mathrm{Tr}\frac{V_1'(X_1)}{x-X_1}\frac{V_2'(y)-V_2'(X_2)}{y-X_2} - \mathrm{Tr}\frac{1}{x-X_1}X_2\frac{V_2'(y)-V_2'(X_2)}{y-X_2}\right\rangle. \tag{2.67}$$

Retaining the planar terms in the large N limit, and taking $y = V_1'(x) - W(x)$, one obtains the spectral curve of the planar resolvent

$$E(x,y) = 0, \tag{2.68}$$

where

$$E(x,y) = (V_1'(x) - y)(V_2'(y) - x) - P(x,y) + 1, \tag{2.69}$$

and $P(x,y)$ is a polynomial of degree d_1 in x and d_2 in y. It contains low-level correlators in the large z expansion of $W(x)$, such as $p_1(g)$ in the pure gravity spectral curve (2.23).

The coefficients of $P(x,y)$ are determined through the genus zero condition, which can be imposed in a number of ways. For example, in Section 2.2.2 we stipulated that the planar resolvent possesses a certain number of branch points, constraining the form of the discriminant (2.24). Similarly, we may enforce this condition here through mandating that the resolvent possesses a certain branch structure. Another method which is particularly useful for complicated spectral curves involves noting that the genus zero condition is equivalent to the existence of a rational parameterisation of the algebraic curve: $x = \mathcal{X}(s), y = \mathcal{Y}(s)$, which are single-valued functions on the punctured Riemann sphere. Following [12, 14] a consistent parameterisation can be given for (2.68),

$$x = \mathcal{X}(s) = \gamma s + \sum_{k=0}^{d_2} \frac{\alpha_k}{s^k}, \quad y = \mathcal{Y}(s) = \frac{\gamma}{s} + \sum_{j=0}^{d_1} \beta_j s^j, \tag{2.70}$$

where the coefficients are determined by demanding that the Laurent series expansion about the poles reproduce the asymptotic expansion of the spectral curve.

As previously discussed in Section 2.2.3, the continuum limit is defined by isolating the nonanalytic dependence of observables on the fugacities. In the pure gravity case the only relevant fugacity was g, representing the bulk cosmological constant, and consequently the continuum limit was defined by the critical value of g and the scaling behaviour could be characterised by the critical exponent $\gamma_s = -1/2$. For the Ising matrix model, the presence of two fugacities, (g, c), offers the possibility of higher order critical behaviour. For arbitrary c, there exists a point where g is critical, corresponding to the pure gravity continuum limit, as in the one-matrix model. However, there also exists a value of c and g for which both the matter and geometry become critical. At this higher order point the confluence of both matter and spacetime excitations shift the string susceptibility to $\gamma_s = -1/3$.

Let us realise this explicitly, and compute the scaling one-loop function for (2.68), with $V_1 = V_2$, and $t_m = 0$ for $m > 3$. The spectral curve is given by

$$x^3 + y^3 - (t_2 - 1)(x^2 y + x y^2) + \frac{(t_2 - 1)}{t_3}(x^2 + y^2) - t_3 x^2 y^2 + \frac{(t_3^2 - t_2^2 + 2t_2 - 2)}{t_3} xy + c_1(t_2, t_3)(x + y) + c_2(t_2, t_3) = 0, \quad (2.71)$$

where c_1 and c_2 depend only on the couplings. These are fixed through the rational parameterisation, given by (2.70) for $d_1 = d_2 = 2$. The coefficients of the rational parameterisation are determined by demanding they reproduce the large x asymptotic behaviour of the solutions of (2.71), $y(x)$, on each sheet. These expressions are quite large and so we shall not reproduce them here. The critical point may be determined by requiring that sufficiently many derivatives vanish, consistent with the expectation of higher order critical behaviour $y \sim (x - x_c)^{4/3}$ where x_c represents a branch point. This yields $t_{2,c} = 2(1 + \sqrt{7})$ and $t_{3,c} = \sqrt{10}$, and we may then easily determine the branch point x_c through the rational parameterisation. We then use the prescription argued for in Section 2.2.3, taking the $\varepsilon \to 0$ limit with $t_3 = t_{3,c} e^{-\varepsilon^2 \mu}$ and $x = x_c e^{\varepsilon z}$, but now holding $t_2 = t_{2,c}$. Using (2.31) we can identify the scaling function with $\gamma_s = -1/3$, which is given, up to an overall factor, by

$$\tilde{W}(z, \mu) = \mu^{2/3} \left(\left(z + \sqrt{z^2 - 1} \right)^{4/3} + \left(z - \sqrt{z^2 - 1} \right)^{4/3} \right). \quad (2.72)$$

For generic potentials in the one- and two- matrix models it is possible to achieve a wider variety of multicritical behaviours, describing gravity interacting with an array of different conformal matter. For the one-matrix model one can achieve critical behaviour corresponding to conformal matter given by the $(2m-1, 2)$ diagonal minimal models (nomenclature will be explained in the following section), characterised by $\gamma_s = -1/m$ [15]. For the two-matrix model, sufficiently tuned potentials can give critical behaviour corresponding to the (p, p') diagonal minimal models for arbitrary integers p, p' [14]. The multicritical points of multi-matrix models are less well-explored, hampered by issues with actually computing objects like the planar resolvent. In this thesis we will focus on the latter problem for the particular case of the Potts model.

2.4 Conformal Field Theory

2.4.1 A brief overview

For statistical models of spin systems on fixed lattices, it is well known that at a critical point, where the correlation length of spins diverges and one obtains a continuous phase transition, the long range excitations of the theory can be described by a scale invariant quantum field theory. In two-dimensions, such scale invariance is enhanced to the larger symmetry group of conformal transformations. This group may be characterised as the set of diffeomorphisms under which the metric transforms by a scale factor, hence preserving angles, and in two-dimensions the conformal group is infinite dimensional. This makes local conformal symmetry a powerful tool in the analysis of quantum field theories, by allowing one to compute correlation functions non-perturbatively, and even without a defined action. Here we will outline some of the basic elements of two-dimensional conformal field theory (CFT) relevant to the systems discussed in this thesis. A more complete treatment of this subject may be found in [16, 17].

Using complex coordinates $z = x^0 + ix^1, \bar{z} = x^0 - ix^1$, two-dimensional conformal transformations may be identified with the set of holomorphic transformations $z \to f(z)$. By observing the action of infinitesimal holomorphic transformations, $z \to z + \sum_n \epsilon_n z^{n+1}$, on functions, one can deduce the algebra of the local conformal group, called the Witt algebra,

$$[l_n, l_m] = (n-m)l_{m+n}, \quad l_n := -z^{n+1}\frac{\partial}{\partial z}. \tag{2.73}$$

There is also an identical copy of the algebra describing antiholomorphic transformations, written in terms of a corresponding set of generators $\{\bar{l}_n\}$. When studying the action of symmetry transformations on quantum states, one must consider projective representations, since states in the Hilbert space differing by a scale factor should be identified. This is equivalent to considering representations of a centrally extended algebra. The unique central extension of the holomorphic

Witt algebra is given by the Virasoro algebra,

$$[L_n, L_m] = (n-m)L_{n+m} + \frac{c}{12} n(n^2-1)\delta_{n+m,0}, \tag{2.74}$$

where c is an extensive quantity denoting the central charge of the given CFT under consideration.

In ordinary quantum field theory, one quantises on a constant time hypersurface and the Hamiltonian, as the generator of time translations, allows one to connect different time slices. In CFT, due to scale invariance, and the fact that we predominantly work in Euclidean spacetimes, we may quantise on a surface of constant radius, and take the Virasoro generator L_0, which generates scale transformations, as the analogue of the Hamiltonian. To be completely precise, we take the sum $L_0 + \bar{L}_0$ up to a constant factor as the full Hamiltonian. This choice is called radial quantisation. The origin is taken to correspond to the asymptotic past and complex infinity corresponds to the asymptotic future. With this framework, states in the asymptotic past are localised at the origin, and we can therefore identify states with local operators. This is the state-operator correspondence, and it allows us to work with either states or corresponding local fields in the description of conformal field theories.

The set of states of a CFT must form a representation of the holomorphic and antiholomorphic copies of the Virasoro algebra. For now we will consider the holomorphic sector only, with the story playing out the same way for the anitholomorphic sector. We label states by their eigenvalue under L_0, which we call the conformal dimension. A primary state of conformal dimension Δ is a highest weight state of a given representation, satisfying

$$L_0 |\Delta\rangle = \Delta |\Delta\rangle , \quad L_n |\Delta\rangle = 0,\ n > 0. \tag{2.75}$$

Repeated action of the generators L_n for $n < 0$ produces descendant states with ever increasing conformal dimension

$$L_0(L_n |\Delta\rangle) = (\Delta - n)(L_n |\Delta\rangle). \tag{2.76}$$

The primary state, together with its descendants, forms a highest weight representation of the Virasoro algebra, called a Verma module. To find an irreducible representation, one must quotient out any submodules generated by descendant states that are also primary. Such descendant states are known as null or singular states, and the presence of such states provides powerful constraints on the theory by, for example, implying correlation functions satisfy certain partial differential equations. Another necessary concept is the fusion product of two representations

$$\mathcal{R}_i * \mathcal{R}_j = \bigoplus_k \mathcal{N}_{i,j}{}^k \mathcal{R}_k, \quad \mathcal{N}_{i,j}{}^k \in \mathbb{N}, \tag{2.77}$$

expressing the product of two representations, $\mathcal{R}_i, \mathcal{R}_j$, in terms of a sum of representations. The complete set of fusion products between irreducible representations of a given CFT is called the fusion algebra.

2.4.2 Minimal models

An important class of CFT are the minimal models. Specified by two coprime integers p, p', with $p < p'$, the (p, p') minimal model is the CFT with central charge

$$c = 1 - 6\frac{(p-p')^2}{pp'}, \tag{2.78}$$

and a finite number of primary states, with conformal weights given by the Kac formula,

$$\Delta_{r,s} = \frac{(p'r - ps)^2 - (p'-p)^2}{4pp'}, \tag{2.79}$$

where $1 \leqslant r < p$, and $1 \leqslant s < p'$.

Each Verma module built from primary states with conformal dimension (2.79) has two null vectors, the confluence of which give rise to an infinite number of descendant null vectors in the spectrum, and thus to an infinite number of constraints on the correlators of the theory. This in turn leads to a significant truncation of the fusion algebra, such that we only need to consider a finite set of primary states for the algebra to be closed.

From these degenerate representations one can generate full conformal field theories by combining holomorphic and antiholomorphic Verma modules. A

particularly simple example is the A-series, or diagonal, minimal models, for which the Hilbert space of states is given by the following tensor product of holomorphic and antiholomorphic irreducible representations of conformal dimension (2.79),

$$\mathcal{H}^{A}_{(p,p')} = \frac{1}{2}\bigoplus_{r=1}^{p'-1}\bigoplus_{s=1}^{p-1}\mathcal{R}_{r,s}\otimes\bar{\mathcal{R}}_{r,s}. \tag{2.80}$$

This encompasses the critical and tricritical Ising models for $(p',p) = (4,3)$ and $(5,4)$ respectively. The states involved in the diagonal models are spinless, having zero eigenvalue under the spin operator $L_0 - \bar{L}_0$.

A more complicated construction is given by the D-series minimal models, which combine degenerate representations with conformal dimensions differing by integers, and consequently possessing states with non-zero spin:

$$\mathcal{H}^{D}_{(p,p')} = \frac{1}{2}\bigoplus_{r=_2 1}^{p'-1}\bigoplus_{s=1}^{p-1}|\mathcal{R}_{r,s}|^2 \bigoplus \frac{1}{2}\bigoplus_{\substack{1\leqslant r\leqslant p'-1\\ r=\frac{p'}{2}\bmod 2}}\bigoplus_{s=1}^{p-1}\mathcal{R}_{r,s}\otimes\bar{\mathcal{R}}_{p'-r,s}, \tag{2.81}$$

where $=_2$ means r increases in steps of 2. This encompasses the critical and tricritical Potts model for $(p',p) = (6,5)$ and $(7,6)$ respectively.

2.4.3 Boundary conformal field theory

Physical systems usually have a finite number of conformally invariant and physically realisable boundary states, corresponding to various boundary conditions imposed on the lattice. We will now review the description of these boundaries in CFT, detailing the construction for diagonal theories, and discussing the boundary states of various other systems, the 3-state Potts model in particular.

The canonical way of introducing a boundary is to fix it to be the real axis in the complex plane $\mathrm{Im}(z) = 0$. The CFT is then defined on the upper half plane (UHP). The set of admissible diffeomorphisms, $z \to z + \epsilon(z)$, $\bar{z} \to \bar{z} + \bar{\epsilon}(\bar{z})$, must preserve this boundary, and therefore implies that the holomorphic and antiholomorphic transformations must coincide on the real axis, $\epsilon(z) = \bar{\epsilon}(\bar{z})$. Thus, the number of generators is halved, with $L_n = \bar{L}_n$, but we are still left with an infinite-dimensional copy of the local conformal group.

To describe the construction of boundary states it is convenient to consider a semi-annular domain on the UHP with inner and outer radii identified, and two separate boundary configurations for $z > 0$ and $z < 0$ with $\mathrm{Im}(z) = 0$, which we will call a and b. Equivalently, this may be regarded as a cylinder with different boundary conditions at each end. This may be mapped to the finite strip via $w = \frac{L}{\pi}\mathrm{Ln}(z)$, and subsequently mapped to the annulus under the mapping $\zeta = \exp\left(-\frac{2\pi i w}{T}\right)$. The annular geometry is useful since, under radial quantisation, it may be regarded as a segment of the full complex plane, for which we have already discussed the construction of states and representations.

The condition of conformal invariance in the annular geometry may be written as the following constraint acting on the boundary state $|a\rangle$:

$$(L_n - \bar{L}_{-n})\,|a\rangle = 0. \tag{2.82}$$

Boundary states satisfying this condition are conformally invariant boundary states. Solutions to this linear system are spanned by a set known as the Ishibashi states,

$$|j\rangle\rangle = \sum_n |j,n\rangle \otimes U\,|\overline{j,k}\rangle\,, \tag{2.83}$$

where $|j,n\rangle$ is the n^{th} state in the Verma module j, $|\overline{j,n}\rangle$ is the corresponding antiholomorphic state, and U is an anti-unitary operator satisfying

$$UL_n = \bar{L}_n U, \quad U\,|\overline{j,n}\rangle = |\overline{j,n}\rangle^*\,. \tag{2.84}$$

Thus we possess an Ishibashi state for each primary state in the theory, and any linear combination of these also defines a conformally invariant boundary state. However, the set of physical boundary states satisfies not only conformal invariance, but some auxiliary constraints.

To proceed we define the following functions, known as characters,

$$\chi_j(q) = \mathrm{Tr}\, q^{L_0 - c/24}, \tag{2.85}$$

where the trace is taken over the entire set of states of a given Verma module j. For $q = e^{2i\pi\tau}$ the set of characters associated with the minimal models transform

amongst themselves under modular transformations. In particular, under $\tau \to -1/\tau$,

$$\chi_i(q) = \sum_j S_{ij}\chi_j(\tilde{q}), \quad \tilde{q} = e^{-\frac{2i\pi}{\tau}}, \tag{2.86}$$

where the subscripts i, j label primary states and the modular S-matrix is given by

$$S_{(r,s),(r',s')} = \sqrt{\frac{8}{pp'}}(-1)^{(r+s)(r'+s')} \sin \pi r r' \frac{(p-p')}{p'} \sin \pi s s' \frac{(p-p')}{p}. \tag{2.87}$$

Moreover, Ishibashi states satisfy the following orthogonality condition,

$$\langle\langle i| \, (\tilde{q}^{\frac{1}{2}})^{(L_0+\bar{L}_0-c/12)} \, |j\rangle\rangle = \delta_{ij}\chi_j(\tilde{q}). \tag{2.88}$$

Following Cardy [18], the auxiliary relations determining the set of physical boundary states may be found by using the constraints of modular invariance of the partition function Z_{ab}. This may be computed in two different ways. We may calculate it in the annular geometry with time flowing in the 'L' direction and the boundary state $|a\rangle$ evolving into $|b\rangle$,

$$Z_{ab} = \langle b| \, (\tilde{q}^{\frac{1}{2}})^{(L_0+\bar{L}_0-c/12)} \, |a\rangle \, . \tag{2.89}$$

Equivalently, we may regard it as resulting from periodic time evolution on the strip with boundary conditions $|a\rangle$ and $|b\rangle$. Then, if the Hilbert space decomposes into irreducible representations as

$$\mathcal{H}_{ab} = \oplus_i \, n^i{}_{ab}\mathcal{R}_i, \quad n^i{}_{ab} \in \mathbb{N}, \tag{2.90}$$

then the partition function is given by

$$Z_{ab} = \sum_i n^i{}_{ab}\chi_i(q). \tag{2.91}$$

We may then equate expressions (2.89) and (2.91). Expanding (2.89) in Ishibashi states, and using properties (2.86) and (2.88), we may identify the coefficients of the characters, obtaining Cardy's consistency conditions:

$$\sum_i S_{ij} n^i{}_{ab} = \langle a|j\rangle\rangle\langle\langle j|b\rangle \, . \tag{2.92}$$

This is a nonlinear constraint relating the coefficients of the boundary states $|a\rangle \, , |b\rangle$, with respect to the Ishibashi basis, to the integer multiplicities $n^i{}_{ab}$.

For the minimal models (2.92) is solved by

$$|a\rangle = \sum_j \frac{S_{a,j}}{\sqrt{S_{I,j}}} |j\rangle\rangle, \tag{2.93}$$

which automatically satisfies (2.92) for $a = I$, and holds generally when the integer multiplicities $n^i{}_{ab}$ equal the fusion coefficients (2.77). Consider, for example, the critical Ising model. This has three primary states: $|I\rangle$ with conformal weight 0, $|\epsilon\rangle$ with weight $\frac{1}{2}$, and $|\sigma\rangle$ with weight $\frac{1}{16}$. The physical boundary states are then:

$$|I\rangle = \frac{1}{\sqrt{2}} |I\rangle\rangle + \frac{1}{\sqrt{2}} |\epsilon\rangle\rangle + \frac{1}{2^{1/4}} |\sigma\rangle\rangle, \tag{2.94}$$

$$|\epsilon\rangle = \frac{1}{\sqrt{2}} |I\rangle\rangle + \frac{1}{\sqrt{2}} |\epsilon\rangle\rangle - \frac{1}{2^{1/4}} |\sigma\rangle\rangle, \tag{2.95}$$

$$|\sigma\rangle = |I\rangle\rangle - |\epsilon\rangle\rangle. \tag{2.96}$$

$|I\rangle$ and $|\epsilon\rangle$ are identified with the fixed spin boundary conditions since they differ by the sign of the state corresponding to the spin field operator. The remaining boundary state corresponds to the free boundary condition.

2.4.4 3-state Potts model

The 3-state Potts model on a fixed lattice is a generalisation of (2.58), where the spins of the spin system are allowed to occupy one of three different states. There is a nearest neighbour interaction between these spins governed by the Hamiltonian

$$H = -J \sum_{\langle i,j \rangle} \delta(s_i, s_j), \quad s_i \in \{1, 2, 3\}. \tag{2.97}$$

We take the coupling constant $J > 0$, corresponding to ferromagnetic interactions. The set of physical boundary states in the antiferromagnetic model were recently discussed in [19].

The CFT describing the critical 3-state Potts model is the (6,5) D-series minimal model (2.81), with central charge $c = 4/5$. As the Hilbert space is non-diagonal, the corresponding analysis required to construct the physical boundary states becomes more complicated. However, this theory possesses a larger, infinite-dimensional symmetry algebra, called the W_3 algebra, of which the Virasoro algebra is a subset.

This phenomenon may be regarded as arising due to the confluence of a spin-3 current in the spectrum with the spin-2 current that generates conformal transformations (the stress-energy tensor) [20]. The critical Potts model has another description as a diagonal minimal model of this extended W_3 algebra. Therefore the analysis of the previous section still holds.

The bulk spectrum consists of four Verma modules with respect to the W_3 algebra, two of which occur twice. The primary states are labelled $|I\rangle$ with conformal weight 0, $|\epsilon\rangle$ with weight $\frac{2}{5}$, $|\psi\rangle, |\psi^\dagger\rangle$ with weight $\frac{2}{3}$, and $|\sigma\rangle, |\sigma^\dagger\rangle$ with weight $\frac{1}{15}$. For each of these states, one can construct corresponding W-Ishibashi states, and construct six physical boundary states as linear combinations of them using the Cardy construction. In [18] it was argued that the physical boundary states $|I\rangle, |\psi\rangle, |\psi^\dagger\rangle$ represent fixed boundary conditions, and the states $|\epsilon\rangle, |\sigma\rangle, |\sigma^\dagger\rangle$ represent mixed boundary conditions, where two out of three available spin states are permitted at the boundary.

These states give a complete set of physical boundary states that are invariant under the W_3 algebra, but they do not exhaust the set of conformally invariant physical boundary states. For $c = 4/5$ there are ten degenerate representations of the Virasoro algebra, and thus ten Ishibashi states one could construct. Through considering cylinder partition functions between W-boundary states and Virasoro Ishibashi states, Affleck, Oshikawa and Saleur [21] discovered two more physical boundary states violating W-symmetry. One represented free boundary conditions, while the other they dubbed the 'New' boundary condition. They argued that the New boundary condition may be understood as arising from free boundary conditions on a fixed lattice with negative Boltzmann weight interactions between boundary spins. It was subsequently proven that these exhaust the physical set of boundary states in [22]. See [23] for a complete treatment using the Coulomb gas approach.

One of the main aims of this thesis is to realise these physical boundary states, implemented through corresponding boundary conditions, on the random lattice. In particular, we will return to the 3-state Potts model in Chapters 4 and 5.

2.4.5 q-state Potts model

The q-state Potts model further generalises (2.97) by allowing the spins to occupy one of q different states, $s_i \in \{1, 2, \ldots, q\}$. For $q = 2$ and 3 we recover the Ising model and the 3-state Potts model respectively. For $q > 4$ the model has a first order phase transition, and consequently there is no CFT description. For $q = 1$ and 4, one still obtains a continuous phase transition; the former may be identified with the $(3, 2)$ minimal model [16], whereas the latter can be described as an orbifold of the compactified free boson [24]. This $q = 4$ CFT is non-rational, and consequently the discussion of boundary states in Section 2.4.3 does not apply.

It is possible to reformulate the fixed lattice description as a probability distribution of random graphs living on the same fixed lattice. This is known as the Fortuin-Kasteleyn cluster representation [25], and it allows one to generalise the model to arbitrary values of q. In particular, one obtains a continuous phase transition for $0 < q \leqslant 4$. Within this range there exists an infinite set of q's for which the central charge is of the form [26],

$$c = 1 - \frac{6}{m(m+1)}, \quad q = 2\left(1 + \cos\frac{2\pi}{m+1}\right), \; m \in \mathbb{N}. \tag{2.98}$$

This central charge coincides with the unitary minimal models, although the spectrum, which consists of a finite number of primary states, will only partially overlap with that of the corresponding minimal model [27]. To the best of our knowledge the Hilbert space and conformally invariant boundary states have not been determined for arbitrary m. Remarkably, for general $0 < q \leqslant 4$, the spectrum of primary states has been identified [28, 29], but the structure of the representations and the fusion algebra are still largely unknown.

2.4.6 Dilute q-state Potts model

The dilute q-state Potts model on a fixed lattice is defined like the ordinary q-state Potts model, except that we allow for vacant sites on the lattice, and the total number of spins may fluctuate. The model is characterised by the Hamiltonian [30],

$$H = -\sum_{\langle i,j \rangle} t_i t_j (J + \delta(s_i, s_j)) - \mu \sum_i t_i, \quad s_i \in \{1, 2, \ldots, q\}, \tag{2.99}$$

where the variable t_i is 0 if the site i is vacant and 1 otherwise, and μ is a chemical potential specifying the average number of occupied sites on the lattice. In contrast to the q-state Potts model there is a second coupling, allowing for higher order tricritical behaviour. We will discuss the specific cases of the $q = 2$ (dilute Ising) and $q = 3$ (dilute Potts) models.

The tricritical point of the dilute Ising model is described by the tricritical Ising CFT. This CFT is equivalent to the diagonal (5,4) minimal model CFT, which possesses six primary states. We may therefore follow the analysis of Section 2.4.3 and determine the set of physical boundary states, which are in one-to-one correspondence with the set of primary states. In [31, 32] it was argued that we have the following identification between these states and boundary conditions on the lattice:

Boundary condition	fixed	partially fixed	vacant	free
Boundary state	$\|0\rangle, \|3/2\rangle$	$\|1/10\rangle, \|3/5\rangle$	$\|7/16\rangle$	$\|3/80\rangle$

where we have labelled boundary states by the conformal weight of the primary state they are associated with. Thus we find that, compared to the critical Ising model, we obtain three additional boundary states, one where the boundary is dominated by vacancies, and two for which the boundary possesses vacancies and fixed spins, which we call partially fixed.

Similarly the tricritical point of the dilute Potts model is described by the tricritical Potts CFT, which is equivalent to the (7,6) D-series minimal model. The set of physical boundary states has been determined in [33]. In terms of the lattice realisation, one still finds physical boundary states corresponding to the fixed, mixed, free, and New boundary conditions. Like the tricritical Ising model, one also finds additional boundary conditions coming from the admixture of vacancies. These are three partially fixed and three partially mixed boundary conditions, and a single pure vacancy state.

2.4.7 Liouville theory

A model of particular relevance to 2D quantum gravity is the Liouville conformal field theory. This is given by the following action,

$$S_L = \frac{1}{4\pi}\int_{\mathcal{M}} d^2\xi\sqrt{\hat{g}}(\partial_a\phi\partial^a\phi + Q\phi R[\hat{g}] + 4\pi\mu e^{2b\phi}), \tag{2.100}$$

where $\hat{g}$ is a fixed background metric, $Q = b + b^{-1}$ is a background charge, and the coupling b and bulk cosmological constant μ are free parameters. The central charge of the theory is given by $c = 1 + 6Q^2$.

In contrast to minimal models, Liouville theory is a non-rational CFT with an infinite number of primary states. In complex coordinates these are given by

$$|P\rangle = \lim_{z,\bar{z}\to 0} V_{\frac{Q}{2}+iP}(z)\bar{V}_{\frac{Q}{2}-iP}|0\rangle\,, \quad V_\alpha =: e^{2\alpha\phi(z)} :\,, \tag{2.101}$$

where states are labelled by the Liouville momentum parameter P. Since there is a continuum of primary states the Hilbert space may be expressed as an integral over a continuous set of irreducible representations, which is conventionally taken to be diagonal.

One may impose a boundary condition on the Liouville field ϕ through the addition of the following boundary term to (2.100),

$$\int_{\partial\mathcal{M}} d\zeta\left(\frac{QK}{2\pi}\phi + \mu_B e^{b\phi}\right), \tag{2.102}$$

where $d\zeta$ denotes the line element along the boundary, K denotes the geodesic curvature, and μ_B is the boundary cosmological constant. It is convenient to parameterise μ_B in terms of an auxiliary variable, σ,

$$\mu_B = \zeta\cos 2\pi b\sigma, \quad \zeta^2\sin\pi b^2 = \mu. \tag{2.103}$$

As in the rational case, one may construct a physical boundary state to each primary state. These were first identified in [34] using the boundary conformal bootstrap, and are given by

$$|\sigma\rangle = \int_0^\infty dP\Psi_\sigma(P)\,|P\rangle\rangle, \tag{2.104}$$

$$\Psi_\sigma(P) = (\pi\mu\gamma(b^2))^{-iP/b}\frac{\Gamma(1+2iPb)\Gamma(1+2iP/b)}{2^1/4(-2i\pi P)}\cos 4\pi\sigma P, \tag{2.105}$$

where $|P\rangle\rangle$ denotes the Ishibashi state corresponding to the primary state $|P\rangle$. These are the FZZT boundary states of Liouville theory.

A different set of boundary conditions is described by the ZZ boundary states, first computed in [35]. These states will play no significant role in this thesis. For a more complete treatment of Liouville theory, see [36, 37]. Regarding boundary states [38] provides a cogent discussion, particularly with respect to ZZ boundary states.

2.5 Liouville Gravity

2.5.1 Gauge fixing the 2D gravity path integral

Although an important theory in its own right, the role of conformal field theory in this thesis is through its connection to the theory of dynamical triangulations, where it facilitates the physical interpretation of various random lattice constructions. We will outline the connection to the discretised theory through the path integral approach to (2.1).

As we noted, the Einstein-Hilbert action is particularly simple in two-dimensions such that, if we fix the topology, which we always assume, the action depends only upon the area of surfaces under consideration. A suitable diffeomorphism invariant measure on the space of metric and matter configurations may be defined implicitly through a metric on these configuration spaces, the details of which may be found in [37, 39]. These measures are then further refined through restricting to the conformal gauge, $g = e^\phi\hat{g}$ with fixed $\hat{g}$, as first advocated in [40].

The reason for choosing conformal gauge is that, in two-dimensions, any metric may be written as $f^*g = e^\phi\hat{g}(\tau)$, where f^* represents a diffeomorphism, ϕ a Weyl rescaling, and $\hat{g}(\tau)$ is a representative fiducial metric in the moduli space, the space of metrics modulo diffeomorphisms and Weyl rescalings. We may therefore recast the integration over general two-dimensional metrics as an integral over the space of diffeomorphisms parameterised by some ζ, the space of Weyl rescalings

parameterised by ϕ, and the moduli space parameterised by τ,

$$\mathcal{D}g_{\mu\nu} \to d\zeta \mathcal{D}\phi d\tau J. \tag{2.106}$$

As the action and measure are diffeomorphism invariant, we can complete the integral over diffeomorphisms, which then factors out. The change of variables introduces a Jacobian given by the Fadeev-Popov determinant [41], which can be expressed as a functional integral over ghost fields

$$J = \int \mathcal{D}b\mathcal{D}c e^{-S_{\rm gh}[b,c]}, \quad S_{\rm gh} = \frac{1}{2\pi}\int d^2\xi \sqrt{g} b_{\alpha\beta} g^{\beta\sigma}\nabla_\sigma c^\alpha. \tag{2.107}$$

The measures for ϕ, the ghost sector, and the matter sector still depend implicitly on the gauge fixed metric, and therefore on the field ϕ. This dependence can be made explicit through the relations

$$\mathcal{D}_{e^\phi \hat{g}} X = e^{\frac{c_M S_L}{48\pi}} \mathcal{D}_{\hat{g}} X, \tag{2.108}$$

$$\mathcal{D}_{e^\phi \hat{g}} b \mathcal{D}_{e^\phi \hat{g}} c = e^{-\frac{26 S_L}{48\pi}} \mathcal{D}_{\hat{g}} b \mathcal{D}_{\hat{g}} c, \tag{2.109}$$

$$\mathcal{D}_{e^\phi \hat{g}} \phi = e^{\frac{S_L}{48\pi}} \mathcal{D}_{\hat{g}} \phi, \tag{2.110}$$

where S_L is given by the Liouville action (2.100). Relations (2.108), (2.109) have been derived through various methods [40]. The analysis for the Liouville measure is more complicated as the associated metric defined on the space of configurations depends implicitly upon ϕ itself [37]. By taking an ansatz for the final effective action and using consistency principles to determine the relevant coefficients, it was argued in [42, 43], that the Liouville measure must transform in a similar way to the matter and ghost measure, hence relation (2.110).

After a suitable rescaling of the field ϕ, the gauge fixed gravitational path integral is given by

$$\mathcal{Z}_h = \int d\tau \mathcal{D}_{\hat{g}}\phi \mathcal{D}_{\hat{g}} b \mathcal{D}_{\hat{g}} c \mathcal{D}_{\hat{g}} X \exp\left(-S_M[X,\hat{g}] - S_L[\phi,\hat{g}] - S_{\rm gh}[b,c,\hat{g}]\right). \tag{2.111}$$

The final theory obtained is a full fledged conformal field theory consisting of matter, Liouville, and ghost fields. They are coupled through the requirement that the conformal anomaly vanishes:

$$c_M + c_L - 26 = 0. \tag{2.112}$$

The effective theory given by (2.111) is known as Liouville gravity.

2.5.2 Bulk and boundary spectrum

The physical observables of Liouville gravity are represented by the gravitationally dressed matter states,

$$\lim_{z,\bar{z}\to 0} c\bar{c}\mathcal{O}_M(z,\bar{z})e^{2\alpha\phi(z,\bar{z})}\left|0\right\rangle, \tag{2.113}$$

where $c, \bar{c}$ are ghost fields and $\mathcal{O}_M$ represents a matter field. The parameter α is tuned so that, together, the net conformal weight of the matter and Liouville operator is one in the holomorphic and antiholomorphic sectors. This is equivalent to demanding that the operator is diffeomorphism invariant.

The physical Hilbert space of bulk states was determined by Lian and Zuckerman [44] for the case where the matter sector is given by the diagonal minimal models. Following the formalism of [45], the spectrum of physical states has also been determined for the case where the matter sector is given by the diagonal W_q minimal models [46]. These generalise the previously discussed W_3 minimal models.

The physical boundary states are constructed as a tensor product of boundary states in the matter, Liouville, and ghost sectors

$$\left|\sigma;\lambda\right\rangle = \left|\lambda\right\rangle_M \otimes \left|\sigma\right\rangle_{\text{FZZT}} \otimes \left|B\right\rangle_{\text{gh}}. \tag{2.114}$$

Together these are called the FZZT-Cardy branes. They have been extensively studied for the case of diagonal minimal matter [47, 48].

In this thesis we study the marked disc amplitude with prescribed boundary conditions, which is given by the first derivative of the disc partition function with respect to the boundary cosmological constant, $\partial_{\mu_B}\mathcal{Z}^{\text{disc}}$. Following [47], this may be computed for the (p',p) diagonal minimal model by first calculating

$$\partial_\mu \mathcal{Z}^{\text{disc}} = \lim_{z,\bar{z}\to 0}\left\langle\sigma;\lambda\right| c\bar{c}e^{2b\phi}\left|0\right\rangle, \tag{2.115}$$

where, from (2.100), it can be seen that the derivative with respect to μ corresponds to the insertion of the operator (2.113) for $\mathcal{O}_M = I$. This may then be integrated with respect to μ and differentiated with respect to μ_B to obtain

$$\tilde{W}(\sigma,\mu) = \partial_{\mu_B}\mathcal{Z}^{\text{disc}} = (\sqrt{\mu})^{p/p'}\cosh\left(\frac{\pi\sigma}{b}\right). \tag{2.116}$$

For $(p',p) = (5,4)$, this gives the scaling limit of the Ising one-loop function (2.72).

2.5.3 KPZ/DDK scaling

To cement the relationship between the discretised picture we first described and the continuum approach, we compare how the partition function scales with area. In the discretised theory, this scaling relation is given in terms of the string susceptibility γ_s by (2.29). In Liouville gravity, one must consider the fixed area partition function, given by inserting a delta function constraint $\delta(A - \int d^2\xi\sqrt{\hat{g}}e^{2b\phi})$ in (2.111). Under a shift of the Liouville field $\phi \to \phi + \ln A/2b$ the entire partition function scales as

$$\mathcal{Z}_h(A) = A^{-\frac{Q}{4b}\chi-1}\mathcal{Z}(1), \tag{2.117}$$

where we use the Gauss-Bonnet theorem to evaluate the contribution from the action.

The background charge Q may be determined from (2.112), and requiring consistency with the semiclassical limit of Liouville theory, given by $b \to 0$ when $c_M \to -\infty$, fixes the coupling b. Finally using the definition of γ_s in (2.29), we find

$$\gamma_s = \frac{1}{12}\left(c_M - 1 - \sqrt{(c_M-1)(c_M-25)}\right). \tag{2.118}$$

In the pure gravity scenario, with $c_M = 0$, this gives $\gamma_s = -1/2$, consistent with the scaling of the discretised model of Section 2.2.3. This formula is an example of the KPZ/DDK relations [49].

More generally, these formulae relate the conformal dimension of spinless primary states, corresponding to fixed lattice conformal field theories, and the analogous states when the matter theory is coupled to Liouville gravity. Calculating the scaling exponents of the partition function and correlation functions in the discretised theory and comparing with the continuum theory gives implicit confirmation of both the discretisation procedure adopted, and the prescription taken for constructing the continuum limit. Thus, we may use the matrix model prescription to calculate observables that may be difficult to compute in Liouville gravity.

Chapter 3

Boundary Conditions in the q-state Potts Model

3.1 Overview

In the previous chapter, we explained how the one-matrix model with a cubic potential formulates a discretisation of random surfaces (2.32), and how we may consider the Ising spin system on random planar graphs via the two-matrix model (2.59). With general polynomial potentials, we may use the multicritical points of the one- and two-matrix models to study the diagonal $(2m-1,2)$ and (p,p') minimal models, respectively, coupled to gravity. These models are solvable in the planar limit, and there are methods to compute subleading terms of the one-loop and multi-loop functions to all orders in the large N expansion [12, 15, 50].

In order to consider more general spin systems coupled to gravity, we need to study higher-order multi-matrix models. Unfortunately, as first pointed out in [51], and later in [52], multi-matrix models containing more than 2 degrees of freedom tend to be intractable. Those that can be solved use methods quite specific to the particular form of the model, and do not generalise (see [53, 54] cataloguing various solvable models).

In this chapter, we study properties of the planar one-loop function of the q-states Potts model coupled to 2D discretised quantum gravity. We use the multi-matrix model formulation

$$Z_q = \int \prod_{i=1}^{q} [dX_i] e^{-N\mathrm{Tr}\left(\sum_{i=1}^{q} V(X_i) - \sum_{\langle i,j\rangle} X_i X_j\right)}. \tag{3.1}$$

The X_i are $N \times N$ Hermitian matrices, each representing one of the q spin states, and $[dX_i]$ denotes integration over all the independent components. The potential $V(z) = U(z) - z^2/2$, where $U(z) = \sum_{k=2}^{n} t_m z^m/m$, controls the type of polygonulation of discrete 2-manifolds generated by the formal Feynman graph expansion in $\{t_2, t_3, \ldots\}$(we use $n = 3$, corresponding to triangulations).

At first, this model seems intractable. The non-trivial cycle of couplings between matrices prevents simultaneous diagonalisation, so that some techniques that are useful for single matrix models, such as orthogonal polynomials, are rendered inadequate. However, due to the particular structure of this partition function, it is in fact solvable. Kazakov [55] computed the solution for the case $q = 1$ and $q = 0$, and for $q = 2$ it reduces to the well-known Ising model on a random lattice, for which the one-loop function has been computed [13, 56]. Later, Daul and Zinn-Justin computed the one-loop function corresponding to the fully magnetised boundary condition on the spins, and associated critical exponents, for the $q = 3$ case [57, 58]. For all allowed values of q, in the sense that one obtains finite-sheeted resolvents, Eynard and Bonnet [59] subsequently computed the one-loop function using a loop equation method.

In [60, 61], a formalism was developed to compute a larger set of loop amplitudes, including auxiliary boundary conditions on Potts spins as well as the free and partially magnetised conditions. This formulation was illustrated by application to the $q = 1, 2, 3$ Potts models and the known results reproduced. In this chapter we show how to use these methods to develop systematically the loop amplitudes for these boundary conditions at all allowed q-values, and compute the associated critical exponents.

This chapter is organised as follows. In Section 2 we define the model and observables of the theory. In Section 3 we outline the method of determining the one-loop functions. In Section 4 we apply this construction to arbitrary q and p, giving the allowed values of each, along with the degree of the discriminant in each case. In Section 5 we outline some consequences of the previous propositions on the allowed one-loop functions, and derive the critical exponents of the general

solution, and in Section 6 we discuss our results. The results of this chapter have been reported in [62].

3.2 Defining the Model

We use the model defined by (3.1) to describe the q-state Potts model on a random planar lattice. We are interested in computing the correlation functions of matrices corresponding to various boundary conditions. These are captured by the resolvents

$$W_{(p)}(z) = \frac{1}{N}\left\langle \mathrm{Tr}\frac{1}{z - \sum_{k=1}^{p} X_k}\right\rangle, \tag{3.2}$$

where we use the S_q symmetry of the model to identify the resolvent generated by $\sum_{i=1}^{p} X_i$ with the resolvents generated by the $\sum_{i=1}^{p} X_{\sigma(i)}$ for all $\sigma \in S_q$. Therefore, only sums of matrices matter.

For $W_{(p)}(z)$ with arbitrary orderings of $\{X_1, \cdots X_p\}$, the corresponding resolvent generates discretised surfaces with a boundary composed of the permitted matrices. Interpreting the matrices as spins, we find that the resolvents generate the Potts model coupled to random surfaces with a single outer boundary (i.e. a disc for genus zero surfaces), where the boundary admits a restricted subset of spins, given by the matrices used to define the relevant resolvent. For example, the single matrix resolvent, given by (3.2) with $p = 1$, corresponds to the Potts model with a single spin on the boundary, and this would give the fixed spin boundary condition in the continuum CFT. In general, we map the resolvents onto the various conformal boundary conditions admitted by the Potts model CFT.

As in the case of the one-matrix model, for a given Hermitian matrix X with eigenvalues $\{x_i\}_{i=1}^{N}$, we define the large N eigenvalue density distribution

$$\rho_X(x) = \lim_{N\to\infty} \frac{1}{N}\left\langle \sum_{i=1}^{N} \delta(x - x_i)\right\rangle, \tag{3.3}$$

and the planar resolvent is then given by the Stieltjes transform

$$W_X(z) = \int_{\mathrm{supp}\,\rho_X} dx \frac{\rho_X(x)}{z - x}, \quad z \notin \mathrm{supp}\,\rho_X. \tag{3.4}$$

One then finds the eigenvalue density distribution by computing the discontinuity of the genus zero resolvent along its compact ('physical') cut, and with this one can compute various correlation functions in the same limit. We can analogously define eigenvalue density distributions and planar resolvents for any of the other resolvents given in (3.2).

For a given pair of Hermitian matrices X and Y, with eigenvalues $\{x_k\}_{k=1}^N$ and $\{y_l\}_{l=1}^N$, and a coupling given through the HCIZ integral formula [63, 64]

$$I = \frac{1}{N^2} \ln \left(\frac{\det_{1 \leqslant k,l \leqslant N} e^{N x_k y_l}}{\Delta(x)\Delta(y)} \right), \tag{3.5}$$

we associate a set of functions which we call G-functions, which we introduce following [65]. Assuming (3.5) has a smooth large N limit such that it only depends on the eigenvalue density distributions of X and Y, ρ_X and ρ_Y respectively, we write

$$\frac{\partial}{\partial x} \frac{\delta}{\delta \rho_X(x)} I = \operatorname{Re} G_X^Y(x) - \operatorname{Re} W_X(x), \tag{3.6}$$

where x is an eigenvalue of X. Furthermore we have

$$\operatorname{Re} G_X^Y(x) = G_X^Y(x)_0 + G_X^Y(x)_1, \tag{3.7}$$

and similarly for $W_X(x)$, where the subscript '0' refers to the physical sheet, and the subscript '1' refers to an adjoining sheet, connected through a compact cut along the real axis. The left hand side of (3.6) is an entire function of x and has no cuts on the support of ρ_X. We can therefore analytically continue to complex values $x \mapsto z$ and express the right hand side as functions defined on one sheet (say '0'). Equivalently, we may consider derivatives with respect to the eigenvalue density distribution of Y, obtaining an expression in terms of a separate G-function, $G_Y^X(z)$, and the resolvent $W_Y(z)$.

We therefore define the G-functions, for a pair of Hermitian matrices X and Y as

$$G_Y^X(z) = \frac{1}{N} \frac{\partial}{\partial z} \ln \left\langle \det_{1 \leqslant k,l \leqslant N} e^{N x_k y_l} \right\rangle_{y_N = z}, \quad z \notin \operatorname{supp} \rho_Y, \tag{3.8}$$

$$G_X^Y(z) = \frac{1}{N} \frac{\partial}{\partial z} \ln \left\langle \det_{1 \leqslant k,l \leqslant N} e^{N x_k y_l} \right\rangle_{x_N = z}, \quad z \notin \operatorname{supp} \rho_X, \tag{3.9}$$

where it is understood that one takes the derivative with respect to an eigenvalue within the support of the relevant eigenvalue density distribution, here taken to be the N^{th} eigenvalue, and then analytically continues the function away from the support. These functions satisfy the property $G_Y^X(G_X^Y(z)) = z + \mathcal{O}(1/N)$ [65]. Moreover, since the left hand side of (3.6) is an entire function of the eigenvalue, the G-function and associated resolvent have the same discontinuity across the real axis

$$\begin{aligned} G_Y^X(z)_0 - G_Y^X(z)_1 &= W_Y(z)_0 - W_Y(z)_1, \\ G_X^Y(z)_0 - G_X^Y(z)_1 &= W_X(z)_0 - W_X(z)_1. \end{aligned} \tag{3.10}$$

In the following, we determine the resolvents of the model in terms of these G-functions, to which they are related by an entire function.

3.3 One-Loop Functions: Key Results

In this section, we recall the principal results of [61], and establish the procedure for determining the one-loop functions.

Lemma 3.3.1. *Let $h > 0$ and abbreviate the integral transformations*

$$\gamma_\pm(X) = \int_{\mathbb{R}} dP_\pm f(P) e^{-\frac{N}{2}\mathrm{Tr}P_\pm^2} e^{N\mathrm{Tr}P_\pm X/\sqrt{e^{\pm 2h}-1}} \tag{3.11}$$

$$\gamma'_\pm(P) = \int_\Gamma dX f(X) e^{N\mathrm{Tr}PX\sqrt{1-e^{\mp 2h}}} \tag{3.12}$$

where the subscripts below the integrals indicate the integration cycle for the corresponding eigenvalues. Then, up to an overall factor, the partition function in (3.1) *can be written as*

$$Z_q = \int_{\mathbb{R}} dP_+ e^{-\frac{N}{2}(1-e^{-2h})\mathrm{Tr}P_+^2} (\gamma'_+[e^{-N\mathrm{Tr}U}](P_+))^q \tag{3.13}$$

$$= \int_{\mathbb{R}} dX_0 \gamma_+[(\gamma'_+[e^{-N\mathrm{Tr}U}])^p](X_0)\gamma_-[(\gamma'_-[e^{-N\mathrm{Tr}U}])^{q-p}](X_0) \tag{3.14}$$

$$\begin{aligned} = \int_{\mathbb{R}} dX_0 \Bigg(& \prod_{i=1}^q \int_\Gamma dX_i e^{-N\mathrm{Tr}U(X_i)} \\ & \times \gamma_+[1]\left(X_0 + 2\sinh h \sum_{i=1}^p X_i\right) \\ & \times \gamma_-[1]\left(X_0 - 2\sinh h \sum_{i=p+1}^q X_i\right). \end{aligned} \tag{3.15}$$

With these integral transforms, the coupling terms between matrices in the action (3.1) can be decomposed into simpler expressions with the introduction of new fiducial matrices. These new matrices, $\sqrt{1-e^{-2h}}P_+$, $\sqrt{1-e^{2h}}P_-$, and X_0, couple to separate sums of the original set of matrices, as well as each other. Note that the parameter h is introduced alongside the auxiliary matrices $P_\pm$, and thus Z_q does not depend on it. In [61] it was shown that as $h \to \infty$ the resolvent of X_0 is equivalent to the resolvent of the sum of random matrices that P_+ couples to, and thus possesses the required eigenvalue density distribution. This leads to the following result.

Proposition 3.3.2. *Let the random matrix P_+ be defined as in Lemma 3.3.1, and set $Y = \sqrt{1-e^{-2h}}P_+$. Then for $N \to \infty$ and $h \to \infty$, the spectral density of the sum of p matrices, distributed according to* (3.1)*, is given by*

$$\rho_{(p)}(z) = \frac{1}{2\pi i}\left(G^Y_{(p)}(z)_0 - G^Y_{(p)}(z)_1\right), \tag{3.16}$$

where $G^Y_{(p)}(z)$ is the functional inverse of

$$G^{(p)}_Y(z)_0 = \frac{p}{q}(z - W_Y(z)_1) + \frac{q-p}{q}W_Y(z)_0. \tag{3.17}$$

The label (p) refers to the sum of matrices being studied, i.e. if we take $X_{(p)} = \sum_{k=1}^{p} X_k$, then $G_Y^{X_{(p)}} = G^{(p)}_Y$.

This argument rests on the fact that these G-functions have the same cut on the physical plane as the $W_Y(z)$ resolvents (3.10). Using the result of this proposition, once we calculate the G-functions, we can determine the eigenvalue density distribution, from which one can calculate the correlators of the theory.

To determine the G-functions, we use the saddle-point equation about the eigenvalues for a given matrix in (3.1), say, $X \coloneqq X_i$ for some $i \in \{1, \ldots, q\}$:

$$U'(z) = W_X(z)_0 + G^Y_X(z)_0. \tag{3.18}$$

In analysing the $p = 1$ case for integer q, we assume $W_X(z)_0$ has an asymptotic expansion such that $\lim_{z\to\infty} zW_X(z)_0 = 1$. This can be seen from the formal definition of the resolvent (3.2). Then, we can immediately infer from (3.18) that $G^X_Y(z)_0$ has two sheets, connected by a semi-infinite square-root branch cut (taking

$U(z)$ to be cubic), which we denote C_∞. Furthermore, Proposition 3.3.2 implies that $G_Y^X(z)_0$ has at least two sheets connected by a compact cut, which we denote C_F. If the resulting branch structure does not terminate there, we can analytically continue to the other sheets, and use Proposition 3.3.2 to write down expressions for $G_Y^X(z)$ on all of its other sheets.

This derivation fixes the undetermined coefficients in the asymptotic expansion of the resolvent $W_X(z)$ by demanding that the G-functions have finitely many sheets. Starting from the physical sheet, '0', we analytically continue through C_F, to the next sheet, then C_∞ to the sheet above, and repeating in this way, we eventually reach a sheet on which there is no longer a branch cut through which we can analytically continue the function to higher sheets.

3.4 The G-functions for arbitrary (p, q)

Proposition 3.4.1. *The only values of q for which the $p = 1$ generating function can be described by an algebraic equation are given by*

$$q = 2(1 + \cos \nu\pi) \in (0, 4), \tag{3.19}$$

where $\nu = n/m$, and n, m are coprime.

Proof. This result was first observed by Eynard and Bonnet for the one-loop function in [59]. Here we establish it by computing the discontinuities across the branch cuts of the generating function and determining the values of q for which they vanish. The analytic structure of $G_Y^X(z)$ is described in Fig.3.1. Eliminating $W_Y(z)_1$ between (3.17) and (3.10), we have

$$G_Y^X(z)_1 = z + (1 - q)G_Y^X(z)_0 + (q - 2)W_Y(z)_0. \tag{3.20}$$

Sheet 1 is connected to sheet 0 by C_F. Circling C_∞ gives us

$$G_Y^X(z)_2 = z + (1 - q)G_Y^X(z)_{-1} + (q - 2)W_Y(z)_0. \tag{3.21}$$

Now we can eliminate $W_Y(z)_0$ between the last two equations to get

$$G_Y^X(z)_2 = G_Y^X(z)_1 + (q - 1)(G_Y^X(z)_0 - G_Y^X(z)_{-1}). \tag{3.22}$$

This demonstrates that we can generate all subsequent $G_Y^X(z)_K$ with $G_Y^X(z)_{-1,0,1}$ as initial data.

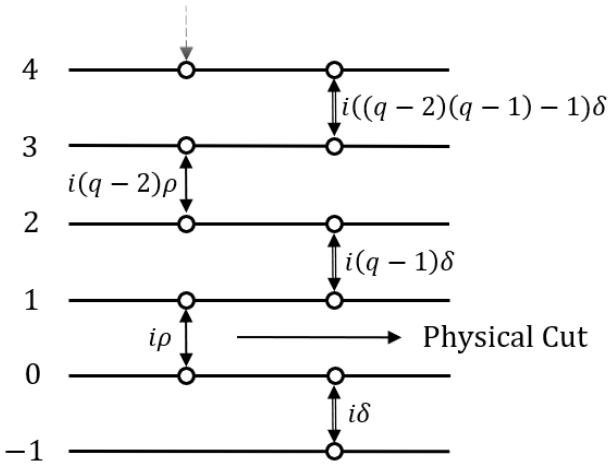

Figure 3.1: Analytic structure of $G_Y^X(z)$ for general q for (3.1) with a cubic potential. Each horizontal line denotes a sheet of the function and each circle a branch cut. The left-most circles represent C_F and the right-most represent C_∞. Branch cuts are labelled by discontinuities between the upper and lower sheet.

Circling successively $C_F, C_\infty, C_F, C_\infty, \ldots$ gives

$$\begin{aligned} G_Y^X(z)_3 &= G_Y^X(z)_0 + (q-1)(G_Y^X(z)_1 - G_Y^X(z)_{-1}) \\ G_Y^X(z)_4 &= G_Y^X(z)_{-1} + (q-1)(G_Y^X(z)_2 - G_Y^X(z)_0) \\ G_Y^X(z)_5 &= G_Y^X(z)_{-1} + (q-1)(G_Y^X(z)_3 - G_Y^X(z)_1) \\ &\vdots \\ G_Y^X(z)_K &= G_Y^X(z)_{K-6} + (q-1)(G_Y^X(z)_{K-2} - G_Y^X(z)_{K-4}). \end{aligned} \tag{3.23}$$

We note that this is a linear relationship amongst the $G_Y^X(z)_K$s, so we can read off the identical relationship for the coefficients of the discontinuous parts, ρ_K and δ_K, across the finite and infinite cuts respectively. We further note that the coefficient of any fixed power of z also satisfies the same equation – in particular α_K, the coefficient of the z itself, will be important later in the computation of the discriminant.

From the above linear recursion relationship, we see that the ρ_K, δ_K and α_K, defined above, all satisfy the difference equation

$$y_K = (q-1)(y_{K-2} - y_{K-4}) + y_{K-6}, \quad K \geqslant 6, \tag{3.24}$$

with appropriate initial data generated by the expressions $\{y_0, y_2, y_4\}$ for even K, and $\{y_1, y_3, y_5\}$ for odd K. We can separate the solutions of this into those for which K is an odd number and those for which K is even. The solutions of this difference equation in the even case are of the form

$$y_K = Ax^{K/2}, \tag{3.25}$$

where A is a constant and x satisfies

$$x^3 - (q-1)(x^2 - x) - 1 = 0, \tag{3.26}$$

whose solutions are

$$\begin{aligned} x &= 1, \\ x &= \frac{q - 2 \pm i\sqrt{4 - (q-2)^2}}{2} = e^{\pm i\theta}, \end{aligned} \tag{3.27}$$

assuming $q \leqslant 4$.

If the functions are algebraic, there must be a sheet for which the discontinuous parts ρ_K or δ_K vanish. Using the boundary conditions for the difference equation, we have the following:

$$C_F \;:\; \begin{cases} \rho_{2k} &= \frac{1}{\sqrt{q(q-4)}} x^{-(k+1)}(x^{2(k+1)} - 1), \\ \rho_{2k+1} &= -\rho_{2k} \end{cases} \quad k \geqslant 1, \tag{3.28}$$

$$C_\infty \;:\; \begin{cases} \delta_{2k} &= \frac{1}{q-4} x^{-(k+1)}(x-1)(x^{2k+1} - 1), \\ \delta_{2k-1} &= -\delta_{2k} \end{cases} \quad k \geqslant 1. \tag{3.29}$$

The vanishing of ρ_K or δ_K in (3.28) (3.29) fixes x to be a root of unity whence, using (3.27), we find that q must satisfy (3.19) and hence that $q < 4$. □

Proposition 3.4.2. *If $\theta = \nu\pi = \frac{n\pi}{m}$, with $n < m$ mutually prime, $n = 1, 3, \ldots$ is odd, and m may be even or odd. Then the allowed values of p are*

$$p = 1 + \frac{\sin(M+1)\theta}{\sin M\theta}, \quad M = 1, \ldots, m-1, \tag{3.30}$$

if the sheets terminate on a compact cut, and

$$p = 1 + \frac{\sin(M+\frac{3}{2})\theta}{\sin(M+\frac{1}{2})\theta}, \quad M = 0, \ldots, m-1, \tag{3.31}$$

if the sheets terminate on an infinite cut. We denote this set of solutions Case 1.

If $\theta = \nu\pi = \frac{n\pi}{m}$, with $n < m$ mutually prime, $n = 2, 4, \ldots, m-1$ is even, then the only allowed values of p are those for which the sheets terminate on a compact cut:

$$p = 1 + \frac{\sin(M+1)\theta}{\sin M\theta}, \quad M = 1, \ldots, m-1. \tag{3.32}$$

We denote this set of solutions Case 2.

Proof. Going back to (3.17) and (3.10), we can eliminate $W_Y(z)_1$ between these two equations, but keep p general, to find

$$G_Y^{(p)}(z)_0 = \frac{p}{q}\Big(z + G_Y^X(z)_0 - G_Y^X(z)_1\Big) + \left(1 - \frac{2p}{q}\right) W_Y(z)_0\,. \tag{3.33}$$

But $W_Y(z)_0$ also appears in (3.20), so can be eliminated, and we obtain

$$(q-2)G_Y^{(p)}(z)_0 = (p-1)\Big(z - G_Y^X(z)_1\Big) + (q-p-1)G_Y^X(z)_0\,. \tag{3.34}$$

Note that $q = 2$ has to be dealt with separately but one can show that the results we will obtain are true even in that case. Circling C_F gives

$$(q-2)G_Y^{(p)}(z)_1 = (p-1)\Big(z - G_Y^X(z)_0\Big) + (q-p-1)G_Y^X(z)_1\,. \tag{3.35}$$

Note that formula (3.34) is trivially correct for $p = 1$ and that

$$\begin{aligned}(q-2)G_Y^{(q-p)}(z)_0 &= (q-p-1)\Big(z - G_Y^X(z)_1\Big) + (p-1)G_Y^X(z)_0 \\ &= (q-2)z - (p-1)\Big(z - G_Y^X(z)_0\Big) - (q-p-1)G_Y^X(z)_1 \\ &= (q-2)\Big(z - G_Y^{(p)}(z)_1\Big),\end{aligned} \tag{3.36}$$

which is the correct duality relationship between p and $q-p$ functions, observed in [60].

Going back to (3.34) and circling cuts in the sequence $C_F, C_\infty, C_F, C_\infty, \ldots$ generates sheets with positive labels, so following on from (3.35) we have

$$\begin{aligned}(q-2)G_Y^{(p)}(z)_2 &= (p-1)\Big(z - G_Y^X(z)_{-1}\Big) + (q-p-1)G_Y^X(z)_2 \\ (q-2)G_Y^{(p)}(z)_3 &= (p-1)\Big(z - G_Y^X(z)_{-1}\Big) + (q-p-1)G_Y^X(z)_3 \\ (q-2)G_Y^{(p)}(z)_4 &= (p-1)\Big(z - G_Y^X(z)_0\Big) + (q-p-1)G_Y^X(z)_4 \\ &\vdots \\ (q-2)G_Y^{(p)}(z)_K &= (p-1)\Big(z - G_Y^X(z)_{K-4}\Big) + (q-p-1)G_Y^X(z)_K\,.\end{aligned} \tag{3.37}$$

Circling cuts in the sequence $C_\infty, C_F, C_\infty, C_F, \ldots$ generates sheets with negative labels:

$$\begin{aligned}
(q-2)G_Y^{(p)}(z)_{-1} &= (p-1)\Big(z - G_Y^X(z)_2\Big) + (q-p-1)G_Y^X(z)_{-1} \\
(q-2)G_Y^{(p)}(z)_{-2} &= (p-1)\Big(z - G_Y^X(z)_3\Big) + (q-p-1)G_Y^X(z)_{-1} \\
(q-2)G_Y^{(p)}(z)_{-3} &= (p-1)\Big(z - G_Y^X(z)_4\Big) + (q-p-1)G_Y^X(z)_0 \\
&\vdots \\
(q-2)G_Y^{(p)}(z)_{-K} &= (p-1)\Big(z - G_Y^X(z)_{K+1}\Big) + (q-p-1)G_Y^X(z)_{K-3}\,.
\end{aligned} \tag{3.38}$$

Note that, because the $G_Y^X(z)_K$s and $y_K \propto z$ all satisfy (3.24), so do the $G_Y^{(p)}(z)_{-K}$ and the only difference is the initial data. Therefore, all $G_Y^{(p)}(z)_{-K}$ can be expressed as linear combinations of $\{z, G_Y^X(z)_{-1,0,1}\}$; and the coefficients, $\rho_K^{(p)}$, $\delta_K^{(p)}$ and $\alpha_K^{(p)}$ of the discontinuous parts and of z, respectively, can be found.

Using these relationships, it is straightforward to find that

$$\rho_{2M}^{(p)} = \frac{(1-p)\sin M\theta + \sin(M+1)\theta}{\sin\theta} = -\rho_{2M+1}^{(p)}, \tag{3.39}$$

$$\delta_{2M+1}^{(p)} = -\frac{(1-p)\sin(M+\frac{1}{2})\theta + \sin(M+\frac{3}{2})\theta}{\sin\frac{1}{2}\theta} = -\delta_{2M+2}^{(p)}, \tag{3.40}$$

$$\rho_{-2M-1}^{(p)} = \frac{(1-p)\sin(M+1)\theta + \sin M\theta}{\sin\theta} = -\rho_{-2M-2}^{(p)}, \tag{3.41}$$

$$\delta_{-2M}^{(p)} = -\frac{(1-p)\sin(M+\frac{1}{2})\theta + \sin(M-\frac{1}{2})\theta}{\sin\frac{1}{2}\theta} = -\delta_{-2M-1}^{(p)}, \tag{3.42}$$

for $M = 0, 1, 2, \ldots$. For the coefficients of z we get

$$\begin{aligned}
\alpha_{2M+1}^{(p)} &= \frac{-(p-2)\cos\frac{1}{2}\theta + (p-1)\cos(M+\frac{1}{2})\theta - \cos(M+\frac{3}{2})\theta}{2\sin\frac{1}{2}\theta\sin\theta}, \\
\alpha_{2M+1}^{(p)} &= \alpha_{2M+2}^{(p)}, \\
\alpha_{-2M}^{(p)} &= \alpha_{-2M-1}^{(p)}.
\end{aligned} \tag{3.43}$$

with $M = 0, \pm1, \pm2\cdots$.

For general p the sheet structure can terminate: on an even positive label sheet in which case $\rho_{2M}^{(p)} = 0$; on an odd positive label sheet in which case $\delta_{2M+1}^{(p)} = 0$; on an odd negative label sheet in which case $\rho_{-2M-1}^{(p)} = 0$; and on an even negative label sheet in which case $\delta_{-2M}^{(p)} = 0$. Clearly, to be finite sheeted it must terminate

on both a positive and a negative label sheet. The ρ's and δ's have some general properties which help in classifying everything:

(i) The absolute values of $\rho^{(p)}_{2M}$ etc. have period m in M. Therefore, we need only consider $0 \leq M < m$ in determining whether $G^{(p)}_Y(z)$ is finite sheeted.

(ii) Note that if $\rho^{(p)}_{2M} = 0$ then

$$\begin{aligned} \rho^{(p)}_{-2(m-M-1)-1} &= \frac{(1-p)\sin(m-M)\theta + \sin(m-M-1)\theta}{\sin\theta}, \\ &= \frac{(1-p)\sin(n\pi - M\theta) + \sin(n\pi - (M+1)\theta)}{\sin\theta}, \\ &= (-1)^{n+1}\rho^{(p)}_{2M} = 0\,. \end{aligned} \tag{3.44}$$

Similarly, if $\delta^{(p)}_{2M+1} = 0$ then $\delta^{(p)}_{-2(m-M-1)} = 0$. It follows that, if the structure terminates at a positive label sheet, it will also terminate at a negative label sheet (though these results do not necessarily identify the lowest label sheet on which the structure actually terminates).

(iii) In Case 2 observe that

$$\begin{aligned} \rho^{(p)}_{2(M+1)} &= (-1)^{n/2}\frac{(1-p)\sin((M+1)\frac{n\pi}{m} - \frac{n\pi}{2}) + \sin((M+2)\frac{n\pi}{m} - \frac{n\pi}{2})}{\sin\theta}, \\ &= (-1)^{n/2}\frac{(1-p)\sin((M+1-\frac{m}{2})\frac{n\pi}{m}) + \sin((M+2-\frac{m}{2})\frac{n\pi}{m})}{\sin\theta}, \\ &= (-1)^{n/2}\frac{(1-p)\sin((M-\frac{m-1}{2}+\frac{1}{2})\frac{n\pi}{m}) + \sin((M-\frac{m-1}{2}+\frac{3}{2})\frac{n\pi}{m})}{\sin\theta}. \end{aligned} \tag{3.45}$$

But m is odd, so $k = \frac{m-1}{2}$ is an integer, and we find

$$\rho^{(p)}_{2(M+1)} = (-1)^{n/2}\delta^{(p)}_{2(M-k)+1}, \tag{3.46}$$

and similarly, that

$$\rho^{(p)}_{-2M-1} = (-1)^{n/2}\delta^{(p)}_{-2(k-M)}. \tag{3.47}$$

It follows that termination on even or odd sheets generates the same set of p values for which $G^{(p)}_Y(z)$ is finite sheeted; whether it actually terminates on an even or an odd sheet is determined by which one has lower label.

3.4.1 Case 1: $\theta = \nu\pi = \frac{n\pi}{m}$, $n < m$ are mutually prime, $n = 1, 3, \ldots$ is odd, m may be even or odd

By properties (ii) it follows that all p values for which $G_Y^{(p)}(z)$ is finite sheeted are given by $\rho_{2M}^{(p)} = 0$, $M > 0$, or by $\delta_{2M+1}^{(p)} = 0$, $M \geq 0$, giving two sequences:

$$S_1 : p = 1 + \frac{\sin(M+1)\theta}{\sin M\theta}, \qquad M = 1, \ldots m-1, \tag{3.48}$$

$$S_2 : p = 1 + \frac{\sin(M+\frac{3}{2})\theta}{\sin(M+\frac{1}{2})\theta}, \qquad M = 0, \ldots m-1, \tag{3.49}$$

where S_1, for $M = 1, \ldots m-1$, terminates on sheet $2M$, i.e. $2, 4, \ldots, 2(m-1)$ and S_2, for $M = 0, \ldots m-1$, terminates on sheet $2M+1$, i.e. $1, 3, \ldots, 2m-1$.

Note that S_1 and S_2 are distinct, so we can find the negative label on which they terminate by inserting the values of p from (3.48) and (3.49) respectively into the expressions $\rho_{-2M'-1}^{(p)}$ (3.41) and $\delta_{-2M'}^{(p)}$ (3.42) and solving for M'. This gives:

- S_1: $M = 1, \ldots m-1$ terminates on sheet $-2(m-M)+1$,
- S_2: $M = 0, \ldots m-1$ terminates on sheet $-2(m-M-1)$.

Note that for every allowed p there are exactly $2m$ sheets, the same as for $p = 1$, which is always case $M = m-1$ in S_1.

Now we can show that $S_1 \neq S_2$ are distinct. If they were not, then we would have for some M, M'

$$\sin(M+\frac{3}{2})\theta \, \sin M'\theta = \sin(M+\frac{1}{2})\theta \, \sin(M'+1)\theta, \tag{3.50}$$

$$\Rightarrow (2(M-M')+1)\frac{n\pi}{m} = 2\ell\pi, \tag{3.51}$$

which is a contradiction because n is odd.

3.4.2 Case 2: $\theta = \nu\pi = \frac{n\pi}{m}$, $n < m$ are mutually prime and $n = 2, 4, \ldots, m-1$ is even

By properties (ii) and (iii) it follows that all p values for which $G_Y^{(p)}(z)$ is finite sheeted are given by $\rho_{2M}^{(p)} = 0$, $M > 0$, so in this case there is only one sequence given by

$$p = 1 + \frac{\sin(M+1)\theta}{\sin M\theta}, \qquad M = 1, \ldots m-1. \tag{3.52}$$

Note that the special case $p = 1$ is $M = m - 1$.

By property (iii) we see, for $M = \frac{m+1}{2}, \ldots, m-1$, that $\delta^{(p)}$ is zero for a lower labelled sheet than $\rho^{(p)}$, so for positive labels:

- $M = 1 \ldots \frac{m-1}{2}$ terminates on sheet $2M$,
- $M = \frac{m+1}{2} \ldots m - 1$ terminates on sheet $2M - m$.

Using property (i) we see that for negative labels:

- $M = 1 \ldots \frac{m-1}{2}$ terminates on sheet $-m + 2M + 1$,
- $M = \frac{m+1}{2} \ldots m - 1$ terminates on sheet $-2(m - M) + 1$.

Note that for every allowed p there are exactly m sheets, the same as for $p = 1$.

□

Proposition 3.4.3. *The degree of the discriminant of the G-functions, for all values of (p, q), is given by*

$$\deg \Delta(z) = 2m(2m-1) - m, \tag{3.53}$$

in Case 1, and

$$\deg \Delta(z) = m(m-1) - \frac{1}{2}(m-1), \tag{3.54}$$

in Case 2.

Proof. We can examine the α_K (3.43), the coefficient of z in the recurrence relation for the G-functions, and determine the degree of the discriminant. We note the following properties:

(i) First note that $\alpha_{-1} = \alpha_0 = 0$ and that in general $\alpha_{2M+1} = \alpha_{2M+2}$ so that $G_Y^X(z)_{2M+2} - G_Y^X(z)_{2M+1} \propto \sqrt{z} +$ lower order terms.

(ii) Now we prove that there are no other cases where $\alpha_K = \alpha_{K'}$ in the finite sheet structure. For $\alpha_{2M+1} = \alpha_{2M'+1}$ we require

$$\cos(M + \frac{3}{2})\theta = \cos(M' + \frac{3}{2})\theta, \tag{3.55}$$

with $M, M' = -1, \ldots, m-2$, in Case 1, or $M, M' = -1, \ldots, \frac{1}{2}(m-3)$, in Case 2. The first possibility is that $M = M' + m$, if n is even, or $M = M' + 2m$, if n is odd; but then M falls outside the allowed range. The second possibility is that

$$(M + \frac{3}{2})\theta = 2N\pi - (M' + \frac{3}{2})\theta, \qquad N = 1, 2, \ldots, \tag{3.56}$$

so that

$$(M + M' + 3)\frac{n}{m} = 2N. \tag{3.57}$$

In Case 2 this is satisfied if $M + M' + 3 = m$, which can only be true if $M = M' = \frac{1}{2}(m-3)$, which proves the result. In Case 1 this is satisfied if $M + M' + 3 = 2m$, which can only be true if one of M or M' is $m-1$, which is out of range, and thus proves the result.

Now we can compute the leading power of z in the discriminant. In Case 1

$$\Delta(z) = \prod_{K<K'} \left(G_Y^X(z)_K - G_Y^X(z)_{K'}\right)^2, \tag{3.58}$$

$$= \prod_{M=-1}^{m-2} \left(G_Y^X(z)_{2M+2} - G_Y^X(z)_{2M+1}\right)^2 \prod_{K'-K>1} \left(G_Y^X(z)_K - G_Y^X(z)_{K'}\right)^2. \tag{3.59}$$

So for $2m$ sheets we have m terms in the product giving a factor z, and $2m(2m-1)/2 - m$ terms giving a factor z^2. Therefore

$$\deg\Delta(z) = 2m(2m-1) - m. \tag{3.60}$$

In Case 2

$$\Delta(z) = \prod_{K<K'} \left(G_Y^X(z)_K - G_Y^X(z)_{K'}\right)^2, \tag{3.61}$$

$$= \prod_{M=-1}^{\frac{1}{2}(m-5)} \left(G_Y^X(z)_{2M+2} - G_Y^X(z)_{2M+1}\right)^2 \prod_{K'-K>1} \left(G_Y^X(z)_K - G_Y^X(z)_{K'}\right)^2. \tag{3.62}$$

This time there are m sheets and we have $\frac{1}{2}(m-1)$ terms in the product giving a factor z, and $m(m-1)/2 - \frac{1}{2}(m-1)$ terms giving a factor z^2. Therefore

$$\deg\Delta(z) = m(m-1) - \frac{1}{2}(m-1). \tag{3.63}$$

Next, we can examine the $\alpha_K^{(p)}$ and show that the degree of the discriminant is the same as it is for $p = 1$ for all values of p for which $G_Y^{(p)}(z)$ is finite sheeted.

(i) First note that $\alpha_{-1}^{(p)} = \alpha_0^{(p)} = 0$ and that $\alpha_L^{(p)} \neq 0$ if $L \neq 0, -1$, as is easily shown from (3.43), and that in general $\alpha_{2M+1}^{(p)} = \alpha_{2M+2}^{(p)}$, so that $G_Y^{(p)}(z)_{2M+2} - G_Y^{(p)}(z)_{2M+1} \propto \sqrt{z} +$ lower order terms.

(ii) It is straightforward to prove that there are no other cases where $\alpha_L^{(p)} = \alpha_{L'}^{(p)}$ in the finite sheet structure. Setting $\alpha_{2K+1}^{(p)} = \alpha_{2K'+1}^{(p)}$ and using (3.43) gives

$$p - 1 = \frac{\sin(\frac{1}{2}(K + K' + 3)\theta)}{\sin(\frac{1}{2}(K + K' + 1)\theta)}. \tag{3.64}$$

Using (3.48),(3.49), or (3.52), as appropriate, and considering each in turn, it can be shown there are no $K \neq K'$ and both in the physical range.

(iii) For a given q the number of sheets for $G_Y^{(p)}(z)$ is the same as for $G_Y^X(z)$ if p is an allowed value as shown for Case 1 and Case 2. It follows from this, and (i) and (ii) immediately above, that the degree of the discriminant is the same as well.

□

Lastly, we outline what happens in the $q \geqslant 4$ cases. Now the sheet structure does not terminate, and so a solution cannot be written in terms of algebraic functions. Nevertheless a solution can be obtained for the $q = 4, p = 1$ function by explicitly solving a double Riemann-Hilbert problem in terms of elliptic functions [58]; one then finds that the value of p is unconstrained. In the case of $q > 4$ we find an ever increasing weighting for C_F and C_∞, which rules out any possibility of algebraic solutions.

3.5 Properties of the General Solution

3.5.1 Allowed values of p

By construction, the general (q, p) solution allows a $p = 1$ boundary resolvent function. However, our results show that other integer values of p for a given allowed value of q are not necessarily allowed, even when $p < q$. We observe the following:

(i) $p = 2$ is not allowed if $\theta = \nu\pi = \frac{n\pi}{m}$, with n even, $n < m$ mutually prime (Case 2). From (3.32) this would imply

$$1 = \frac{\sin(M+1)\theta}{\sin M\theta} \Rightarrow \theta = \frac{2\ell+1}{2M+1}\frac{\pi}{2}, \tag{3.65}$$

which is a contradiction.

(ii) $p = 2$ is allowed if $\theta = \nu\pi = \frac{n\pi}{m}$, with n odd, $n < m$ mutually prime (Case 1). It appears in the series when C_F vanishes (3.30) if m is odd, in which case $M = \frac{m-1}{2}$, and it appears in the series for C_∞ (3.31) if m is even, in which case $M = \frac{m}{2} - 1$.

(iii) $p = 3$ is allowed only if $q = 3$. We do not have a simple analytic proof of this, but we have checked every case of $\theta = \frac{n\pi}{m}$ up to $m = 170$.

There are two further values of p which appear generically but are not in general integers:

(i) $p = q$ is always allowed. For Case 1, set $M = 0$ in the C_∞ series. For Case 2, set $M = \frac{m+1}{2}$ in the C_F series.

(ii) $p = q/2$ occurs for Case 1: if m is even set $M = \frac{m}{2}$ in the C_F series; if m is odd set $M = \frac{m-1}{2}$ in the C_∞ series. It is not allowed for Case 2 as is easily proved by contradiction.

3.5.2 Critical exponents

When we we have finite sheeted functions, the critical exponents can be computed directly from the discriminant,

$$\Delta(z) \coloneqq \prod_{i<j} \left(G_Y^X(z)_i - G_Y^X(z)_j\right)^2. \tag{3.66}$$

We use the following lemma, adapted from [66].

Lemma 3.5.1. *Let z_0 be a branch point of order p over z_0, then the sum of orders of all branch points over some z equals the multiplicity of z_0 as a root of the discriminant. Thus, the sum of orders of all branch points in the finite part of the Riemann surface equals the degree of the polynomial $\Delta(z)$.*

Proof. According to the theorem on symmetric functions, the discriminant is a polynomial in z. Given a branch point of order p over z_0, then $G_Y^X(z)$ on $p+1$ sheets will have the form

$$G_Y^X(z)_i = a_0 + b(z-z_0)^{1/(p+1)} + \cdots, \tag{3.67}$$

where the different branches of the $(p+1)^{\text{th}}$ root correspond to different i. There can also be other branch points over z_0. For all of them a_0 will be different. The contribution of the branch point to the discriminant is $(z-z_0)^{\frac{2}{p+1}\frac{(p+1)p}{2}} = (z-z_0)^p$. □

As we approach the critical point, the branch point of C_∞ merges with the right-most branch point of C_F, which we denote z_0. By hypothesis, at criticality we have one central branch point, about which the function behaves as $(z-z_0)^{r/s}$ for $r, s \in \mathbb{Z}$. The contribution of this branch point to the discriminant is then $(z-z_0)^{\frac{2r}{s}\sum_{i<j}} = (z-z_0)^{\frac{r}{s}n(n-1)}$, where n is the number of sheets this branch point connects, which we assume to be the total number of sheets of $G_Y^X(z)$. Meanwhile we have contributions from the left-most branch point of C_F, about which we obtain square-root behaviour. For a given n there will be $(n-2)/2$ of these for Case 1, and $(n-1)/2$ for Case 2. By Lemma 3.5.1, in Case 1 the degree of the discriminant will be given by

$$\deg \Delta(z) = \binom{2m-2}{2} + \frac{r}{s}2m(2m-1), \tag{3.68}$$

while for Case 2, the degree of the discriminant will be given by

$$\deg \Delta(z) = \binom{m-1}{2} + \frac{r}{s}m(m-1), \tag{3.69}$$

where m is defined as in Proposition 3.4.2.

From (3.53) and (3.54) in the preceding section we have the degree of the discriminant, and this should not change as we vary the couplings of the model. Comparing both, we find that the critical exponent in Case 1 is given by

$$\frac{r}{s} = \frac{2m-1}{2m}, \tag{3.70}$$

and in Case 2 it is given by

$$\frac{r}{s} = \frac{m-1}{m}, \tag{3.71}$$

which depends only on the number of sheets of the function. The string exponent is defined in terms of the resolvent as

$$W_{(p)}(z - z_c) \sim (z - z_c)^{1-\gamma_s}. \tag{3.72}$$

Due to (3.10) the singular behaviour of $G^Y_{(p)}(z)$ about C_F is the same as the behaviour of $W_{(p)}(z)$, and so we can relate our result for the former into a statement about the latter. Therefore we recover the known results $\gamma_s = -\frac{1}{2}, -\frac{1}{3}, -\frac{1}{5}$ for $q = 1, 2, 3$, in agreement with the values found in [59].

It should, however, be noted that the string exponent appearing in (3.72) is only certain to agree with the susceptibility defined by the KPZ/DDK relation (2.118) if the conformal field theory coupled to gravity is unitary. In the KPZ/DDK relation the cosmological constant is taken as the coupling to the dressed identity operator, whereas in the matrix model the scaling variable couples to the dressed lowest dimension operator, which is not necessarily the identity for non-unitary conformal field theories [15].

3.6 Discussion

We have classified all algebraic solutions for the one-loop function of the q-state Potts model coupled to random planar graphs with p allowed spins on the boundary. We found that there is a discrete series of allowed values of q that admit a $p = 1$ boundary condition, in agreement with the calculation of [59] using loop equations, and the results of [67, 68] using separate methods. For each of these we then determined the discrete series of allowed values of p, and we computed the discriminant of the general solution, using it to analyse the critical behaviour of the theory, and finding agreement with [59]. In the case of $q = 3$ this results in another boundary condition for $p = 3/2$, in addition to the usual $p = 1, 2$, and 3 solutions. We conjecture that this extra boundary condition may play the role of the New boundary condition

that appears in the fixed lattice spin system, but we have not established such a firm connection. Attempting to justify this statement motivates the following chapter, where we study Kramers-Wannier duality on the random lattice.

There are a number of avenues of inquiry one may pursue regarding this work. It would be interesting to calculate cylinder functions on the random lattice to enable confirmation of our identification of boundary conditions, as in [69]. This would require extending our results to higher order in topology and pushing beyond the planar limit, as performed for the $O(n)$ model in [70], using the algebraic curves found here as the starting point of the topological recursion procedure [50].

We would also like to understand the $q/2$ condition itself for general q, and determine what it corresponds to physically, if anything. If it is not the New boundary condition, then there is no apparent analogue on the fixed lattice. Discrepancies between fixed lattice and random lattice results have been observed in the past for the $O(n)$ model; in the strong coupling regime, corresponding to $n > 2$ and central charge greater than one, new exotic critical points were discovered [71, 72] which were not known to exist on the flat lattice. The q-state Potts model appears to be related to the $O(n)$ model [59, 73] and so one might expect similar features to be present in the former. We have found no new critical behaviour for $q < 4$ in the (q, p) parameter space of the q-state Potts model on random planar graphs, but we have not excluded an analogue of the new critical behaviour of the $O(n)$ model in the corresponding $q > 4$ strong coupling regime.

Chapter 4

Kramers-Wannier Duality on a Random Lattice

In the previous chapter we found that for the particular case of the 3-state Potts model, there are four allowed values for the boundary counting parameter, $p = 1, 3/2, 2, 3$. The integer values of p have a straightforward interpretation as resolvent functions for which one, two, or three spin values are allowed at the boundary. However the $p = 3/2$ case has no easy physical interpretation that is local in terms of the microscopic theory.

As discussed in Chapter 2, the critical point of the 3-state Potts model on a fixed lattice is described by a $(6, 5)$ D-series conformal field theory (CFT). Affleck et al. [21] showed that there are eight physical boundary states in this case that are invariant under boundary-preserving conformal transformations. Seven states are accounted for by boundary conditions with a) fixed spins (three states), b) mixed spins (three states), c) free spins (one state). The eighth state is called the New boundary condition. The corresponding microscopic lattice picture involves negative Boltzmann weights in the statistical spin model and lacks a simple intuitive physical interpretation. We outline this result in Appendix C.

It is tempting to conjecture that the $p = 3/2$ state is, in the scaling limit, the random lattice analogue of the New boundary condition. To confirm this, or otherwise, would require the extension of our methods to compute cylinder amplitudes. In this chapter we will take an alternative approach and explicitly construct the one-loop function for the New boundary condition on the random

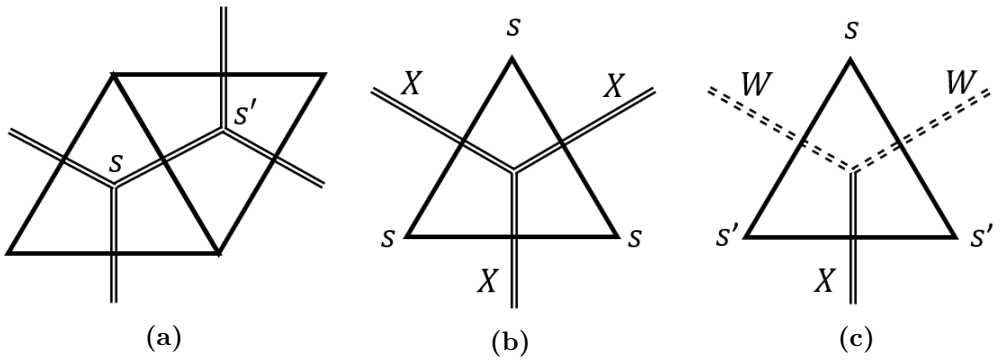

Figure 4.1: a) $\mathcal{M}_2$: spins s, s' living on the faces of T; b) $\hat{\mathcal{M}}_2$: the vertex in $\hat{T}$ when all spins on the vertices of a triangle in T take the same value; c) $\hat{\mathcal{M}}_2$: the vertex in $\hat{T}$ for $q = 2$ when all spins on the vertices of a triangle in T do not take the same value.

lattice, using the relationship between boundary conditions in the original model, and boundary conditions in the Kramers-Wannier dual theory.

This chapter is organised as follows. We first revisit the Ising model and discuss how one may construct the Kramers-Wannier dual on a random lattice in Section 4.1. Following this, we study the 3-state Potts model in Section 4.2. We construct the Kramers-Wannier dual to the 3-state Potts matrix model, and construct the one-loop functions corresponding to boundary conditions of the 3-state Potts model in the dual theory. Using the relationship between boundary conditions in the original model and the dual theory we study the New boundary condition, using the mixed boundary condition of the dual theory, and discuss our findings in Section 4.3. The results of this chapter have been reported in [62].

4.1 Ising Model

Kramers-Wannier duality, originally described for the Ising model on flat lattices, provides a relationship between the high-temperature and low-temperature expansions of the partition function on a lattice and its dual respectively, see [74] for a review. On random lattices Kramers-Wannier duality was first studied in [6, 75]. The situation is quite different from the flat lattice because the coordination numbers of the two lattices are radically different; one is finite (three in the case of the models considered in this thesis), while the other is unconstrained.

In the graphs we have considered, the spins are located at the face of each triangle in T, see Fig. 4.1a. We associate weights 1 to an edge in the dual graph, $\hat{T}$, connecting identical spins, and $e^{-2\beta}$ to an edge connecting different spins. Starting with the Ising model, $q = 2$, these weights are reproduced by the quadratic term in the matrix model action

$$\mathcal{S}_2 = \mathrm{Tr}\left(\frac{1}{2}\frac{1}{1-e^{-4\beta}}(X_1^2 + X_2^2 - 2e^{-2\beta}X_1X_2) - \frac{g}{3}(X_1^3 + X_2^3)\right), \qquad (4.1)$$

while the cubic term generates the vertices of $\hat{T}$; we refer to this model as $\mathcal{M}_2$. By redefining the couplings and scaling the matrices, we recover the form given in (3.1) for $q = 2$.

In the dual theory, $\hat{\mathcal{M}}_2$, the Ising spins are located on the vertices of the triangles, rather than the faces. These combinatorics can be described by a new matrix model defined as follows:

(i) An edge connecting two vertices with the same spin carries weight 1, and is represented by a matrix X in the dual lattice, see Fig.4.1b.

(ii) An edge connecting two vertices with opposite spins carries weight $e^{-2\hat{\beta}}$, and is represented by a matrix W in the dual lattice, see Fig.4.1c.

(iii) There are two types of cubic vertex on the dual lattice corresponding to the cases when the three spins on the surrounding triangle are equal or not, see Figs.4.1b & 1c.

This leads to the action

$$\hat{\mathcal{S}}_2 = \mathrm{Tr}\left(\frac{1}{2}X^2 + \frac{e^{2\hat{\beta}}}{2}W^2 - \frac{\hat{g}}{3}(X^3 + 3XW^2)\right). \qquad (4.2)$$

Boundary configurations for the two models are different as shown in Fig 4.2. In $\hat{\mathcal{M}}_2$ a boundary condition is given by the spin values on the vertices of triangles lying on the boundary of T; whereas in $\mathcal{M}_2$ the spins are specified on the vertex of order one on the edge in $\hat{T}$ that is dual to the boundary edge of T.

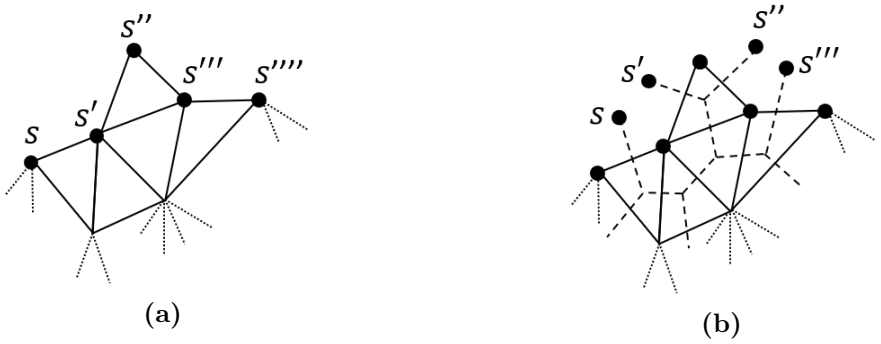

Figure 4.2: Boundary spin configurations in a) $\hat{\mathcal{M}}_2$ and b) $\mathcal{M}_2$.

$\mathcal{S}_2$ and $\hat{\mathcal{S}}_2$ are related by the change of variables [6]

$$X \to \frac{\lambda}{\sqrt{2}}(X_1 + X_2), \quad W \to \frac{\lambda}{\sqrt{2}}(X_1 - X_2), \quad \hat{g} \to \frac{\lambda^{-3}}{\sqrt{2}}g, \tag{4.3}$$

where

$$\lambda = (1 + e^{-2\beta}), \text{ and } \tanh\hat{\beta} = e^{-2\beta}. \tag{4.4}$$

Note that the relationship between β and $\hat{\beta}$ is the same as for a fixed lattice. The partition functions of $\mathcal{M}_2$ and $\hat{\mathcal{M}}_2$ are therefore equivalent but the relationship is more subtle for graphs with boundaries.

The resolvent for the free boundary condition in $\mathcal{M}_2$, $W_{(2)}(z)$, can be calculated in the dual picture by computing the resolvent $W_X(z)$, which describes the *fixed* boundary condition in $\hat{\mathcal{M}}_2$, with the action $\hat{S}$. The two resolvents have the same scaling properties as each other and as the fixed spin resolvent $W_{(1)}(z)$ [6]. Similarly the resolvent $W_W(z)$, describing a boundary with alternating spins in $\hat{\mathcal{M}}_2$, is equivalent in $\mathcal{M}_2$ to $W_{X_1-X_2}(z)$ which describes a system with an applied imaginary boundary magnetic field weighting the boundary spins by $e^{i\frac{\pi s}{2}}$. Note that this resolvent allows only boundaries of length 0 mod 2, and has a different scaling exponent from $W_{(1)}(z)$; in fact the resolvent $W_{Z_\alpha}(z)$ where

$$Z_\alpha = (1-\alpha)X_1 - (1+\alpha)X_2 = W - \alpha X \tag{4.5}$$

can be computed explicitly [69, 76] and for $\alpha \neq 0$ has the same scaling exponent as $W_{(1)}(z)$, so we conclude that the boundary condition described by W is unstable in the infra-red. This is also the case for the fixed lattice Ising model, and consistent

with the fact that the fixed and free boundary conditions appear as Cardy states in the $c = \frac{1}{2}$ boundary CFT, but the alternating spin boundary condition does not [18].

4.2 3-state Potts Model

We can easily extend these ideas to the Potts model. The matrix model, $\mathcal{M}_3$, for spins defined on the faces of the triangulations has action

$$\mathcal{S}_3 = \mathrm{Tr}\left(\frac{\mu(c)}{2}(\sum_{i=1}^{3} M_i^2 - 2cM_1M_2 - 2cM_1M_3 - 2cM_2M_3) - \frac{g}{3}(\sum_{i=1}^{3} M_i^3)\right), \quad (4.6)$$

where

$$\mu(c) = \frac{(1-c)}{(1+c)(1-2c)} \text{ and } c = \frac{1}{e^{\beta}+1}. \quad (4.7)$$

The Boltzmann weights are then

$$e^{\beta(\delta_{\sigma_k,\sigma_l}-1)} = \begin{cases} 1 & \text{if } \sigma_k = \sigma_l \\ \frac{c}{1-c} & \text{if } \sigma_k \neq \sigma_l \end{cases} \quad (4.8)$$

as on the flat lattice.

To construct the dual matrix model, we map the spins on the faces of the triangulation T to phase factors $s \in \{1, \omega, \omega^2\}$ on the vertices of T, where $\omega = e^{i\frac{2\pi}{3}}$. To connect adjacent spins, we use the following matrices: U, which increases the phase by $\frac{2\pi}{3}$, $U^\dagger$ which increases the phase by $\frac{4\pi}{3}$, and X which preserves the phase. The X matrix has Boltzmann weight 1, since it connects identical spins, whereas U and $U^\dagger$ have Boltzmann weight $e^{-\hat{\beta}}$, as they connect differing spins. Since the change in phase is dependent on the direction in which we go along the edge, the quadratic part of the action, that measures the contribution from neighbouring vertices with different spins, must be proportional to $UU^\dagger$. The cubic vertices can be derived by generalising Figs.4.1b & 1c to $q = 3$. These considerations lead to the following action for the dual model $\hat{\mathcal{M}}_3$

$$\hat{\mathcal{S}}_3 = \frac{1}{2}\mathrm{Tr}(X^2 + 2e^{\hat{\beta}}UU^\dagger) - \hat{g}X(UU^\dagger + U^\dagger U) - \frac{\hat{g}}{3}(U^3 + U^{\dagger 3} + X^3). \quad (4.9)$$

As in the Ising model, $\mathcal{M}_3$ and $\hat{\mathcal{M}}_3$ are related through a linear transformation of the matrix variables:

$$\begin{aligned} X =& \frac{\lambda}{\sqrt{3}}(M_1 + M_2 + M_3), \quad U = \frac{\lambda}{\sqrt{3}}(M_1 + \omega M_2 + \omega^2 M_3), \\ U^\dagger =& \frac{\lambda}{\sqrt{3}}(M_1 + \omega^2 M_2 + \omega M_3), \quad \hat{g} = \frac{\lambda^{-3}}{\sqrt{3}} g, \quad \lambda = \sqrt{\frac{1-c}{1+c}}, \end{aligned} \tag{4.10}$$

with

$$e^{\hat{\beta}} = 1 + \frac{3}{e^\beta - 1}, \tag{4.11}$$

the same relationship between temperature and dual temperature as for the flat lattice. Note that both $\mathcal{S}_3$ and $\hat{\mathcal{S}}_3$ inherit the permutation symmetry of the original Potts model through permutations of $\{X_1, X_2, X_3\}$, and the exchange of U and $U^\dagger$ respectively.

The loop functions we are interested in do not all have the same straightforward form in the dual model. For the fixed spin boundary in $\hat{\mathcal{M}}_3$, all spins on the boundary vertices are the same, see Fig.4.3a, which corresponds to the resolvent $W_X(z)$; this is equivalent by (4.10) to the free boundary condition in $\mathcal{M}_3$. The free spin boundary condition in $\hat{\mathcal{M}}_3$ has graphs of the form Fig.4.3c which correspond to the resolvent $W_{X+U+U^\dagger}(z)$; this is equivalent by (4.10) to the fixed boundary condition in $\mathcal{M}_3$. The mixed boundary condition in $\hat{\mathcal{M}}_3$, Fig.4.3b, is expected to be dual to the New boundary condition in $\mathcal{M}_3$. The generating function for these graphs is slightly harder to construct. To ensure that, for example, only 1 and ω appear on the boundary, U can only be followed by X or $U^\dagger$ and not another U, and there must be an equal number of U and $U^\dagger$ for periodicity. The loop function that accounts for all these features is

$$W_{\text{mixed}}(z) = \frac{1}{N} \left\langle \text{Tr} \frac{1}{(z - (X + U \frac{1}{z-X} U^\dagger)} \right\rangle. \tag{4.12}$$

Using the matrix model technology available at the present moment we do not know how to compute this function. However, we can justify that this is the correct expression.

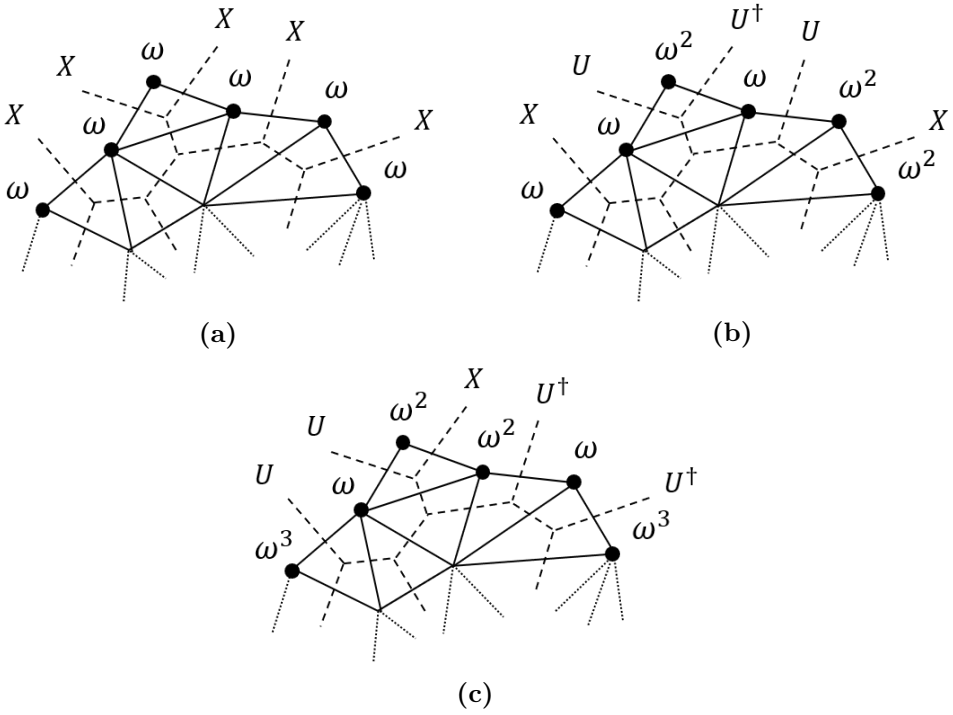

Figure 4.3: Examples of diagrams corresponding to various boundary conditions in $\hat{\mathcal{M}}_3$; a) Fixed spin, b) Mixed spin, c) Free spin.

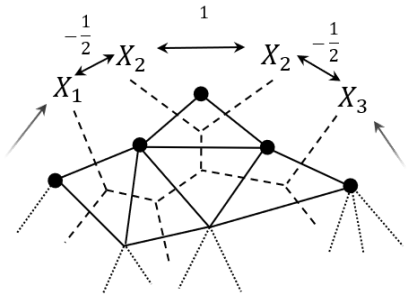

Figure 4.4: Example diagram in $\mathcal{M}_3$ corresponding to $\langle \mathrm{Tr} \cdots X_1 X_2 X_2 X_3 \cdots \rangle$ with associated boundary interactions represented by solid lines between the spins X_i.

In [21] it was argued that the New boundary condition corresponds to deleting the Boltzmann weights (4.8) for edges of the graph belonging to the boundary and instead assigning the weights[1]

$$w_{kl} = \begin{cases} 1 & \text{if } \sigma_k = \sigma_l, \\ -\frac{1}{2} & \text{if } \sigma_k \neq \sigma_l. \end{cases} \tag{4.13}$$

For example, as shown in Fig.4.4, neighbouring spins on the boundary of a given triangulation will contribute a factor of $-1/2$ when they differ and 1 when they

[1]See Appendix C, summarising the arguments that lead to this expression.

are the same. Therefore the amplitude will possess a weight of $(-1/2)^2$ due to the boundary interactions of this segment. This procedure is straightforward to implement in $\hat{\mathcal{M}}_3$, and gives the loop function

$$W_{\text{New}}(z) = \frac{1}{N}\left\langle \text{Tr}\frac{1}{z-(X-\frac{1}{2}U-\frac{1}{2}U^\dagger)}\right\rangle \tag{4.14}$$

which, by (4.10), is equivalent to the mixed boundary condition in $\mathcal{M}_3$.

Similarly, it is possible to use the S_3 symmetry to show that this implementation holds when we map (4.12) in $\hat{\mathcal{M}}_3$ to $\mathcal{M}_3$. To see this, we first note that the asymptotic expansion of (4.12) generates a restricted sum of length n words in the free algebra generated by $\{X, U, U^\dagger\}$. We then map these allowed words using (4.10) to a weighted sum of words in the free algebra generated by $\{M_1, M_2, M_3\}$. Permutation symmetry with respect to exchange of M_2, M_3 means that only the real part of the expectation value of these words contribute. This leads to the following proposition.

Proposition 4.2.1. *Under the mapping*

$$X = \sum_{\sigma\in\Delta} M_\sigma,\ U = \sum_{\sigma\in\Delta} \omega^{\sigma-1}M_\sigma,\ U^\dagger = \sum_{\sigma\in\Delta}\omega^{1-\sigma}M_\sigma, \tag{4.15}$$

the real part of the sum of allowed length n words in the free algebra generated by $\{X, U, U^\dagger\}$ *maps to the following sum of length n words in the free algebra generated by* $\{M_1, M_2, M_3\}$*,*

$$2^{n-1}\sum_{\sigma_1,\cdots,\sigma_n\in\Delta}\left(-\frac{1}{2}\right)^{\sum_{k=1}^n(1-\delta(\sigma_k,\sigma_{k+1}))} M_{\sigma_1}\cdots M_{\sigma_n},\quad \sigma_{n+1}=\sigma_1, \tag{4.16}$$

where $\Delta = \{1, 2, 3\}$*.*

Proof. Let W_n be the sum of allowed length n words in $\{V, U, U^\dagger\}$. Then for $n > 0$,

$$W_n = XW_{n-1} + \sum_{k=2}^{n} UX^{k-2}U^\dagger W_{n-k}, \tag{4.17}$$

where we take $W_0 = 1$. Under (4.15) we have

$$W_n = \sum_{\sigma_1,\cdots\sigma_n\in\Delta} C_n(\sigma_1,\cdots,\sigma_n)M_{\sigma_1}\cdots M_{\sigma_n}. \tag{4.18}$$

The recurrence relation on the words can then be expressed as a recurrence relation on the coefficients $C_n(\sigma_1, \cdots \sigma_n)$,

$$C_n(\sigma_1, \cdots, \sigma_n) = C_{n-1}(\sigma_2, \cdots \sigma_n) + \sum_{k=2}^{n} \omega^{\sigma_1 - \sigma_k} C_{n-k}(\sigma_{k+1}, \cdots, \sigma_n), \tag{4.19}$$

where $C_1(\sigma) = C_0 = 1$. We can now prove by induction that for $n > 1$ this recurrence relation is equivalent to[2]

$$C_n(\sigma_1, \cdots, \sigma_n) = (1 + \omega^{\sigma_1 - \sigma_2}) C_{n-1}(\sigma_2, \cdots, \sigma_n). \tag{4.20}$$

For $n = 2$ the recurrence relation gives

$$C_2(\sigma_1, \sigma_2) = C_1(\sigma_2) + \omega^{\sigma_1 - \sigma_2} C_0 \tag{4.21}$$

$$= (1 + \omega^{\sigma_1 - \sigma_2}) C_1(\sigma_2). \tag{4.22}$$

Now assume the result holds up to some $n = l$. Then we must show that (4.19) is equivalent to (4.20) for $n = l + 1$. By repeatedly applying this hypothesis we find

$$\omega^{\sigma_1 - \sigma_2} C_l(\sigma_2, \cdots, \sigma_{l+1}) = \omega^{\sigma_1 - \sigma_2} C_{l-1}(\sigma_3, \cdots, \sigma_{l+1}) + \omega^{\sigma_1 - \sigma_3} C_{l-1}(\sigma_3, \cdots, \sigma_{l+1}) \tag{4.23}$$

$$= \omega^{\sigma_1 - \sigma_2} C_{l-1}(\sigma_3, \cdots, \sigma_{l+1)} + \cdots + \omega^{\sigma_1 - \sigma_{k+1}} C_0 \tag{4.24}$$

$$= \sum_{k=2}^{l+1} \omega^{\sigma_1 - \sigma_k} C_{l+1-k}(\sigma_{k+1}, \cdots, \sigma_{l+1}). \tag{4.25}$$

Hence the proposition holds for $n = l + 1$. Thus, since it also holds for $n = 2$, it is true for all n. Using this result we can easily solve the recursion,

$$C_n(\sigma_1, \cdots, \sigma_n) = \prod_{k=1}^{n-1} (1 + \omega^{\sigma_k - \sigma_{k+1}}). \tag{4.26}$$

By taking the real part of this, we recover (4.16). □

Therefore we find that the mixed boundary condition in $\hat{\mathcal{M}}_3$ is equivalent to a boundary condition in $\mathcal{M}_3$ with the weights for spins on the boundary given by (4.13).

It is interesting to examine the boundary conditions generated by $W_U(z)$ and $W_{U^\dagger}(z)$; these are the $\mathbb{Z}_3$ analogues of the boundary condition generated by $W_W(z)$

[2]We would like to thank an anonymous contributor to Mathematics StackExchange for drawing attention to this feature.

in the Ising case. Evaluating the resolvent series expansion and using the underlying S_3 symmetry under exchange of the matrices shows that only boundaries of length $0 \mod 3$ appear, analogous to the appearance of boundaries of length $0 \mod 2$ in $W_W(z)$. Crucially, as we observed above, this boundary condition has a different scaling dimension and flows to the free boundary condition under Z_2 symmetric boundary perturbations [69]. We expect the same behaviour to hold for the $q = 3$ case; as soon as a perturbation ϵX is added the restriction on boundary length disappears and the boundary condition will flow to the free boundary condition in the infra-red.

4.3 Discussion

In this chapter we examined the Kramers-Wannier dual theory for $q = 3$, extending the work of [6] for $q = 2$, and showed that the relationship between boundary conditions in the original and dual theories on a fixed lattice [22] extends to the same statistical system on a random lattice. Within this framework we discovered that there is one boundary condition in the original theory and the dual that is not a simple resolvent, and we argued that this is the New boundary condition in the original theory, and the mixed boundary condition in the dual.

Regarding ways we could extend this work, foremost would be calculating resolvents in the dual theory explicitly. The matrix model is a mixed Hermitian-complex matrix model, with a particular structure that has not been studied in the literature. However, as the 3-state Potts matrix model is solvable, it is reasonable to expect that the dual theory is also a solvable matrix model, and, in particular, that its mixed boundary condition loop function (4.12) can be computed. Computing the dual loop functions would allow us to directly study their scaling behaviour, and enable clear comparison with the loop functions of the original model. This leads us to the topic of the next chapter, where we develop a combinatorial method for computing planar resolvents.

Chapter 5

Boundary Conditions in the 3-state Potts Model

Since the work of Eynard and Bonnet [59], it has been known that the planar resolvent, corresponding to the fixed spin boundary conditions of the 3-state Potts model on random planar graphs, may be computed through the method of loop equations. The work of Atkin, Niedner and Wheater [60], building on the saddle-point approach of Daul [57], and subsequently Zinn-Justin [58], demonstrated that the saddle-point method may be used to compute the planar eigenvalue density distribution for the sum of p random matrices in the q-state Potts model, and thus a wider variety of boundary conditions. As discussed in Chapter 2, the method of loop equations has a direct combinatorial interpretation, expressing the possible ways of decomposing random graphs after the removal of a marked edge. Whether one could recover the results of [60] in this language is the the question we seek to address in this chapter.

This chapter is organised as follows. In Section 5.1 we describe the formalism we use to discuss loop equations for general multi-matrix models, which we subsequently demonstrate for the particular case of the two-matrix model with a generic cubic potential. In Section 5.2 we then describe an algorithm for computing and systematically solving loop equations. We immediately apply this to the case of the 3-state Potts model in Section 5.3, where we illustrate the algorithm in detail for the $p = 1$ fixed spin resolvent. We then discuss the case of the $p = 2$ mixed and $p = 3$ free boundary conditions, and describe general features of the spectral curve.

Further to this, we discuss some non-standard boundary conditions, which includes a case where the loop equation method fails. Finally, in Section 5.4 we consider the case of the dilute Ising model, followed by the dilute 3-state Potts model in Section 5.5, before concluding with a discussion of some implications of our results.

5.1 Formalism

Consider a generic multi-matrix model in n Hermitian matrix degrees of freedom $\mathbf{X} = \{X_i\}_{i=1}^n$ of the form

$$Z = \int \prod_{i=1}^{n} [dX_i]\, e^{-N \mathrm{Tr} V(\mathbf{X})}, \tag{5.1}$$

where $V(\mathbf{X})$ is a potential function which is a polynomial of degree $d+1$ in the n matrices of $\mathbf{X}$, and depends on couplings $\{t_i\}_{i=2}^{\infty}$. We are interested in computing the planar resolvent of a given matrix, say $X := X_1$.

Define the following resolvent functions with boundary insertions

$$W_{w(\mathbf{X})}(z) = \frac{1}{N} \left\langle \mathrm{Tr} \frac{1}{2} \Big(w(\mathbf{X}) + \bar{w}(\mathbf{X}) \Big) \frac{1}{z - X} \right\rangle, \tag{5.2}$$

where $w(\mathbf{X})$ is a word in the free algebra generated by $\mathbf{X}$ and $\bar{w}(\mathbf{X})$ the reversed word, but with the constraint that X is not the first or last letter of the word. On the left hand side we will proceed to label the resolvent functions by the indices labelling the matrices that comprise the word $w(\mathbf{X})$ for the sake of brevity. Hence, one may write

$$W_{(2,1,3)}(z) = \frac{1}{N} \left\langle \mathrm{Tr} \frac{1}{2} (X_2 X_1 X_3 + X_3 X_1 X_2) \frac{1}{z - X} \right\rangle. \tag{5.3}$$

Furthermore, we define the following trace correlation functions analogously,

$$p_{w(\mathbf{X})} = \frac{1}{N} \left\langle \mathrm{Tr} \frac{1}{2} (w(\mathbf{X}) + \bar{w}(\mathbf{X})) \right\rangle. \tag{5.4}$$

Define the level of a resolvent function of the form (5.2) as the length of the associated word, $L(w(\mathbf{X}))$, such that, for example, (5.3) with $L(X_2 X_1 X_3) = 3$ denotes a level-3 resolvent function. Similarly, we index trace correlation functions of a given level by the set of words of appropriate length.

The number of inequivalent trace correlation functions of a given level is generally much smaller than the size of the corresponding set of words. Due to cyclicity of the trace and symmetry under reversal of the word (which has been arranged by construction in (5.4)), there is a D_k symmetry for the correlators, where D_k is the dihedral group of order k. There may also be a global symmetry, G, of the matrix model potential, given by

$$G = \{g \in \mathrm{Aut}(\mathbf{X}) : V(g(\mathbf{X})) = V(\mathbf{X})\}. \tag{5.5}$$

An example of this would be permutation symmetry amongst the matrix degrees of freedom. Therefore, defining the set of irreducible trace correlation functions of level k as $\mathcal{P}_k$, we may write

$$\mathcal{P}_k \cong \mathbf{X}^k/(D_k \times G). \tag{5.6}$$

The number of inequivalent correlators is then given by the cardinality of this set.

Similarly we define the set of irreducible resolvent functions of level k as $\mathcal{W}_k$. The number of independent resolvent functions is also constrained, although not as severely as the correlation functions are. Define the operator Δ, acting on resolvent functions as follows:

$$\Delta^k W_{w(\mathbf{X})}(z) := \frac{1}{N}\left\langle \mathrm{Tr}\frac{1}{2}\Big(X^k w(\mathbf{X}) + \bar{w}(\mathbf{X})X^k\Big)\frac{1}{z-X}\right\rangle \tag{5.7}$$

$$= z^k W_{w(\mathbf{X})}(z) - \sum_{i=1}^{k} z^{k-i} p_{X^{k-1}w(\mathbf{X})}. \tag{5.8}$$

We may omit words for which any sub-word consisting only of the matrix X adjoins the loop operator $(z-X)^{-1}$, since these may be expressed in terms of the Δ operator to a power given by the length of the adjoining sub-word in X, acting on a lower-level resolvent function. Moreover, the presence of the loop operator means that, relative to the correlation functions, the dihedral symmetry is reduced as $D_k \to \mathbb{Z}_2$, corresponding to symmetry under reversal of the words defining the resolvent functions. Finally, having fixed X as the representative matrix of the

loop operator, the defining word only respects the subgroup $G' \subseteq G$, consisting of elements $g \in \mathrm{Aut}(\tilde{\mathbf{X}})$, where $\tilde{\mathbf{X}} = \mathbf{X} \setminus X$. Therefore we may write

$$\mathcal{W}_k \cong (\tilde{\mathbf{X}} \times \mathbf{X}^{k-2} \times \tilde{\mathbf{X}})/(\mathbb{Z}_2 \times G'). \tag{5.9}$$

For example, consider a three-matrix model with matrix degrees of freedom X_1, X_2, X_3, with a $\mathbb{Z}_2$ symmetry under exchange of X_1 and X_2. Then for the resolvent functions with respect to X_1, one would find $W_{(3,2,1,2,3)} \neq W_{(3,1,2,1,3)}$, and therefore the representative words comprise two distinct elements of $\mathcal{W}_5$, whereas the same words are identified in $\mathcal{P}_5$ as one has $p_{3,2,1,2,3} = p_{3,1,2,1,3}$.

Loop equations are Schwinger-Dyson equations of the matrix model, expressing the invariance of the matrix integral under infinitesimal reparameterisations $X_i \to X_i + \varepsilon \delta X_i$. There is some freedom as to which variations one can consider. In Chapter 2 we outlined one approach, specific to the two-matrix model, where one studies reparameterisations using products of the resolvent operator (2.65). The approach we adopt here is to consider variations of the form

$$\delta X_i = w_1(\mathbf{X}) \frac{1}{z - X} w_2(\mathbf{X}) + \bar{w}_2(\mathbf{X}) \frac{1}{z - X} \bar{w}_1(\mathbf{X}). \tag{5.10}$$

One then evaluates the loop equation by equating the first order contribution from the Jacobian, which may be computed using the split rule (2.51), with the contribution from the potential (2.49). These reparameterisations are manifestly Hermitian, and the resulting constraints may be expressed in terms of the resolvent functions (5.2) and trace correlation functions (5.4).

We can classify loop equations by the level of their highest-level resolvent functions. If $V'(\mathbf{X})$ is degree d in $\tilde{\mathbf{X}}$[1], then level-k loop equations are given by (5.10) with $L(w_2) = k - d - L(w_1)$. We can therefore define a corresponding set of level k variations,

$$\mathcal{V}_k = \left\{ (w_1, w_2) \in \mathbf{V}_m \times \overline{\mathbf{V}}_{k-d-m} : m = k - d, \cdots \lceil (k-d)/2 \rceil \right\}, \tag{5.11}$$

[1]The degree will generally be different for variations corresponding to different $X_i \in \mathbf{X}$.

where $\mathbf{V}_m = \mathbf{X}^{m-1} \times \tilde{\mathbf{X}}$ and $\overline{\mathbf{V}}_m = \tilde{\mathbf{X}} \times \mathbf{X}^{m-1}$. That is, the words w_1 and w_2 are constrained such that the letters in contact with the loop operator are in $\tilde{\mathbf{X}}$. This is so that the resulting loop equations are distinct from lower-level loop equations.

The key idea of the loop equation approach we adopt is to compute the Schwinger-Dyson constraints for each matrix degree of freedom by a sufficiently large set of variations. We aim to compute loop equations up to a certain level $n_{\max}$, which denotes the level at which the number of algebraically independent constraints outnumber the total number of independent resolvent functions present in the constraints, and then eliminate the resolvent functions so that we obtain an algebraic equation for the planar (level-0) resolvent. This may be regarded as a discrete version of the approach outlined in Chapter 2, since one may expand the product of resolvent operators as an infinite sum of words in matrices of arbitrary length multiplying a single resolvent operator. It is hoped that this refined set of equations contains more information than if one only considers a finite set of reparameterisations by products of loop operators, allowing us to compute the planar resolvent.

5.1.1 The two-matrix model with generic cubic potential

To illustrate our formalism and demonstrate the strength of the loop equation approach, let us consider the simple example of a two-matrix model with a generic cubic potential:

$$\begin{aligned} V(M_1, M_2) =& \frac{1}{2(\alpha\beta - \gamma^2)}(\alpha M_1^2 + \beta M_2^2 - 2\gamma M_1 M_2) \\ &+ \frac{1}{3}(aM_1^3 + 3bM_1^2 M_2 + 3dM_1 M_2^2 + eM_2^3). \end{aligned} \tag{5.12}$$

This furnishes an example of a multi-matrix model which is not solvable through any known saddle-point or orthogonal polynomial approach. In particular, the loop equation method of Chapter 2 is not sufficient to compute the planar resolvent. However, as first demonstrated in [6], one may compute the resolvent of this model using our more granular loop equation strategy.

For (5.12) the following are the minimal set of reparameterisations:

$$\delta M_i = \frac{1}{z - M_1}, \tag{5.13}$$

$$\delta M_i = M_2 \frac{1}{z - M_1} + \text{h.c.}, \tag{5.14}$$

$$\delta M_i = M_2^2 \frac{1}{z - M_1} + \text{h.c.}, \tag{5.15}$$

$$\delta M_i = M_2 \frac{1}{z - M_1} M_2, \tag{5.16}$$

for $i \in \{1, 2\}$. Calculating the corresponding loop equations yields the following relations, where the action of the Δ operator is given by (5.7) for $k = 1$, i.e. $\Delta^1 = \Delta$, and we suppress the z-dependence of the resolvent functions[2]:

$$W^2 = -dW_{(2,2)} + \frac{\gamma W_2}{\gamma^2 - \alpha\beta} - a\Delta^2 W - 2b\Delta W_2 + \frac{\alpha \Delta W}{\alpha\beta - \gamma^2}, \tag{5.17}$$

$$0 = -eW_{(2,2)} + \frac{\beta W_2}{\alpha\beta - \gamma^2} - b\Delta^2 W - 2d\Delta W_2 + \frac{\gamma \Delta W}{\gamma^2 - \alpha\beta}, \tag{5.18}$$

$$WW_2 = \frac{\gamma W_{(2,2)}}{\gamma^2 - \alpha\beta} - a\Delta^2 W_2 - b\Delta W_{(2,2)} - bW_{(2,1,2)} - dW_{(2,2,2)} + \frac{\alpha \Delta W_2}{\alpha\beta - \gamma^2}, \tag{5.19}$$

$$W = \frac{\beta W_{(2,2)}}{\alpha\beta - \gamma^2} - b\Delta^2 W_2 - d\Delta W_{(2,2)} - dW_{(2,1,2)} - eW_{(2,2,2)} + \frac{\gamma \Delta W_2}{\gamma^2 - \alpha\beta}, \tag{5.20}$$

$$WW_{(2,2)} = \frac{\gamma W_{(2,2,2)}}{\gamma^2 - \alpha\beta} - a\Delta^2 W_{(2,2)} - b\Delta W_{(2,2,2)} - bW_{(2,1,2,2)} - dW_{(2,2,2,2)} + \frac{\alpha \Delta W_{(2,2}}{\alpha\beta - \gamma^2}, \tag{5.21}$$

$$Wp_2 + W_2 = \frac{\beta W_{(2,2,2)}}{\alpha\beta - \gamma^2} - b\Delta^2 W_{(2,2)} - d\Delta W_{(2,2)} - dW_{(2,1,2,2)} - eW_{(2,2,2,2)} + \frac{\gamma \Delta W_{(2,2)}}{\gamma^2 - \alpha\beta}, \tag{5.22}$$

$$W_2^2 = \frac{\alpha W_{(2,1,2)}}{\alpha\beta - \gamma^2} + \frac{\gamma W_{(2,2,2)}}{\gamma^2 - \alpha\beta} - aW_{(2,1,1,2)} - 2bW_{(2,1,2,2)} - dW_{(2,2,2,2)}, \tag{5.23}$$

$$2W_2 = \frac{\gamma W_{(2,1,2)}}{\gamma^2 - \alpha\beta} + \frac{\beta W_{(2,2,2)}}{\alpha\beta - \gamma^2} - bW_{(2,1,1,2)} - 2dW_{(2,1,2,2)} - eW_{(2,2,2,2)}. \tag{5.24}$$

These are eight independent equations in eight unknowns which may be eliminated to give a single algebraic equation for the resolvent $W(z)$. This spectral curve is degree 4 in both the resolvent and the boundary cosmological constant. We can, at most, tune the parameters of the model to achieve critical behaviour of the form $W(z) \sim (z - z_c)^{4/3}$, which is characteristic of the critical Ising model universality class.

[2]Note that W_2 is distinct from the resolvent $W_{(2)}$ (3.2), which denotes the resolvent of the sum of two matrices.

5.2 General Strategy

In practice, for complicated multi-matrix models, one needs to consider a large number of loop equations - on the order of hundreds for many of the highly symmetric three-matrix models we will consider. Each of these encode a combinatorial relation relating a random graph with prescribed boundary conditions to a different set of random graphs with various boundary conditions when a marked edge has been removed. Many of these are not independent, and so we need a systematic approach for eliminating the higher-order resolvent functions.

For all $v \in \mathcal{V}_n$ we obtain a corresponding loop equation, which we denote

$$\sum_{w \in \mathcal{W}_n} M^{(n)}_{v,w}\left(\{t_i\},\{p_i\}\right)\, W_w(z) + \mathcal{R}_v\Big[\bigcup_{n'<n} \mathcal{W}_{n'}\Big] = 0, \tag{5.25}$$

where $\mathcal{R}_v$ denotes the remaining terms in the loop equation containing resolvent functions with level $m < n$. The coefficient matrix $M^{(n)}_{v,w}$ will generically depend on resolvent functions of level $m \leqslant \lfloor n/2 \rfloor$, which has been suppressed in (5.25). Starting with (5.25) for level $n = n_{\max}$, one may identify a linearly independent set of constraints with respect to the level-n resolvent functions by using the Gaussian elimination algorithm on $(M^{(n)})^T$. Gaussian elimination reduces $(M^{(n)})^T$ to a matrix, $T^{(n)}$, in row echelon form. The rows of $(M^{(n)})_{ji}$ which form a linearly independent basis are then the rows for which $j \in \mathcal{I}_n$ where

$$\mathcal{I}_n = \bigcup_i \{\min j : T^{(n)}_{ij} = 0 \ \forall j\}. \tag{5.26}$$

One may then solve the linearly independent set of equations to express the level-n resolvent functions in terms of lower order resolvent functions. Using these expressions to remove the level-n resolvent functions from the remaining constraints, one obtains a set of constraints linear in resolvent functions of top-level $n_{\max} - 1$, which may include distinct loop equations from those computed using variations $v \in \mathcal{V}_{n-1}$. Together with (5.25) for $v \in \mathcal{V}_{n_{\max}-1}$ we obtain an augmented set of relations at level $n_{\max} - 1$.

We can then iterate this calculation, going from level $n_{\max} - 1$ to $n_{\max} - 2$, then $n_{\max} - 2$ to $n_{\max} - 3$, and so on. This procedure fails at a level, say m, where the

level-m resolvent functions enter non-linearly in the loop equations. The critical level at which this occurs is $n_{\text{crit.}} = \lfloor \frac{n}{2} \rfloor$, as there are variations for which the Jacobian contribution is quadratic in level-$n_{\text{crit.}}$ resolvent functions.

5.3 3-state Potts Model

We now return to the Potts model (3.1) for $q = 3$. The 3-state Potts model on random planar triangulations is given by the following matrix integral

$$Z = \int \prod_{i=1}^{3} [dX_i] e^{-N \text{Tr}\left(\sum_{i=1}^{3} \frac{(t_2-1)}{2} X_i^2 + \frac{t_3}{3} X_i^3 - X_1 X_2 - X_2 X_3 - X_3 X_1 \right)}, \tag{5.27}$$

which possesses a global S_3 symmetry. In this section we will demonstrate how one can use the algorithm described in the previous section to compute the fixed-spin one-loop function in detail, following which we we will discuss the mixed and free boundary conditions. We then consider resolvents with unclear physical interpretation, including an 'odd' boundary condition where the loop equations close, and the U boundary condition of Chapter 4, which fails to be solvable through this method. Details of the asymptotic expansion for the planar resolvents for the fixed, mixed, and free boundary conditions, calculated using this method may, be found in Appendix B.

5.3.1 Fixed boundary conditions

The problem of calculating the planar resolvent with fixed spin boundary conditions has been addressed multiple times in the literature. It was first successfully solved using loop equations by Eynard and Bonnet in [59]. They used reparameterisations involving products of resolvent operators, similar to the variations (2.65) considered for the two-matrix model of Chapter 2, and were able to solve the resulting loop equations for general values of q for which the resolvent is described by an algebraic function. This problem was also studied earlier by Bonnet [77] and Carroll et al. [6] using loop equations in a similar manner to the approach we are using. However, both failed to give a closed set of constraints that give the spectral curve. In the former, a complete set of loop equations was not given due to considering

an insufficient set of variations at each level, whereas the latter used an explicitly combinatorial method to derive loop equations, but a closed set was not found as they did not include variations of sufficiently high level.

With $n_{\max} = 5$ the total number of inequivalent loop equations is 64. Although this is a closed and consistent system of polynomial equations, many of them are not independent, and so to determine the spectral curve only a subset of these is required. Using the elimination procedure described above we have identified such a subset consisting of 20 loop equations which, to the best of our knowledge, form a minimal closed set of constraints from which one may extract the resolvent. These are given as follows, where we have again suppressed the z-dependence of the resolvent functions, and we take $W = W_{(1)}(z)$:

1. $\delta X_1 = \frac{1}{z-X_1}$

$$t_3\Delta^2 W + (t_2-1)\Delta W - 2W_2 = W^2 \tag{5.28}$$

2. $\delta X_1 = X_2\frac{1}{z-X_1} + \text{h.c.}$

$$t_3\Delta^2 W_2 + (t_2-1)\Delta W_2 - W_{(2,2)} - W_{(2,3)} = WW_2 \tag{5.29}$$

3. $\delta X_2 = \frac{1}{z-X_1}$

$$t_3 W_{2,2} + (t_2-1)W_2 - W_2 - \Delta W = 0 \tag{5.30}$$

4. $\delta X_2 = X_2X_3\frac{1}{z-X_1} + \text{h.c.}$

$$t_3\Delta^2 W_{(2,3)} + (t_2-1)\Delta W_{(2,3)} - W_{(2,2,3)} - W_{(2,3,2)} = WW_{(2,3)} \tag{5.31}$$

5. $\delta X_2 = X_2\frac{1}{z-X_1} + \text{h.c.}$

$$t_3 W_{(2,2,2)} + (t_2-1)W_{(2,2)} - W_{(2,3)} - \Delta W_2 = W \tag{5.32}$$

6. $\delta X_3 = X_2\frac{1}{z-X_1} + \text{h.c.}$

$$t_3 W_{(2,2,3)} + (t_2-1)W_{(2,3)} - W_{(2,2)} - \Delta W_2 = 0 \tag{5.33}$$

7. $\delta X_1 = X_2 X_3 X_2 \frac{1}{z-X_1} + \text{h.c.}$

$$t_3\Delta^2 W_{(2,3,2)} + (t_2-1)\Delta W_{(2,3,2)} - W_{(2,2,3,2)} - W_{(2,3,2,3)} = W W_{(2,3,2)} \quad (5.34)$$

8. $\delta X_2 = X_3 X_2 \frac{1}{z-X_1} + \text{h.c.}$

$$t_3 W_{(2,2,3,2)} + (t_2-1)W_{(2,3,2)} - W_{(2,2,3)} - \Delta W_{(2,3)} = p_1 W \quad (5.35)$$

9. $\delta X_1 = X_1 X_2 X_3 \frac{1}{z-X_1} + \text{h.c.}$

$$t_3\Delta^3 W_{(2,3)} + (t_2-1)\Delta^2 W_{(2,3)} - W_{(2,1,2,3)} - W_{(2,1,3,2)} = W_{(2,3)} + W\Delta W_{(2,3)} \quad (5.36)$$

10. $\delta X_2 = X_3 X_3 \frac{1}{z-X_1} + \text{h.c.}$

$$t_3 W_{(2,2,3,3)} + (t_2-1)W_{(2,2,3)} - W_{(2,2,2)} - \Delta W_{(2,2)} = 0 \quad (5.37)$$

11. $\delta X_2 = X_1 X_3 \frac{1}{z-X_1} + \text{h.c.}$

$$t_3 W_{(2,1,3,3)} + (t_2-1)W_{(2,1,3)} - W_{(2,1,2)} - \Delta^2 W_2 = 0 \quad (5.38)$$

12. $\delta X_1 = X_2 \frac{1}{z-X_1} X_2$

$$t_3 W_{(2,1,1,2)} + (t_2-1)W_{(2,1,2)} - W_{(2,2,2)} - W_{(2,3,2)} = W_2^2 \quad (5.39)$$

13. $\delta X_1 = X_2 X_1 X_3 \frac{1}{z-X_1} + \text{h.c.}$

$$t_3\Delta^2 W_{(2,1,3)} + (t_2-1)\Delta W_{(2,1,3)} - W_{(2,1,3,2)} - W_{(2,1,3,3)} = p_1 W_2 + W W_{(2,1,3)} \quad (5.40)$$

14. $\delta X_1 = X_2 X_1 X_2 \frac{1}{z-X_1} + \text{h.c.}$

$$t_3\Delta^2 W_{(2,1,2)} + (t_2-1)\Delta W_{(2,1,2)} - W_{(2,1,2,2)} - W_{(2,1,2,3)} = p_1 W_2 + W W_{(2,1,2)} \quad (5.41)$$

15. $\delta X_2 = X_1 X_2 \frac{1}{z-X_1} + \text{h.c.}$

$$t_3 W_{(2,1,2,2)} + (t_2-1)W_{(2,1,2)} - W_{(2,1,3)} - \Delta^2 W_2 = p_1 W \quad (5.42)$$

16. $\delta X_3 = X_2 \frac{1}{z-X_1} X_2$

$$t_3 W_{(2,3,3,2)} + (t_2 - 1) W_{(2,3,2)} - W_{(2,2,2)} - W_{(2,1,2)} = 0 \tag{5.43}$$

17. $\delta X_2 = X_2 X_3 \frac{1}{z-X_1} X_2 + \text{h.c.}$

$$t_3 W_{(2,2,2,2,3)} + (t_2 - 1) W_{(2,2,2,3)} - W_{(2,1,2,3)} - W_{(2,3,2,3)} = 2W_{(2,3)} \tag{5.44}$$

18. $\delta X_2 = X_2 X_2 \frac{1}{z-X_1} X_3 + \text{h.c.}$

$$t_3 W_{(2,2,2,2,3)} + (t_2 - 1) W_{(2,2,2,3)} - W_{(2,2,3,3)} - W_{(2,1,3,3)} = W_{(2,3)} + p_1 W_2 \tag{5.45}$$

19. $\delta X_2 = X_1 X_2 \frac{1}{z-X_1} X_2 + \text{h.c.}$

$$t_3 W_{(2,1,2,2,2)} + (t_2 - 1) W_{(2,1,2,2)} - W_{(2,1,1,2)} - W_{(2,1,3,1)} = p_1 W_2 + \Delta W_2 \tag{5.46}$$

20. $\delta X_2 = X_2 X_1 X_2 \frac{1}{z-X_1} + \text{h.c.}$

$$t_3 W_{(2,1,2,2,2)} + (t_2 - 1) W_{(2,1,2,2)} - W_{(2,1,2,3)} - \Delta W_{(2,1,2)} = p_{1,2} W + \Delta W_2 \tag{5.47}$$

In our terminology, (5.28) is a level-1 loop equation, equations (5.29), (5.30) are level-2 loop equations, (5.31), (5.32) and (5.33) are level-3 loop equations, equations (5.34)-(5.43) are level-4 and (5.44) - (5.47) are level-5 loop equations.

The only level-5 resolvent functions are $W_{(2,2,2,2,3)}$ and $W_{(2,1,2,2,2)}$. Taking these as a basis, the coefficient matrix is

$$(M^{(5)})^T = t_3 \begin{pmatrix} 1 & 1 & 0 & 0 \\ 0 & 0 & 1 & 1 \end{pmatrix}. \tag{5.48}$$

Since this is already in row echelon form, we do not need to implement Gaussian elimination, and we can read off which equations form a linearly independent basis. The first non-zero entry in the first row is the first column, corresponding to (5.44), and the first non-zero entry in the second row is in the third column, corresponding to (5.46). We may therefore use these to eliminate the level-5 resolvent functions from (5.45) and (5.47), yielding

$$W_{(2,1,3,3)} + W_{(2,2,3,3)} - W_{(2,3,2,3)} - W_{(2,1,2,3)} + p_1 W_2 - W_{(2,3)} = 0, \tag{5.49}$$

$$W_{(2,1,2,3)} + \Delta W_{(2,1,2)} - W_{(2,1,1,2)} - W_{(2,1,3,2)} + p_{(1,2)} W - p_1 W_2 = 0. \tag{5.50}$$

The augmented list of level-4 loop equations is then equations (5.34) - (5.43) and (5.49), (5.50).

The set of level-4 resolvent functions is $W_{(2,2,3,2)}, W_{(2,3,2,3)}, W_{(2,1,2,3)}, W_{(2,1,3,2)}$, $W_{2,2,3,3)}$, $W_{(2,1,3,3)}, W_{(2,1,1,2)}, W_{(2,1,2,2)}$ and $W_{(2,3,3,2)}$. The corresponding coefficient matrix is

$$(M^{(4)})^T = \begin{pmatrix} -1 & t_3 & 0 & 0 & 0 & 0 & 0 & 0 & 0 & 0 & 0 & 0 \\ -1 & 0 & 0 & 0 & 0 & 0 & 0 & 0 & 0 & 0 & -1 & 0 \\ 0 & 0 & -1 & 0 & 0 & 0 & 0 & -1 & 0 & 0 & -1 & 1 \\ 0 & 0 & -1 & 0 & 0 & 0 & -1 & 0 & 0 & 0 & 0 & -1 \\ 0 & 0 & 0 & t_3 & 0 & 0 & 0 & 0 & 0 & 0 & 1 & 0 \\ 0 & 0 & 0 & 0 & t_3 & 0 & -1 & 0 & 0 & 0 & 1 & 0 \\ 0 & 0 & 0 & 0 & 0 & t_3 & 0 & 0 & 0 & 0 & 0 & -1 \\ 0 & 0 & 0 & 0 & 0 & 0 & 0 & -1 & t_3 & 0 & 0 & 0 \\ 0 & 0 & 0 & 0 & 0 & 0 & 0 & 0 & 0 & t_3 & 0 & 0 \end{pmatrix}. \tag{5.51}$$

Reduced to row echelon form we find that equations (5.34) - (5.41) and (5.43) form a linearly independent set. Eliminating the level-4 resolvent functions from (5.42), (5.49) and (5.50) respectively, we obtain

$$\begin{aligned}(t_3^2\Delta^2 + t_3(t_2-1)\Delta^2 - t_3(1+W\Delta))W_{(2,3)} - (t_3^2\Delta^2 + t_3(t_2-1)\Delta \\ + t_2 - 2 - t_3W)(W_{(2,1,3)} + W_{(2,1,2)}) + 2(\Delta^2 + t_3p_1)W_2 + p_1W = 0, \end{aligned} \tag{5.52}$$

$$\begin{aligned}\left(t_3\Delta^2 + (t_2-1)\Delta + \frac{(t_2-1)}{t_3} - W\right)W_{(2,3,2)} - (t_3\Delta^2 + (t_2-1)\Delta - W)W_{(2,1,3)} \\ + \frac{(t_2-2)}{5_3}W_{(2,2,3)} - \frac{1}{t_3}W_{(2,2,2)} + \left(t_3\Delta^3 + (t_2-1)\Delta^2 - \left(W + \frac{1}{t_3}\right)\Delta\right)W_{(2,3)} \\ - \frac{1}{t_3}\Delta W_{(2,2)} - \frac{1}{t_3}p_1W = 0, \end{aligned} \tag{5.53}$$

$$\begin{aligned}2\left(t_3\Delta^2 + (t_2-1)\left(\Delta + \frac{1}{t_3}\right)\right) - W\Big)W_{(2,1,3)} - \left(\frac{(t_2+1)}{t_3} + \Delta\right)W_{(2,1,2)} \\ \frac{1}{t_3}(W_{(2,2,2)} + W_{(2,3,2)}) - (t_3\Delta^3 + (t_2-1)\Delta^2 - 1 - W\Delta)W_{(2,3)} \\ - \left(\frac{2}{t_3}\Delta^2 + p_1 - \frac{1}{t_3}W_2\right)W_2 - p_{1,2}W = 0. \end{aligned} \tag{5.54}$$

Therefore the augmented set of level-3 loop equations is (5.31) - (5.33) and (5.52) - (5.54).

The level-3 resolvent functions are $W_{(2,3,2)}, W_{(2,2,3)}, W_{(2,2,2)}$, $W_{(2,1,3)}$, and $W_{(2,1,2)}$. We may eliminate these by repeating the same process as before. The coefficient matrix is

$$(M^{(3)})^T = \begin{pmatrix} -1 & 0 & 0 & 0 & \frac{-1-\alpha}{t_3} & \frac{1}{t_3} \\ -1 & 0 & t_3 & 0 & \frac{t_2-2}{t_3} & 0 \\ 0 & t_3 & 0 & 0 & -\frac{1}{t_3} & \frac{1}{t_3} \\ 0 & 0 & 0 & 2+\alpha & \frac{\alpha+t_2}{t_3} & \frac{2(1-\alpha)}{t_3} \\ 0 & 0 & 0 & 2+\alpha & 0 & -\frac{1+t_2+zt_3}{t_3} \end{pmatrix}, \tag{5.55}$$

where

$$\alpha = t_3(z+W) - t_3 z^2 - t_3 t_2 z - t_2. \tag{5.56}$$

Through Gaussian elimination we identify equations (5.31) - (5.33) and (5.52), (5.53) as a linearly independent set. We may then use these to eliminate the level-3 resolvent functions from (5.54) to yield a single level-2 constraint. This expression is quite large and so we shall not present it here.

We are then left with a system of 4 independent polynomial equations from which we can eliminate $W_{(2,2)}, W_{(2,3)}$, and W_2, to yield a single algebraic equation for the planar resolvent. The spectral curve is degree 8 in the boundary cosmological constant z and degree 5 in $W = W_{(1)}(z)$, and the analytic structure is presented in Fig.5.1. Sheets are labelled starting from the physical sheet, where $\lim_{z\to\infty} zW(z)_0 = 1$, and wind upwards. Single vertical lines correspond to compact branch cuts, while doubled lines correspond to semi-infinite cuts. The horizontal axis is taken to be the z-plane, and so the right-most doubled lines denote branch cuts extending to infinity. Additionally, branch cuts are labelled by discontinuities when traversing from the lower sheet to the upper sheet.

In general, the final result will contain a number of trace correlation functions. Many of these can be expressed in terms of a smaller set of correlation functions through the use of loop equations. In this case, one considers variations of the form (5.10) but omits the loop operator component $(z-X)^{-1}$, yielding constraints on the correlation functions which may be solved in a manner similar to that described for the resolvent functions.

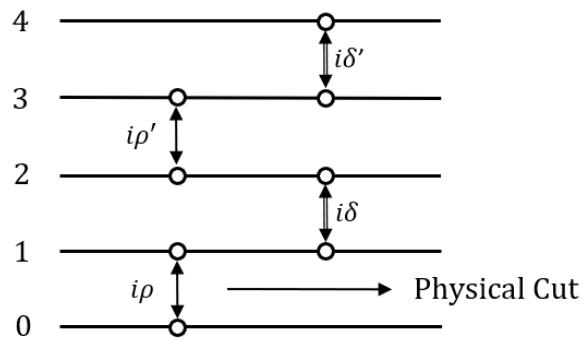

Figure 5.1: Analytic structure of $W_{(1)}(z)$ in the 3-state Potts model.

In Appendix A we complete the calculation of the fixed-spin one-loop function in the formalism of [6]. We demonstrate how one may compute the same loop equations derived in this section using combinatorial arguments, independent of the matrix integral (5.27), and therefore show the equivalence between the loop equation approach for the multi-matrix model we described here, and the combinatorics of coloured random planar graphs.

5.3.2 Mixed boundary conditions

To compute the planar resolvent for the mixed boundary condition we change the basis of the matrix integral (5.27) to $M_1 = X_2 + X_3, M_2 = X_3 + X_1, M_3 = X_1 + X_2$. Under this change of basis the potential becomes

$$V(M_1, M_2, M_3) = \mathrm{Tr}\Bigg(\frac{(3t_2-1)}{8}(M_1^2 + M_2^2 + M_3^2) - \frac{(t_2+1)}{4}(M_1M_2 + M_2M_3 + M_3M_1) + \frac{t_3}{8}(M_1^2M_2 + M_1^2M_3 + M_2^2M_1 + M_2^2M_3 + M_3^2M_1 + M_3^2M_2 - 3M_1M_2M_3 - 3M_3M_2M_1)\Bigg). \quad (5.57)$$

The resulting potential retains the S_3 permutation symmetry of (5.27), but possesses many more interaction terms. The choice of basis is arbitrary, one should be able to reproduce the planar resolvent regardless of how we parameterised the potential. In this case our goal is to compute

$$W_{(2)}(z) = \frac{1}{N}\left\langle \mathrm{Tr}\,\frac{1}{z - M_1}\right\rangle. \quad (5.58)$$

In contrast to the fixed-spin boundary condition, we are able to determine a closed set of algebraic constraints on the planar resolvent only if we extend to level $n_{\max} = 6$ loop equations. The increased number of terms in the potential relative to (5.27) results in a greater number of resolvent functions present in the loop equations. There are $|\mathcal{V}_5| = 64$ possible variations one can consider and $|\mathcal{W}_5| = 54$ resolvent functions up to level 5, but due to redundancies in the resulting system of equations this is not enough to constrain the resolvent. Extending to level 6, $|\mathcal{W}_6| = 144$ and $|\mathcal{V}_6| = 245$. Once redundancies have been removed, these loop equations do possess a closed system of equations. We have not determined a minimal set of equations that form closed algebraic system of equations, and we do not give the full set of constraints here.

The final expression for the spectral curve is degree 10 in the resolvent $W_{(2)}(z)$ and degree 13 in the boundary cosmological constant z. At first glance, this is rather surprising, as it was shown in [60] that the function $G^Y_{(2)}(z)$, which contains the information of the eigenvalue density distribution, satisfies a spectral curve that is degree 5 in $G^Y_{(2)}(z)$ and degree 6 in z. We now show how one can reconcile these two observations.

5.3.3 Mixed boundary saddle-point solution

Under the change of variables $X_\pm = X_1 \pm X_2$ the potential (5.27) becomes

$$V(X_+, X_-, X_3) = \mathrm{Tr}\Bigg(\frac{(t_2-2)}{4}X_+^2 + \frac{t_3}{12}X_+^3 + \frac{(t_2-1)}{2}X_3^2 + \frac{t_3}{3}X_3^3 - X_3X_+ + \frac{1}{4}(t_2\mathbf{I} + t_3X_+)X_-^2\Bigg). \quad (5.59)$$

We can integrate out the final Gaussian term in X_- using the following identity [73],

$$I = \int [dA] e^{-\lambda N \mathrm{Tr} A^2 B} = \frac{(\pi/\lambda N)^{N^2/2}}{2^{N(N-1)/2}} \frac{1}{\sqrt{\det B}\prod_{i<j}(b_i + b_j)}, \quad (5.60)$$

where $[dA] = \prod_{i=1}^N dA_{i,i} \prod_{i<j} d\mathrm{Re}A_{i,j} d\mathrm{Im}A_{i,j}$ and b_i are the eigenvalues of B. Applied to (5.59), one obtains

$$Z \propto \int [dX_+][dX_3] \frac{e^{-N\mathrm{Tr}\left(\frac{(t_2-2)}{4}X_+^2 + \frac{t_3}{12}X_+^3 + \frac{(t_2-1)}{2}X_3^2 + \frac{t_3}{3}X_3^3 - X_3X_+\right)}}{\sqrt{\det B}\prod_{i<j}(b_i + b_j)}, \quad (5.61)$$

where $B = t_2\mathbf{I} + t_3 X_+$.

To calculate the saddle-point equations of (5.61), we follow the approach described in Section 2.3.2 and exploit the $U(N)$ symmetry of the matrix model to diagonalise X_+ and X_3. We set

$$X_+ = U\text{diag}\left(\{\lambda_i\}_{i=1}^N\right)U^\dagger, \quad X_3 = V\text{diag}\left(\{\mu_j\}_{j=1}^N\right), \tag{5.62}$$

with $U, V \in U(N)$. We can then perform the unitary group integrals using the HCIZ formula [63, 64]:

$$\int [dU] e^{N\text{Tr}XUYU^\dagger} \propto \frac{\det\limits_{1\leqslant i,j\leqslant N} e^{Ny_i x_j}}{\Delta(x)\Delta(y)}, \tag{5.63}$$

where $[dU]$ is the normalised Haar measure, and the $\{y_i\}_{i=1}^N$ and $\{x_j\}_{j=1}^N$ are the eigenvalues of the $N \times N$ Hermitian matrices Y and X respectively.

Consider first the saddle-point equation about the eigenvalues of X_+. Diagonalising X_+ and evaluating the integral over the unitary group yields

$$Z \propto \int [dX_3] \int \prod_{i=1}^N d\lambda_i \frac{\Delta(\lambda)}{\Delta(\mu)} \frac{\det_{i,j} e^{N\lambda_i\mu_j} e^{-N\text{Tr}\left(\frac{(t_2-1)}{2}X_3 + \frac{t_3}{3}X_3^3\right) - N\sum_{i=1}^N \frac{(t_2-2)}{4}\lambda_i^2 + \frac{t_3}{12}\lambda_i^3}}{\sqrt{\det B}\prod_{i<j}(b_i+b_j)}. \tag{5.64}$$

We may then write an effective potential for the eigenvalues of X_+,

$$V_{\text{eff.}}(\{\lambda_i\}_{i=1}^N) = \Bigg(\sum_{i=1}^N \frac{(t_2-2)}{4}\lambda_i^2 + \frac{t_3}{12}\lambda_i^3 - \frac{1}{N}\sum_{i<j}\log(\lambda_i - \lambda_j) - \frac{1}{N}\log\det_{i,j} e^{N\lambda_i\mu_j} + \frac{1}{2N}\sum_{i,j}\log\left((t_2 + t_3\lambda_i) + (t_2 + t_3\lambda_j)\right)\Bigg), \tag{5.65}$$

Taking the variation with respect an eigenvalue λ_i, and demanding that this be zero in the large N limit, we find the following saddle-point equation, with $\lambda_i \to z$:

$$\frac{t_3}{4}z^2 + \frac{(t_2-2)}{2}z = W_{(2)}(z) + G^{X_3}_{X_1+X_2}(z) + W_{(2)}\Big(-z - \frac{2t_2}{t_3}\Big), \tag{5.66}$$

where $W_{(2)}(z)$ denotes the resolvent of $X_1 + X_2$ as in (3.2), and the G-function is defined as in (3.8).

The saddle-point equation about the eigenvalues of X_3 is straightforward to compute,

$$t_3 z^2 + (t_2 - 1)z = W_{(1)}(z) + G^{X_1+X_2}_{X_3}(z), \tag{5.67}$$

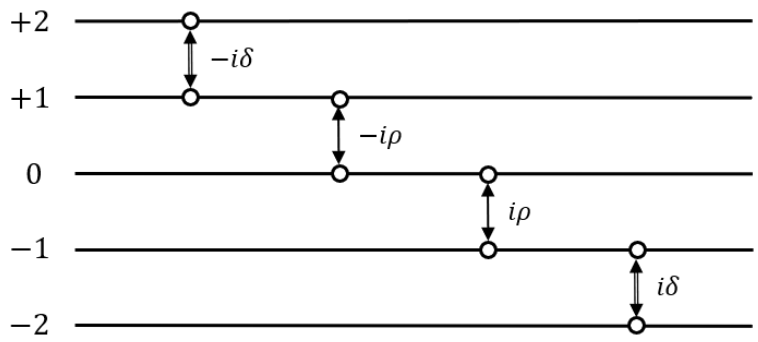

Figure 5.2: Analytic structure of $G^Y_{(2)}(z)$ in the 3-state Potts model.

where $W_{(1)}(z)$ is the single matrix resolvent (3.2). By comparing with (3.18) one finds

$$G^Y_{(1)}(z) = z + G^{X_1+X_2}_{X_3}(z). \tag{5.68}$$

The spectral curve for $G^Y_{(2)}(z)$ derived by Atkin et al. [60] satisfies the following,

$$F_{(2)}(z, G^Y_{(2)}(z)) = F_{(1)}(G^Y_{(2)}(z) - z, G^Y_{(2)}(z)) = 0, \tag{5.69}$$

and so, comparing both, we obtain the following relation,

$$G^Y_{(2)}(z) = G^{X_3}_{X_1+X_2}(z) + z. \tag{5.70}$$

Using their result one can infer the analytic structure of $G^Y_{(2)}(z)$, which is given in Fig.5.2. Therefore, using (5.66) and the branch structure of $G^Y_{(2)}(z)$, we should be able to determine the form of $W_{(2)}(z)$.

Define $U(z) = \frac{t_3}{4}z^2 + \frac{t_2}{2}z$, and label the physical sheet '0', such that the saddle-point equation becomes

$$W_{(2)}(z)_0 + W_{(2)}\Big(-z - \frac{2t_2}{t_3}\Big)_0 + G^Y_{(2)}(z)_0 = U(z). \tag{5.71}$$

Let $W_{(2)}(z)_0$ have a compact branch cut on the interval $C_0^+ = [a, b]$ (and thus $W_{(2)}\Big(-z - \frac{2t_2}{t_3}\Big)_0$ has a cut on $C_0^- = [-b - \frac{2t_2}{t_3}, -a - \frac{2t_2}{t_3}]$), and $G^Y_{(2)}(z)_{-1}$ have a cut on $C_\infty^+ = [c, +\infty)$, as demonstrated in Fig.5.2. We take $a, b, c \in \mathbb{R}$ and $a < b < c$. We now study the branch structure by analytically continuing through the various branch cuts sequentially, and matching discontinuities.

(i) First, analytically continuing through the physical cut C_0^+ takes $W_{(2)}(z)_0 \to W_{(2)}(z)_1$, and we get

$$W_{(2)}(z)_1 + G^Y_{(2)}(z)_{-1} + W_{(2)}\Big(-z-\frac{2t_2}{t_3}\Big)_0 = U(z), \tag{5.72}$$

from which we can infer that $W_{(2)}(z)_1$ has a cut along C_0^-, C_0^+, and C_∞^+.

(ii) Analytically continuing through C_∞^+, we find

$$W_{(2)}(z)_2 + G^Y_{(2)}(z)_{-2} + W_{(2)}\Big(-z-\frac{2t_2}{t_3}\Big)_0 = U(z), \tag{5.73}$$

and consequently $W_{(2)}(z)_2$ has a cut along C_0^- and C_∞^+.

(iii) Circling C_0^-,

$$W_{(2)}(z)_3 + G^Y_{(2)}(z)_{-2} + W_{(2)}\Big(-z-\frac{2t_2}{t_3}\Big)_1 = U(z), \tag{5.74}$$

and so now we have a cut along C_∞^-, C_0^-, C_0^+, and C_∞^+.

(iv) Circling C_∞^+,

$$W_{(2)}(z)_4 + G^Y_{(2)}(z)_{-1} + W_{(2)}\Big(-z-\frac{2t_2}{t_3}\Big)_1 = U(z), \tag{5.75}$$

which implies that $W_{(2)}(z)_4$ has a cut along C_∞^-, C_0^-, and C_∞^+.

(v) If we circle C_0^-, $G^Y_{(2)}(z)_{-1} \to G^Y_{(2)}(z)_0$ and $W_{(2)}\Big(-z-\frac{2t_2}{t_3}\Big)_1 \to W_{(2)}\Big(-z-\frac{2t_2}{t_3}\Big)_0$, which implies that we return to sheet $W_{(2)}(z)_1$, and that these two are connected along C_0^-. Meanwhile, if we circle C_∞^-,

$$W_{(2)}(z)_5 + G^Y_{(2)}(z)_{-1} + W_{(2)}\Big(-z-\frac{2t_2}{t_3}\Big)_2 = U(z), \tag{5.76}$$

from which we deduce that $W_{(2)}(z)_5$ has a cut along C_∞^- and C_∞^+.

(vi) Circling C_∞^+,

$$W_{(2)}(z)_6 + G^Y_{(2)}(z)_{-2} + W_{(2)}\Big(-z-\frac{2t_2}{t_3}\Big)_2 = U(z), \tag{5.77}$$

from which we infer that $W_{(2)}(z)_6$ has branch cuts along C_∞^-, C_0^+, and C_∞^+.

(vii) At this point, if we circle C_∞^-, $G^Y_{(2)}(z)_{-2}$ remains unchanged and $W_{(2)}\Big(-z-\frac{2t_2}{t_3}\Big)_2 \to W_{(2)}\Big(-z-\frac{2t_2}{t_3}\Big)_1$, which tells us that $W_{(2)}(z)_6 \to W_{(2)}(z)_3$. However, if we circle C_0^+, we find

$$W_{(2)}(z)_7 + G^Y_{(2)}(z)_{-2} + W_{(2)}\Big(-z-\frac{2t_2}{t_3}\Big)_3 = U(z), \tag{5.78}$$

and so $W_{(2)}(z)_7$ has cuts along C_∞^-, C_0^-, C_0^+.

(viii) Circling C_∞^- gives

$$W_{(2)}(z)_8 + G^Y_{(2)}(z)_{-2} + W_{(2)}\Big(-z-\frac{2t_2}{t_3}\Big)_4 = U(z), \tag{5.79}$$

and so $W_{(2)}(z)_8$ has cuts along C_∞^-, and C_0^+. If we circle the latter, we find $W_{(2)}\Big(-z-\frac{2t_2}{t_3}\Big)_4 \to W_{(2)}\Big(-z-\frac{2t_2}{t_3}\Big)_1$ and $G^Y_{(2)}(z)_{-2}$ remains unchanged, implying $W_{(2)}(z)_8 \to W_{(2)}(z)_3$.

(ix) Finally, if we circle C_0^- of $W_{(2)}(z)_7$

$$W_{(2)}(z)_9 + G^Y_{(2)}(z)_{-2} + W_{(2)}\Big(-z-\frac{2t_2}{t_3}\Big)_8 = U(z), \tag{5.80}$$

which implies $W_{(2)}(z)_9$ has a single cut along C_0^-, terminating the sheet structure.

The entire analytic structure is depicted in Fig.5.3.

We therefore find that the branch structure predicted by the loop equation solution is in agreement with the solution found in [60]. Moreover, one may explicitly compare the asymptotics of the resolvent on each sheet, given in Appendix B, and see that it is in accord with the saddle-point solution on each sheet, using the asymptotics of $G^Y_{(2)}(z)$ given in [60].

5.3.4 Free boundary conditions

Let us choose a basis for the potential (5.27) given by $M_1 = X_1 + X_2 + X_3, M_2 = X_1 - X_2 + X_3, M_3 = X_1 + X_2 - X_3$. Then computing the resolvent corresponding

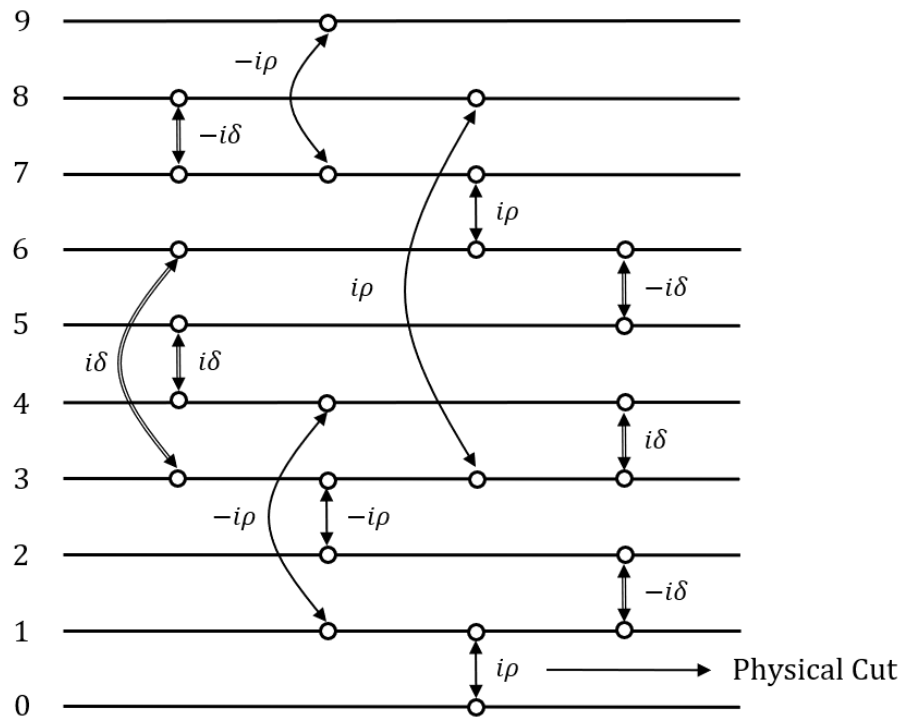

Figure 5.3: Analytic structure of $W_{(2)}(z)$ in the 3-state Potts model.

to the free boundary condition, $W_{(3)}(z)$, is equivalent to computing the planar resolvent of the matrix M_1 with the following potential,

$$V(M_1, M_2, M_3) = \mathrm{Tr}\bigg(\frac{(t_2-2)}{4}M_1^2 + \frac{t_2}{4}(M_2^2 + M_3^2 - M_1M_2 + M_2M_3 - M_3M_1) + \frac{t_3}{8}(M_2^2M_1 + M_3^2M_1 + M_2^2M_3 + M_3^2M_2 - M_1^2M_2 - M_1^2M_3) + \frac{t_3}{12}M_1^3\bigg). \quad (5.81)$$

As in the case of the mixed boundary condition, one must extend to level 6 to find a complete set of constraints.

The model, as written, possesses a $\mathbb{Z}_2$ symmetry relating M_2 and M_3. However, the correlators also possesses a further set of constraints, owing to their origin in the 3-state Potts model, that are not manifest in (5.81). These are given by

$$W_2(z) = \frac{1}{3}\Delta W_{(3)}(z), \quad (5.82)$$

which is easily deduced by rewriting the terms in the original basis and imposing the full S_3 symmetry in the expectation value.

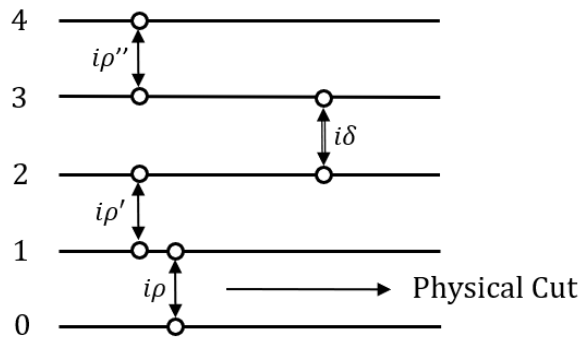

Figure 5.4: Analytic structure of $W_{(3)}(z)$ in the 3-state Potts model.

Applying the elimination procedure and (5.82), one can determine the spectral curve for the free spin resolvent, given by an algebraic equation that is degree 5 in z and degree 5 in the resolvent $W_{(3)}(z)$. Furthermore, with the relation

$$G^Y_{(3)}(z) = z + W_{(3)}(z), \tag{5.83}$$

one recovers the spectral curve for $G^Y_{(3)}(z)$ of Atkin et al. The analytic structure of $W_{(3)}(z)$ is provided in Fig.5.4.

5.3.5 An 'odd' boundary condition

Returning to (5.81), it is also possible to use the loop equation approach to calculate the planar resolvent of M_2. We shall call this the 'odd' boundary condition and label the resolvent $W'(z)$. As with the free spin resolvent, there is a supplementary constraint on the resolvent functions that is not manifest in the potential,

$$W'_1(z) = 2W'_3(z) + \Delta' W'(z), \tag{5.84}$$

where the Δ' is understood to correspond to insertions of the matrix M_2. Once again, we find $n_{\max} = 6$, and the resulting spectral curve is degree 14 in $W'(z)$ and degree 13 in z.

At the moment, it is unclear what the physical interpretation of this object might be. It may be related to the $W_{X_1-X_2}(z)$ one-loop function of the Ising model coupled to 2D gravity [69], but further study of the scaling limit would be needed to demonstrate this.

5.3.6 U boundary conditions

To study the $U = X_1 + \omega X_2 + \omega^2 X_3$ boundary condition we choose the basis $U, U^\dagger$ and $X = X_1 + X_2 + X_3$. The potential is equivalent to the action (4.9) up to a scaling of the matrices,

$$V(X,U,U^\dagger) = \mathrm{Tr}\bigg(\frac{(t_2-3)}{6}X^2 + \frac{t_2}{3}UU^\dagger + \frac{t_3}{9}(UU^\dagger X + XU^\dagger U) + \frac{t_3}{27}(X^3 + U^3 + (U^\dagger)^3)\bigg). \quad (5.85)$$

The structure of the loop equations is quite simple, and one may expect $n_{\max} = 5$, as in the case of the fixed boundary condition. However, unlike the previous cases, applying the algorithm to compute the resolvent of U does not result in a closed system of equations, even if we consider loop equations of level 6. Instead, we obtain a polynomial equation relating the resolvent and the level 1 loop function $W_X(z)$.

We have extended this to level 7 and found that the system of equations still does not close. With the relative simplicity of the potential, this strongly suggests that this resolvent cannot be determined using our loop equation approach.

5.4 Dilute Ising Model

We now turn our attention to the dilute Ising model on random planar graphs, given by the following matrix integral,

$$Z = \int [dY] \prod_{i=1}^{q} [dX_i] e^{-N\mathrm{Tr}\left(\frac{1}{2}Y^2 + \frac{t_0}{3}Y^3 + \sum_{i=1}^{q}\left(\frac{t_2}{2}X_i^2 + \frac{t_3}{3}X_i^3 - YX_i\right)\right)}, \quad (5.86)$$

for $q = 2$. For arbitrary q, this matrix integral represents the dilute q-state Potts model, first studied by Zinn-Justin [58] using the saddle-point method. The parameter t_0 determines the dilution of random graphs, i.e. the number of sites not occupied by the spins $\{X_i\}_{i=1}^q$. For $t_0 = 0$ the integral over Y may be evaluated, and one recovers the q-state Potts model (3.1). The resolvent corresponding to $p = 1$ fixed spin boundary conditions was computed for $q = 1, 2$, and 3, by means of computing the auxiliary G-function (3.8) corresponding to Y-boundary conditions. We will reproduce these results using the loop equation formalism.

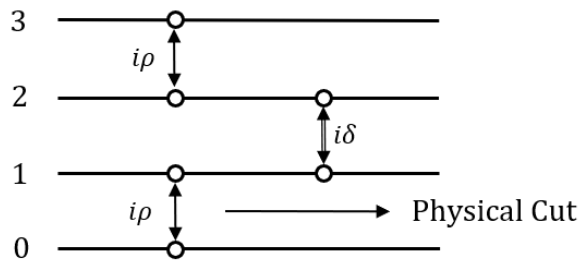

Figure 5.5: Analytic structure of $W_Y(z)$ in the dilute Ising model.

In this section, we will discuss the vacant, fixed, and free boundary conditions in the dilute Ising model. As noted in Chapter 2, these boundary conditions represent three out of the four fixed lattice realisations of the physical conformally invariant boundary states. We have not determined the remaining 'partially fixed' boundary condition, which we expect to be captured by the planar resolvent

$$W_{p.f.}(z) = \frac{1}{N}\left\langle \mathrm{Tr}\,\frac{1}{z-(X_1+Y)}\right\rangle . \tag{5.87}$$

5.4.1 Vacant boundary conditions

The boundary condition in which all the sites on the boundary are left vacant is realised by the resolvent

$$W_Y(z) = \frac{1}{N}\left\langle \mathrm{Tr}\,\frac{1}{z-Y}\right\rangle . \tag{5.88}$$

This may be determined using the loop equation approach with $n_{\max} = 5$, resulting in a spectral curve that is degree 6 in z and degree 4 in $W_Y(z)$. The analytic structure is presented in Fig.5.5.

5.4.2 Fixed boundary conditions

The fixed spin boundary condition, $W_{(1)}(z)$, may be computed using loop equations with $n_{\max} = 5$, resulting in a spectral curve that is degree 8 in z and degree 5 in $W_{(1)}(z)$. The analytic structure is presented in Fig.5.6.

We note that when dilution is turned off we recover the spectral curve (2.71), as expected. The introduction of vacancies fundamentally alters the analytic structure of the Ising spectral curve from a curve that is degree 3 in the resolvent to a

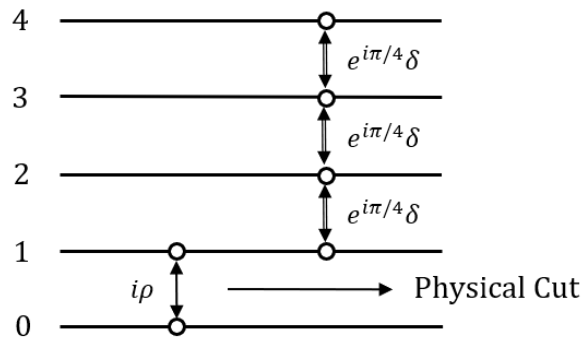

Figure 5.6: Analytic structure of $W_{(1)}(z)$ in the dilute Ising model.

degree 5 curve, and this allows one to generate even higher order critical behaviour. It was argued in [58] that this extra structure admits a new critical point with $\gamma_s = -\frac{1}{4}$, which corresponds to the universality class of the $c = 7/10$ tricritical Ising model coupled to 2D gravity.

5.4.3 Free boundary conditions

To study the free boundary condition we choose the basis $M_1 = X_1 + X_2, M_2 = X_1 - X_2$, and calculate the planar resolvent of M_1. The potential is given by

$$V(Y, M_1, M_2) = N\mathrm{Tr}\bigg(\frac{1}{2}Y^2 + \frac{t_0}{3}Y^3 + \frac{t_2}{4}(M_1^2 + M_2^2) + \frac{t_3}{12}(M_1^3 + 3M_1M_2^2) - YM_1\bigg). \quad (5.89)$$

Extending to level $n_{\max} = 6$ we obtain a closed system of loop equations from which we can compute the spectral curve. The final result is degree 10 in z and degree 10 in $W_{(2)}(z)$. The analytic structure is identical to the mixed boundary condition in the 3-state Potts model, Fig.5.3.

5.5 Dilute Potts Model

Finally, we consider the dilute Potts model on random planar graphs, given by (5.86) for $q = 3$. In this section, we will discuss the vacant and fixed spin boundary conditions, which we have calculated using the loop equation approach.

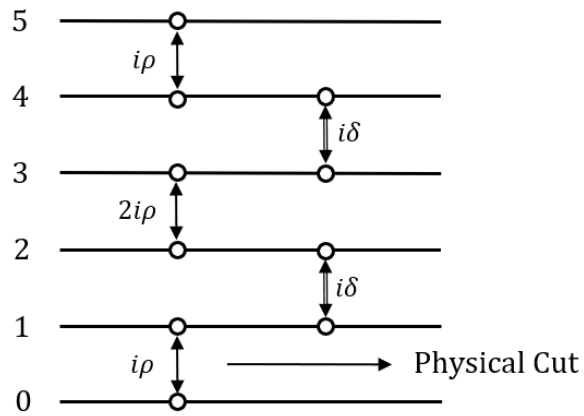

Figure 5.7: Analytic structure of $W_Y(z)$ in the dilute Potts model.

5.5.1 Vacant boundary conditions

The vacant boundary condition $W_Y(z)$ may be calculated by extending to variations of level $n_{\max} = 7$. The spectral curve is degree 10 in the boundary cosmological constant z, and degree 6 in the resolvent $W_Y(z)$. The analytic structure is presented in Fig.5.7.

5.5.2 Fixed boundary conditions

The fixed boundary condition, $W_{(1)}(z)$, may also be calculated with $n_{\max} = 7$. In this case, the spectral curve is degree 16 in the boundary cosmological constant z and degree 9 in the resolvent $W_{(1)}(z)$. The analytic structure is presented in Fig.5.8.

As with the dilute Ising model, one recovers the spectral curve of the critical Potts model when the dilution is turned off. In [58] it was argued that the extra structure generated by introducing dilution allows for a new critical point with $\gamma_s = -\frac{1}{6}$, which corresponds to the universality class of the $c = 6/7$ tricritical Potts model.

5.6 Discussion

In this chapter, we developed an algorithm for systematically computing and solving the loop equations of general multi-matrix models, in the goal of finding the spectral curve for the planar resolvent of a given matrix degree of freedom. We then focused our attention on the 3-state Potts model, where we successfully computed the planar

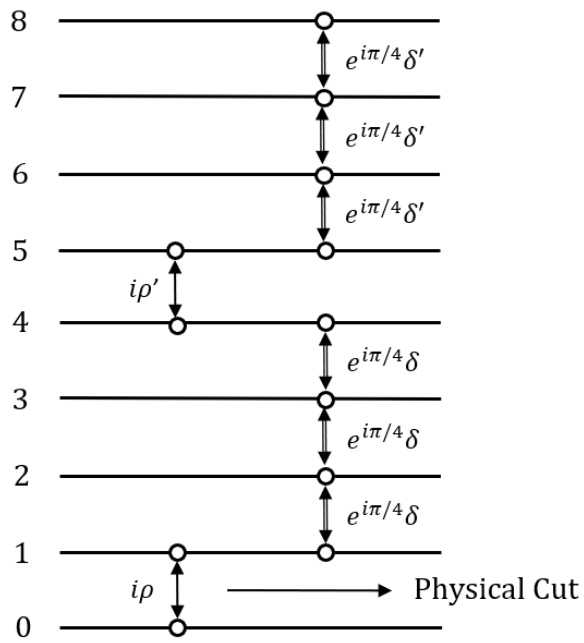

Figure 5.8: Analytic structure of $W_{(1)}(z)$ in the dilute Potts model.

resolvents describing fixed, mixed, and free boundary conditions using this technique. While the fixed and free boundary conditions were manifestly in agreement with the literature, more care was required for the mixed boundary condition. Through studying the analytic structure predicted by the saddle-point solution, we were able to show that this too was consistent with the results of Atkin et al. We then considered some non-standard resolvents, including a new 'odd' boundary condition, which was susceptible to the loop equation strategy, and a U boundary condition which we were not able to solve. Following this, we discussed the dilute Ising and Potts models, where we computed the resolvents corresponding to various boundary conditions, in agreement with the results of Zinn-Justin.

There are many ways to continue this work. Our procedure is algorithmic in nature and so it would be interesting to apply this to a wide variety of models for which the planar resolvent is known or unknown. In the context of three-matrix models more generally, it would be interesting to understand the criteria under which a resolvent is calculable. As we have seen from our results, we were able to calculate the planar resolvent for particular systems with full S_3 symmetry under interchange of the matrix degrees of freedom (5.57), and for systems where there is

a residual $\mathbb{Z}_2$ symmetry under the remaining degrees of freedom, with an auxiliary condition reducing the number of level-1 resolvent functions (5.81). Determining whether this can be elevated to a general principle governing solvability of correlators in the three-matrix model would be an exciting challenge. One immediate offshoot of this would be the calculation of planar resolvents describing boundary conditions that interpolate between the fixed, mixed and free boundary states analogous to [76, 78]. This would allow us to directly study the boundary renormalisation group flow relating the different boundary states, which is expected to induce a partial ordering of the spectrum of boundary states, conforming with the boundary analogue of the c-theorem [79], which was first conjectured in [80], and subsequently proven by Friedan and Konechny [81].

Another interesting avenue of research would be to investigate whether we could generalise the algorithm developed in this chapter for a wider variety of correlators and matrix models, such as the q-state Potts model where q is taken to be non-integer. This is possible for the simple example of the fixed-spin boundary condition [77]. Whether we could do the same for general boundary conditions and reproduce the saddle-point results of Chapter 3 is an open question. This would provide further insight into the nature of the allowed G-functions and corresponding boundary conditions in the q-state Potts model. It would also be useful for studying the expression for the New boundary condition determined in Chapter 4, which is given by a non-standard resolvent function that would not immediately be amenable to calculation through the loop equation method devised in this chapter.

Finally, it would be fruitful to extend our work to the calculation of observables in multi-matrix models beyond the planar limit. It is well known that the planar resolvent forms the initial data for higher-genus and multi-boundary correlators in the one- and two-matrix models [7, 12, 50], and that this may be extended to certain multi-matrix models [70]. It would be interesting to see whether one could reframe the method of loop equations for various boundary conditions in the 3-state Potts model such that one can calculate higher-order correlation functions in an analogous topological recursion procedure. This would allow, for example,

the computation of cylinder amplitudes for different boundary states, and might provide valuable information as to how to interpret the results of Chapter 3.

Chapter 6

Summary

In this thesis, we have discussed the application of random matrix models to 2D Euclidean quantum gravity coupled to matter described by spin systems. Working firmly in the planar limit, we aimed to develop our understanding of boundary conditions in the q-state Potts model on random planar graphs, and pursued this goal along multiple lines of inquiry: we used the saddle-point method; we then turned turned to the case of $q = 3$, and considered Kramers-Wannier duality; and finally, we developed and applied the loop equation method for general boundary conditions.

In Chapter 2, we gave a compressed review of many of the concepts relevant to this work. We described how the quantum gravity path integral may be defined via a lattice regularisation known as dynamical triangulations. We reviewed how the one-loop function, describing 2D geometries with a single boundary, may be computed using combinatorial and matrix model methods, and then described how one may couple spin systems to random planar graphs using multi-matrix models. We introduced and gave a brief overview of conformal field theory, which describes the scaling limit of 2D statistical spin systems, devoting some attention to boundary physics in various models. Following this, we tied these different models together and introduced Liouville gravity, which describes the continuum limit of dynamical triangulations, and surveyed some of its general features.

Subsequently, we introduced the topic of boundary conditions in the q-state Potts model on random planar graphs in Chapter 3. We extended a recent analysis of the one-loop function with $p \leqslant q$ allowed, equally weighted spins on the boundary

and explored the $(q < 4, p \leqslant q)$ parameter space of finite-sheeted resolvents. We reproduced the long-known result that the model possesses a $p = 1$ resolvent, described by an algebraic function, for $q = 2\left(1 + \cos\frac{m}{n}\pi\right)$ with m, n coprime, and computed the corresponding critical exponents. We discovered two distinct sequences of solutions for generic p, depending on the values of m and n, one of which contains $p = 2$ and $p = q/2$, while the other does not. In particular, we found that for $q = 3$, there is a corresponding a $p = 3/2$ boundary condition; we conjectured that this new solution corresponds to the New boundary condition, discovered on the flat lattice by Affleck, Oshikawa and Saleur.

In Chapter 4, in the hope of justifying this conjecture, we turned our attention to Kramers-Wannier duality in the 3-state Potts model, wherein it is known that the New boundary condition is dual to the Mixed boundary condition on the fixed lattice. We constructed the Kramers-Wannier dual of the 3-state Potts model on the random lattice, and explicitly constructed the known boundary conditions. In particular, we were able to show that the mixed boundary condition is dual to a boundary condition on dual graphs that corresponds to Affleck et al.'s identification of the New boundary condition on fixed lattices. However, we found that the mixed boundary condition of the dual, and the corresponding New boundary condition of the original theory were not described by conventional resolvents.

Finally, in Chapter 5, we addressed the question of calculating the one-loop function with general boundary conditions using the combinatorial method of loop equations for general multi-matrix models. Therein we developed a formalism for studying these constraints, and we provided an algorithm for systematically computing loop equations and solving them, in order to generate the spectral curve describing the planar resolvent. We applied this technique to the 3-state Potts model, where we successfully reproduced the $p = 1, 2$, and 3 boundary conditions found by Atkin, Niedner and Wheater. Motivated by this, we attempted to calculate various other boundary conditions, in both the 3-state Potts model and the dilute q-state Potts model. For the 3-state Potts model, we discovered a new boundary condition, which we called the 'odd' boundary condition, which could be calculated

using our formalism, but whose physical interpretation is unclear. Moreover, we appeared to find the limits of this technique, finding a complex boundary condition that was not clearly susceptible to the loop equation strategy. As for the dilute Ising and Potts models, we were successfully able to calculate the vacant and fixed boundary conditions, reproducing the results of Zinn-Justin, and in the former we also computed the free boundary condition.

Where do we go from here? As seen from the discussions in Sections 3.6, 4.3, and 5.6, our work has prompted a number of questions that warrant further investigation, including the calculation of the remaining boundary conditions in the dilute Potts model via saddle-point and loop equation methods, extending our methods to study observables of higher genus, and, of course, understanding the New boundary condition on the random lattice. The questions do not end there. Are there any novel features to be found in the $q > 4$ region of the Potts model? Can we ascribe a physical interpretation to the odd and $p = q/2$ boundary conditions? To what extent can we carve out the space of calculable correlators in multi-matrix models more generally? We have learned much about boundary conditions of the q-state Potts model on random planar graphs, but our understanding is not yet complete.

In summary, we have furthered our understanding of the q-state Potts model on random planar graphs, but there is a great deal left to work out, and more avenues of inquiry to explore. It is the hope of the author that this thesis entices the reader undertake this line of research, and further our understanding of spin systems and boundary conditions on random planar graphs.

Appendices

Appendix A

Combinatorial Solution of the 3-state Potts Model

In this appendix, based on [82], we demonstrate the combinatorial computation of the one-loop function in the 3-state Potts model with fixed-spin fully magnetised boundary conditions, where all of the spins that lie on the boundary have the same orientation. We denote this as

$$\phi(x, g, c) = \sum_{k,l} \mathcal{N}(l; k) g^k x^l c^\nu, \tag{A.1}$$

where we sum over all inequivalent triangulations with k triangles and l boundary links, with a spin $X_i \in \{X_0, X_1, X_2\}$ lying at the centre of each triangle. The bulk cosmological constant is parameterised by g, the boundary cosmological constant by x, and c denotes the Boltzmann weight for Potts spins, with ν being the total number of edges connecting unlike spins on the triangulation. We may repackage (A.1) as follows:

$$\phi(x) = \sum_{n=0}^{\infty} p_n(g, c) x^n, \tag{A.2}$$

where we subsume the g and c dependence of the one-loop function into the coefficients $p_n(g, c)$, which then represent the disc amplitude for triangulations endowed with the Potts spin system, with a boundary of length n. We will calculate (A.2) using the formalism of [6], which builds on the combinatorial solution of the two-matrix model [11, 83], and Tutte recursion [5].

A given boundary condition is specified by the length of the boundary and a string of labels denoting which spins are present and in which order they are arranged on the boundary. For each Potts spin, X_i, this label is a conjugate fugacity, which we denote x_i. Choosing an orientation and a marked edge on a given boundary configuration gives a simple way of ordering the boundary labels; starting with the marked edge, go around the boundary via the prescribed orientation.

With this association, it is natural to treat the fugacities labelling a given boundary configuration as non-commutative variables. Thus, boundary configurations are associated with words generated by the free algebra of these non-commutative variables. The generating function can be expressed as:

$$\Phi = \sum_{w(x_0,x_1,x_2)} w(x_0,x_1,x_2) p_{w(x_0,x_1,x_2)}(g,c), \tag{A.3}$$

where $p_{w(x_0,x_1,x_2)}$ represents the disc amplitude for triangulations with a boundary condition specified by the word $w(x_0,x_1,x_2)$. Note that if we restrict to words in a single letter, this reduces to (A.2).

We define special derivative operators, Δ_i. Acting from the left, these operate on strings of free variables by annihilating words which start with a different variable from x_i, and otherwise removing the leading order x_i,

$$\Delta_i(x_j f(x_i)) = \delta_{i,j} f(x_i). \tag{A.4}$$

We also define right derivative operators,

$$f(x_i) x_j \overleftarrow{\Delta_i} = \delta_{i,j} f(x_i) \tag{A.5}$$

These derivative operators have the physical interpretation of adding a boundary segment to the generating function corresponding to the associated fugacity x_i [6].

The generating function is constrained by geometric recursive relations. As in the case of pure gravity, the effect of removing an edge of a given triangulation in the generating function can give rise to multiple different triangulations. Two of the four possible outcomes of removing a marked edge are detailed in Fig.2.3. A marked edge corresponding to a spin X_i of a given triangulation can be connected either

to a triangle within the triangulation, or another edge, which can be associated to either a different spin X_j or the same spin. By assigning an operation to each of these moves, we can write down the recursion relation for the generating function as a generating equation.

Consider the first decomposition processes shown in Fig.2.3a. By removing an edge connected to a triangle, one generates a diagram where the length of the boundary is increased by one and the new edges have a fugacity conjugate to the spin on the removed triangle. In terms of the original diagram, this new diagram comes with a weight g, due to the removed triangle, a weight c, due to the Boltzmann weight between x_i and x_j, a factor of x_j, due to the new marked edge, and two factors of the derivative operator, Δ_j, due to the removal of an edge of and the addition of two new edges. Collected, this process results in a term $cgx_i\Delta_j^2\Phi$ at the level of the generating function (when $i = j$, there is no factor of c).

Now consider the second decomposition process. By removing an edge connected to another edge, we generate a diagram consisting of two new triangulations with the same number of boundary segments and two new marked edges corresponding to the removed edges, accounting for the deleted spins. In terms of the original diagram, we get a factor of c, due to the Boltzmann weight between x_i and x_j, a factor $x_i\Phi$ to account for the new diagram with the marked edge x_i, and a term $x_j\Phi$ accounting for the second diagram with marked edge x_j. Collected, these are translated into $cx_i\Phi x_j\Phi$ at the level of the generating function. When $i = j$ the Boltzmann weight for x_i to itself is 1, and so the final term is $x_i\Phi x_i\Phi$.

Collecting all possible deconstruction processes that can occur, we can write down the final generating equation,

$$\begin{aligned}\Phi = 1 &+ x_0\Phi\left(x_0 + cx_1 + cx_2\right)\Phi + g(x_0 + cx_1 + cx_2)\Delta_0^2\Phi \\ &+ x_1\Phi\left(cx_0 + x_1 + cx_2\right)\Phi + g(cx_0 + x_1 + cx_2)\Delta_1^2\Phi \\ &+ x_2\Phi\left(cx_0 + cx_1 + x_2\right)\Phi + g(cx_0 + cx_1 + x_2)\Delta_2^2\Phi.\end{aligned} \tag{A.6}$$

This equation cannot be solved in general to obtain the generating function Φ for all possible boundary conditions. We can, however, use this to generate a complete set of loop equations for (A.2).

We first note that by taking derivatives of the generating equation, in the x_0, x_1, and x_2 directions, we can recast it as follows:

$$(1+c)\Delta_0\Phi + (2c^2 - c - 1)(\Phi x_0 \Phi + g\Delta_0^2\Phi) = c(\Delta_1\Phi + \Delta_2\Phi). \tag{A.7}$$

This expression is equivalent to the generating equation, but does not determine the leading constant term in Φ. We take this approach because it simplifies the subsequent analysis and makes comparison with Schwinger-Dyson equations clear.

We can expand the generating function in x_1, x_2, giving a series in the fixed spin generating functions, and the fixed spin generating function with boundary insertions, as functions of x_0,

$$\begin{aligned}\Phi =& \phi + (x_1 + x_2)\phi_1 + (x_1^2 + x_2^2)\phi_{11} + (x_0x_1 + x_0x_2)\Delta_0\phi_1 + \\ & (x_1x_2 + x_2x_1)\phi_{12} + (x_1^3 + x_2^3)\phi_{111} + (x_1x_0x_1 + x_2x_0x_2)\phi_{101} + \\ & (x_0x_1x_1 + x_0x_2x_2)\Delta_0\phi_{11} + (x_0x_1x_2 + x_0x_2x_1)\Delta_0\phi_{12} + \\ & (x_1x_1x_2 + x_2x_2x_1)\phi_{112} + (x_1x_2x_1 + x_2x_1x_2)\phi_{121} + (x_2x_1x_1 + x_1x_2x_2)\phi_{122} + \cdots.\end{aligned} \tag{A.8}$$

The terms $\phi_{w(0,1,2)}$ denote the one-loop function summing over geometries with a boundary carrying the single spin X_0 and a boundary insertion, corresponding to spins ordered as $w(X_0, X_1, X_2)$. We use the permutation symmetry of the model to arrange the labels so that the word $w(0,1,2)$ starts with 1. In this convention, to isolate a given term of the expansion requires operating on Φ with the reverse string of derivative operators. For example,

$$\phi_{112} = \Delta_2\Delta_1\Delta_1\Phi|_{x_1=x_2=0}. \tag{A.9}$$

Furthermore, when applying the derivative operator on the right hand side to functions with cyclic symmetry (such as Φ) it is equivalent to concatenating the

right-hand set of operators with the operators on the left-hand side, but now as right-acting operators. For example,

$$\Delta_1\Delta_0\Phi\overleftarrow{\Delta_1\Delta_2} = \Delta_1\Delta_0\Delta_1\Delta_2\Phi. \tag{A.10}$$

This equivalence can be seen by applying this rule to the series expansion of the generating function. It fails, however, for terms quadratic in the generating function, since they are not cyclic.

By collecting each term in the expansion of the generating function within the generating equation, we can identify constraints for the fixed spin amplitude. There is no known way of demonstrating that any set of constraints we construct results in a closed system of equations, and in principle we can continue to generate constraints that we can't solve to find the fixed spin amplitude.

We will proceed by computing a set of loop equations in the variable x_0. We label these by a corresponding string of variables in the expansion of the generating equation. For example, the loop equation labelled by $w(x_0, x_1, x_2)x_0 \cdots x_0 v(x_0, x_1, x_2)$, where $w(x_0, x_1, x_2)$ and $v(x_0, x_1, x_2)$ are arbitrary words in x_0, x_1, and x_2, will correspond to operating on the generating function with $w(\Delta_0, \Delta_1, \Delta_2)$ on the left and $v(\Delta_0, \Delta_1, \Delta_2)$ on the right and setting x_1 and x_2 to zero, thereby producing an equation in x_0 only.

1. $x_0 \cdots x_0$: The leading order term in (A.7), after taking $x_1, x_2 \to 0$ is

$$(1+c)\Delta_0\phi - (1+c-2c^2)(x_0\phi^2 + g\Delta_0^2\phi) = 2c\phi_1. \tag{A.11}$$

2. $x_1x_0 \cdots x_0x_1$: Following this, we can extract the loop equation corresponding to the string $x_1x_0 \cdots x_0x_1$ by operating on the left and right hand side of the generating equation with Δ_1 and setting $x_1, x_2 \to 0$,

$$(1+c)\phi_{101} - (1+c-2c^2)(x_0\phi_1^2 + g\phi_{1001}) = c(\phi_{111} + \phi_{121}). \tag{A.12}$$

3. $x_1x_0 \cdots$: We can also operate with Δ_1 on the left hand side only. However, this operation is not Hermitian, in the sense that the resulting equation extracted

does not necessarily contain expectation values of Hermitian matrices. This is fixed by adding the conjugate operation, which is where we operate separately with $\overleftarrow{\Delta_1}$ on the right hand side, and add the contributions together,

$$(1+c)\Delta_0\phi_1 - (1+c-2c^2)(x_0\phi\phi_1 + g\Delta_0^2\phi_1) = c(\phi_{11}+\phi_{12}). \tag{A.13}$$

4. $x_2x_1x_0\cdots$: We can then look at mixed strings of the form $x_2x_1x_0\cdots$ (and the conjugate string),

$$(1+c)\Delta_0\phi_{12} - (1+c-2c^2)(x_0\phi\phi_{12} + g\Delta_0^2\phi_{12}) = c(\phi_{121}+\phi_{(122)}), \tag{A.14}$$

where the brackets in the subscript mean symmetrisation between the string and the reversed string,

$$\phi_{(122)} = \frac{1}{2}(\phi_{122}+\phi_{221}). \tag{A.15}$$

Crucially, the fact that terms like ϕ_{122} and ϕ_{221} do not arise independently, but in the symmetrised combination above means we have a smaller set of independent functions.

5. $x_1x_2x_1x_0\cdots$:

$$(1+c)\Delta_0\phi_{121} - (1+c-2c^2)(x_0\phi\phi_{121} + g\Delta_0^2\phi_{121}) = c(\phi_{1212}+\phi_{(1121)}). \tag{A.16}$$

6. $x_1x_0x_2x_0\cdots$:

$$(1+c)\Delta_0\phi_{102} - (1+c-2c^2)(x_0\phi\phi_{102} + p_1\phi_1 + g\Delta_0^2\phi_{102}) = c(\phi_{(1102)}+\phi_{(1201)}). \tag{A.17}$$

7. $x_1x_0x_1x_0\cdots$:

$$(1+c)\Delta_0\phi_{101} - (1+c-2c^2)(x_0\phi\phi_{101} + p_1\phi_1 + g\Delta_0^2\phi_{101}) = c(\phi_{(1101)}+\phi_{(1202)}). \tag{A.18}$$

8. $x_0x_1x_2x_0\cdots$:

$$(1+c)\Delta_0^2\phi_{12} - (1+c-2c^2)(x_0\phi\Delta_0\phi_{12} + \phi_{12} + g\Delta_0^3\phi_{12}) = c(\phi_{(1201)}+\phi_{(1202)}). \tag{A.19}$$

At each level of expansion it appears that we have new objects appearing, implying that we can never arrive at a closed system of equations for the generating function. However, we can appeal to the permutation symmetry of the model once more, and construct loop equations by expanding around another variable, say, x_2. By permutation symmetry, any loop equation for the one-loop function in x_2 (and boundary insertions given by words in the spins X_0, X_1), can always be expressed as a loop equation for the original generating function in x_0.

9. $x_2 \cdots x_2$: First, by expanding the generating equation in x_2 and setting $x_0, x_1 \to 0$, and using permutation symmetry, we find the following loop equation,
$$\phi_1 - (1 + c - 2c^2)g\phi_{11} = c\Delta_0\phi. \tag{A.20}$$

10. $x_1x_2 \cdots x_2x_1$:
$$(1 + c)\phi_{121} - (1 + c - 2c^2)g\phi_{1221} = c(\phi_{111} + \phi_{101}). \tag{A.21}$$

11. $x_1x_2 \cdots$:
$$(1 + c)\phi_{12} - (1 + c - 2c^2)g\phi_{(112)} = c(\phi_{11} + \Delta_0\phi_1). \tag{A.22}$$

12. $x_0x_2 \cdots$:
$$(1 + c)\phi_{11} - (1 + c - 2c^2)(\phi + g\phi_{111}) = c(\phi_{12} + \Delta_0\phi_1). \tag{A.23}$$

13. $x_1x_1x_2 \cdots$:
$$(1 + c)\phi_{(112)} - (1 + c - 2c^2)g\phi_{1122} = c(\phi_{111} + \Delta_0\phi_{11}). \tag{A.24}$$

14. $x_2x_1x_2 \cdots$:
$$(1 + c)\phi_{102} - (1 + c - 2c^2)g\phi_{(1102)} = c(\phi_{101} + \Delta_0^2\phi_1). \tag{A.25}$$

15. $x_2x_0x_2 \cdots$:
$$(1 + c)\phi_{101} - (1 + c - 2c^2)(p_1\phi + g\phi_{(1101)}) = c(\phi_{102} + \Delta_0^2\phi_1). \tag{A.26}$$

16. $x_1x_0x_2\cdots$:

$$(1+c)\phi_{121} - (1+c-2c^2)(p_1\phi + g\phi_{(1121)}) = c(\phi_{(112)} + \Delta_0\phi_{12}). \quad \text{(A.27)}$$

17. $x_0x_1x_2\cdots x_2x_0$:

$$(1+c)\phi_{(1222)} - (1+c-2c^2)(2\phi_{12} + g\phi_{(12222)}) = c(\phi_{1212} + \phi_{(1202)}). \quad \text{(A.28)}$$

18. $x_1x_2\cdots x_2x_0x_0$:

$$(1+c)\phi_{(1222)} - (1+c-2c^2)(\phi_{12} + p_1\phi_1 + g\phi_{(12222)}) = c(\phi_{1122} + \phi_{(1102)}). \quad \text{(A.29)}$$

19. $x_0x_2x_0x_2\cdots$:

$$(1+c)\phi_{(1211)} - (1+c-2c^2)(\phi_{12} + p_{12}\phi + g\phi_{(12111)}) = c(\phi_{(1202)} + \Delta_0\phi_{101}). \quad \text{(A.30)}$$

20. $x_0x_0x_1x_2\cdots$:

$$(1+c)\phi_{(1222)} - (1+c-2c^2)(\phi_{12} + p_1\phi_1 + g\phi_{(12222)}) = c(\phi_{1221} + \Delta_0\phi_{(112)}). \quad \text{(A.31)}$$

This forms the closed system of equations which we can solve to find the algebraic curve describing ϕ. Moreover, the equations we have just described are in one-to-one correspondence with the loop equations derived in Chapter 5 for the fixed boundary condition resolvent $W_{(1)}(z)$. We arrived at these constraints through purely combinatorial arguments, and have thus demonstrated the equivalence between the loop equations due to reparameterisations of the matrix integral (5.27) and the combinatorial recursion method.

Appendix B

Asymptotics

In this appendix we provide the asymptotic expansions for the resolvents of Chapter 5. Labelling of sheets corresponds to the figures describing the analytic structure therein. Source code implementing these calculations may be found in the GitHub repository [84].

B.1 3-state Potts Model

B.1.1 Fixed boundary conditions

The asymptotic behaviour of the planar resolvent $W_{(1)}(z)$ is given by:

$$
\begin{aligned}
W_{(1)}(z)_0 =& \frac{1}{z} + \mathcal{O}(z^{-2}) \\
W_{(1)}(z)_1 =& t_3 z^2 + (t_2 - 1)z - 2t_3^{-1/2} z^{1/2} + \frac{t_2 - 2}{t_3} - \frac{(t_2-2)^2}{4t_3^{3/2}} z^{-1/2} + \mathcal{O}(z^{-3/2}) \\
W_{(1)}(z)_2 =& t_3 z^2 + (t_2 - 1)z + 2t_3^{-1/2} z^{1/2} + \frac{t_2 - 2}{t_3} + \frac{(t_2-2)^2}{4t_3^{3/2}} z^{-1/2} + \mathcal{O}(z^{-3/2}) \\
W_{(1)}(z)_3 =& t_3 z^2 + \frac{(t_2-2)}{2} z - \frac{t_3^{-1/2}}{2\sqrt{2}} z^{1/2} + \frac{(10t_2 - 1)}{8t_3} \\
& - \frac{(4t_2^2 - 20t_2 - 1)}{32\sqrt{2}t_3^{3/2}} z^{-1/2} - \frac{1}{2} z^{-1} + \mathcal{O}(z^{-3/2}) \\
W_{(1)}(z)_4 =& t_3 z^2 + \frac{(t_2-2)}{2} z + \frac{t_3^{1/2}}{2\sqrt{2}} z^{1/2} + \frac{(10t_2 - 1)}{8t_3} \\
& + \frac{(4t_2^2 - 20t_2 - 1)}{32\sqrt{2}t_3^{3/2}} z^{-1/2} - \frac{1}{2} z^{-1} + \mathcal{O}(z^{-3/2})
\end{aligned}
$$

B.1.2 Mixed boundary conditions

The asymptotic behaviour of the planar resolvent $W_{(2)}(z)$ is given by:

$$
\begin{aligned}
W_{(2)}(z)_0 =& z^{-1} + \mathcal{O}(z^{-2}) \\
W_{(2)}(z)_1 =& \frac{t_3 z^2}{4} + \frac{(t_2-2)}{2} z - t_3^{-1/2} z^{1/2} + \frac{(t_2-1)^2}{8t_3^{3/2}} z^{1/2} + \frac{t_2-1}{2t_3} + \frac{1}{2} z^{-1} + \mathcal{O}(z^{-3/2}) \\
W_{(2)}(z)_2 =& \frac{t_3 z^2}{4} + \frac{(t_2-2)}{2} z + t_3^{-1/2} z^{1/2} + \frac{(t_2-1)^2}{8t_3^{3/2}} z^{1/2} + \frac{t_2-1}{2t_3} + \frac{1}{2} z^{-1} + \mathcal{O}(z^{-3/2}) \\
W_{(2)}(z)_3 =& -2z + (1+i) t_3^{-1/2} z^{1/2} - \frac{2t_2}{t_3} + \frac{(1-i)\left(t_2^2 - (6-4i)t_2 + 1\right)}{8t_3^{3/2}} z^{-1/2} + \mathcal{O}(z^{-3/2}) \\
W_{(2)}(z)_4 =& -2z - (1-i) t_3^{-1/2} z^{1/2} - \frac{2t_2}{t_3} - \frac{(1+i)\left(t_2^2 - (6+4i)t_2 + 1\right)}{8t_3^{3/2}} z^{-1/2} + \mathcal{O}(z^{-3/2}) \\
W_{(2)}(z)_5 =& -2z - (1+i) t_3^{-1/2} z^{1/2} - \frac{2t_2}{t_3} - \frac{(1-i)\left(t_2^2 - (6-4i)t_2 + 1\right)}{8t_3^{3/2}} z^{-1/2} + \mathcal{O}(z^{-3/2}) \\
W_{(2)}(z)_6 =& -2z + (1-i) t_3^{-1/2} z^{1/2} - \frac{2t_2}{t_3} + \frac{(1+i)\left(t_2^2 - (6+4i)t_2 + 1\right)}{8t_3^{3/2}} z^{-1/2} + \mathcal{O}(z^{-3/2}) \\
W_{(2)}(z)_7 =& \frac{t_3 z^2}{4} + \frac{1}{2}(t_2-6) z + i t_3^{-1/2} z^{1/2} - \frac{3t_2+1}{2t_3} - \frac{i\left(t_2^2 - 10t_2 + 1\right)}{8t_3^{3/2}} z^{-1/2} \\
& - \frac{1}{2} z^{-1} + \mathcal{O}(z^{-3/2}) \\
W_{(2)}(z)_8 =& \frac{t_3 z^2}{4} + \frac{1}{2}(t_2-6) z - i t_3^{-1/2} z^{1/2} - \frac{3t_2+1}{2t_3} + \frac{i\left(t_2^2 - 10t_2 + 1\right)}{8t_3^{3/2}} z^{-1/2} \\
& - \frac{1}{2} z^{-1} + \mathcal{O}(z^{-3/2}) \\
W_{(2)}(z)_9 =& -4z - \frac{4t_2}{t_3} - z^{-1} + \mathcal{O}(z^{-2})
\end{aligned}
$$

B.1.3 Free boundary conditions

The asymptotic behaviour of the planar resolvent $W_{(3)}(z)$ is given by:

$$
\begin{aligned}
W_{(3)}(z)_0 =& z^{-1} + \mathcal{O}(z^{-2}) \\
W_{(3)}(z)_1 =& \frac{t_3}{9} z^2 + \frac{(t_2-3)}{3} z + \frac{1}{z} + \mathcal{O}(z^{-2}) \\
W_{(3)}(z)_2 =& -\frac{3}{2} z + \frac{3i}{2\sqrt{2} t_3^{3/2}} z^{1/2} - \frac{(18t_2-9)}{8t_3} - \frac{3i(4t_2^2 - 36t_2 + 9)}{32\sqrt{2} t_3^{3/2}} z^{-1/2} - \frac{1}{2} z^{-1} + \mathcal{O}(z^{-3/2}) \\
W_{(3)}(z)_3 =& -\frac{3}{2} z - \frac{3i}{2\sqrt{2} t_3^{3/2}} z^{1/2} - \frac{(18t_2-9)}{8t_3} + \frac{3i(4t_2^2 - 36t_2 + 9)}{32\sqrt{2} t_3^{3/2}} z^{-1/2} - \frac{1}{2} z^{-1} + \mathcal{O}(z^{-3/2}) \\
W_{(3)}(z)_4 =& -\frac{4}{3} z - \frac{2t_2}{t_3} - z^{-1} + \mathcal{O}(z^{-2})
\end{aligned}
$$

B.2 Dilute Ising Model

B.2.1 Vacant boundary conditions

The asymptotic behaviour of the planar resolvent $W_Y(z)$ is given by:

$$W_Y(z)_0 = z^{-1} + \mathcal{O}(z^{-2}) \tag{B.1}$$

$$W_Y(z)_1 = t_0 z^2 + z - 2t_3^{-1/2} z^{1/2} + \frac{t_2}{t_3} - \frac{t_2^2}{4t_3^{3/2}} z^{-1/2} + \mathcal{O}(z^{-3/2}) \tag{B.2}$$

$$W_Y(z)_2 = t_0 z^2 + z + 2t_3^{-1/2} z^{1/2} + \frac{t_2}{t_3} + \frac{t_2^2}{4t_3^{3/2}} z^{-1/2} + \mathcal{O}(z^{-3/2}) \tag{B.3}$$

$$W_Y(z)_3 = 2t_0 z^2 + 2z + \frac{2t_2}{t_3} - z^{-1} + \mathcal{O}(z^{-2}) \tag{B.4}$$

B.2.2 Fixed boundary conditions

The asymptotic behaviour of the planar resolvent $W_{(1)}(z)$ is given by:

$$W_{(1)}(z)_0 = z^{-1} + \mathcal{O}(z^{-1/2})$$

$$\begin{aligned} W_{(1)}(z)_1 =& t_3 z^2 + t_2 z + t_0 z^{-1/2} + \frac{1}{2t_0} - \frac{i}{2t_0^{3/4} t_3^{1/2}} z^{-1/4} + \frac{(t_3 - 2t_0 t_2)}{8t_0^{3/2} t_3} z^{-1/2} \\ &+ \frac{i(t_0 t_2^2 - 2t_3)}{16 t_0^{5/4} t_3^{3/2}} z^{-3/4} - \frac{1}{4} z^{-1} + \mathcal{O}(z^{-5/4}) \end{aligned}$$

$$\begin{aligned} W_{(1)}(z)_2 =& t_3 z^2 + t_2 z - t_0 z^{-1/2} + \frac{1}{2t_0} - \frac{1}{2t_0^{3/4} t_3^{1/2}} z^{-1/4} - \frac{(t_3 - 2t_0 t_2)}{8t_0^{3/2} t_3} z^{-1/2} \\ &- \frac{(t_0 t_2^2 - 2t_3)}{16 t_0^{5/4} t_3^{3/2}} z^{-3/4} - \frac{1}{4} z^{-1} + \mathcal{O}(z^{-5/4}) \end{aligned}$$

$$\begin{aligned} W_{(1)}(z)_3 =& t_3 z^2 + t_2 z + t_0 z^{-1/2} + \frac{1}{2t_0} + \frac{i}{2t_0^{3/4} t_3^{1/2}} z^{-1/4} + \frac{(t_3 - 2t_0 t_2)}{8t_0^{3/2} t_3} z^{-1/2} \\ &- \frac{i(t_0 t_2^2 - 2t_3)}{16 t_0^{5/4} t_3^{3/2}} z^{-3/4} - \frac{1}{4} z^{-1} + \mathcal{O}(z^{-5/4}) \end{aligned}$$

$$\begin{aligned} W_{(1)}(z)_4 =& t_3 z^2 + t_2 z - t_0 z^{-1/2} + \frac{1}{2t_0} + \frac{1}{2t_0^{3/4} t_3^{1/2}} z^{-1/4} - \frac{(t_3 - 2t_0 t_2)}{8t_0^{3/2} t_3} z^{-1/2} \\ &+ \frac{(t_0 t_2^2 - 2t_3)}{16 t_0^{5/4} t_3^{3/2}} z^{-3/4} - \frac{1}{4} z^{-1} + \mathcal{O}(z^{-5/4}) \end{aligned}$$

B.2.3 Free boundary conditions

The asymptotic behaviour of the planar resolvent $W_{(2)}(z)$ is given by:

$$
\begin{aligned}
W_{(2)}(z)_0 =& z^{-1} + \mathcal{O}(z^{-2}) \\
W_{(2)}(z)_1 =& \frac{t_3}{4}z^2 + \frac{t_2}{2}z - t_0^{1/2}z^{1/2} + \frac{1}{2t_0} - \frac{1}{8}t_0^{-3/2}z^{-1/2} + \frac{1}{2}z^{-1} + \mathcal{O}(z^{-3/2}) \\
W_{(2)}(z)_2 =& \frac{t_3}{4}z^2 + \frac{t_2}{2}z + t_0^{1/2}z^{1/2} + \frac{1}{2t_0} + \frac{1}{8}t_0^{-3/2}z^{-1/2} + \frac{1}{2}z^{-1} + \mathcal{O}(z^{-3/2}) \\
W_{(2)}(z)_3 =& (1+i)t_0^{-1/2}z^{1/2} + \frac{(1+i)(4(1+i)t_0t_2+t_3)}{8t_0^{3/2}t_3}z^{-1/2} + \mathcal{O}(z^{-3/2}) \\
W_{(2)}(z)_4 =& -(1-i)t_0^{-1/2}z^{1/2} + \frac{8it_0t_2-(1-i)t_3}{8t_0^{3/2}t_3}z^{-1/2} + \mathcal{O}(z^{-3/2}) \\
W_{(2)}(z)_5 =& -(1+i)t_0^{-1/2}z^{1/2} - \frac{(1+i)(4(1+i)t_0t_2+t_3)}{8t_0^{3/2}t_3}z^{-1/2} + \mathcal{O}(z^{-3/2}) \\
W_{(2)}(z)_6 =& (1-i)t_0^{-1/2}z^{1/2} - \frac{8it_0t_2-(1-i)t_3}{8t_0^{3/2}t_3}z^{-1/2} + \mathcal{O}(z^{-3/2}) \\
W_{(2)}(z)_7 =& it_0^{-1/2}z^{1/2} - \frac{1}{2t_0} + \frac{i(8t_0t_2-t_3)}{8t_0^{3/2}t_3}z^{-1/2} - \frac{1}{2}z^{-1} + \mathcal{O}(z^{-3/2}) \\
W_{(2)}(z)_8 =& -it_0^{-1/2}z^{1/2} - \frac{1}{2t_0} - \frac{i(8t_0t_2-t_3)}{8t_0^{3/2}t_3}z^{-1/2} - \frac{1}{2}z^{-1} + \mathcal{O}(z^{-3/2}) \\
W_{(2)}(z)_9 =& -z^{-1} + \mathcal{O}(z^{-2})
\end{aligned}
$$

B.3 Dilute Potts Model

B.3.1 Vacant boundary conditions

The asymptotic behaviour of the planar resolvent $W_Y(z)$ is given by:

$$
\begin{aligned}
W_Y(z)_0 =& z^{-1} + \mathcal{O}(z^{-2}) \\
W_Y(z)_1 =& t_0z^2 + z - 3t_3^{-1/2}z^{1/2} + \frac{3t_2}{2t_3} - \frac{3t_2^2}{8t_3^{3/2}}z^{-1/2} + \frac{1}{2}z^{-1} + \mathcal{O}(z^{-3/2}) \\
W_Y(z)_2 =& t_0z^2 + z + 3t_3^{-1/2}z^{1/2} + \frac{3t_2}{2t_3} + \frac{3t_2^2}{8t_3^{3/2}}z^{-1/2} + \frac{1}{2}z^{-1} + \mathcal{O}(z^{-3/2}) \\
W_Y(z)_3 =& 3t_0z^2 + 3z + 3t_3^{-1/2}z^{1/2} + \frac{9t_2}{2t_3} + \frac{3t_2^2}{8t_3^{3/2}}z^{-1/2} - \frac{1}{2}z^{-1} + \mathcal{O}(z^{-3/2}) \\
W_Y(z)_4 =& 3t_0z^2 + 3z - 3t_3^{-1/2}z^{1/2} + \frac{9t_2}{2t_3} - \frac{3t_2^2}{8t_3^{3/2}}z^{-1/2} - \frac{1}{2}z^{-1} + \mathcal{O}(z^{-3/2}) \\
W_Y(z)_5 =& 4z + \frac{6t_2}{t_3} + z^{-1} + \mathcal{O}(z^{-2})
\end{aligned}
$$

B.3.2 Fixed boundary conditions

The asymptotic behaviour of the planar resolvent $W_{(1)}(z)$ is given by:

$$
\begin{aligned}
W_{(1)}(z)_0 =& z^{-1} + \mathcal{O}(z^{-2}) \\
W_{(1)}(z)_1 =& t_3 z^2 + t_2 z - t_0^{-1/2} z^{1/2} + \frac{1}{2t_0} - \frac{1}{t_0^{3/4} t_3^{1/2}} z^{-1/4} - \frac{(t_3 - 4t_0 t_2)}{8 t_0^{3/2} t_3} z^{-1/2} \\
& - \frac{(t_0 t_2^2 - 2t_3)}{8 t_0^{5/4} t_3^{3/2}} z^{-3/4} + \mathcal{O}(z^{-5/4}) \\
W_{(1)}(z)_2 =& t_3 z^2 + t_2 z + t_0^{-1/2} z^{1/2} + \frac{1}{2t_0} + \frac{i}{t_0^{3/4} t_3^{1/2}} z^{-1/4} + \frac{(t_3 - 4t_0 t_2)}{8 t_0^{3/2} t_3} z^{-1/2} \\
& - \frac{i(t_0 t_2^2 - 2t_3)}{8 t_0^{5/4} t_3^{3/2}} z^{-3/4} + \mathcal{O}(z^{-5/4}) \\
W_{(1)}(z)_3 =& t_3 z^2 + t_2 z - t_0^{-1/2} z^{1/2} + \frac{1}{2t_0} + \frac{1}{t_0^{3/4} t_3^{1/2}} z^{-1/4} - \frac{(t_3 - 4t_0 t_2)}{8 t_0^{3/2} t_3} z^{-1/2} \\
& + \frac{(t_0 t_2^2 - 2t_3)}{8 t_0^{5/4} t_3^{3/2}} z^{-3/4} + \mathcal{O}(z^{-5/4}) \\
W_{(1)}(z)_4 =& t_3 z^2 + t_2 z + t_0^{-1/2} z^{1/2} + \frac{1}{2t_0} - \frac{i}{t_0^{3/4} t_3^{1/2}} z^{-1/4} + \frac{(t_3 - 4t_0 t_2)}{8 t_0^{3/2} t_3} z^{-1/2} \\
& + \frac{i(t_0 t_2^2 - 2t_3)}{8 t_0^{5/4} t_3^{3/2}} z^{-3/4} + \mathcal{O}(z^{-5/4}) \\
W_{(1)}(z)_5 =& t_3 z^2 + t_2 z - \frac{1}{\sqrt{2} t_0^{1/2}} z^{1/2} + \frac{1}{2t_0} - \frac{1}{2^{7/4} t_0^{3/4} t_3^{1/2}} z^{-1/4} - \frac{(t_3 - 5t_0 t_2)}{4\sqrt{2} t_0^{3/2} t_3} z^{-1/2} \\
& - \frac{(t_0 t_2^2 - 2t_3)}{2^{17/4} t_0^{5/4} t_3^{3/2}} z^{-3/4} - \frac{1}{4} z^{-1} + \mathcal{O}(z^{-5/4}) \\
W_{(1)}(z)_6 =& t_3 z^2 + t_2 z + \frac{1}{\sqrt{2} t_0^{1/2}} z^{1/2} + \frac{1}{2t_0} + \frac{i}{2^{7/4} t_0^{3/4} t_3^{1/2}} z^{-1/4} + \frac{(t_3 - 5t_0 t_2)}{4\sqrt{2} t_0^{3/2} t_3} z^{-1/2} \\
& - \frac{i(t_0 t_2^2 - 2t_3)}{2^{17/4} t_0^{5/4} t_3^{3/2}} z^{-3/4} - \frac{1}{4} z^{-1} + \mathcal{O}(z^{-5/4}) \\
W_{(1)}(z)_7 =& t_3 z^2 + t_2 z - \frac{1}{\sqrt{2} t_0^{1/2}} z^{1/2} + \frac{1}{2t_0} + \frac{1}{2^{7/4} t_0^{3/4} t_3^{1/2}} z^{-1/4} - \frac{(t_3 - 5t_0 t_2)}{4\sqrt{2} t_0^{3/2} t_3} z^{-1/2} \\
& + \frac{(t_0 t_2^2 - 2t_3)}{2^{17/4} t_0^{5/4} t_3^{3/2}} z^{-3/4} - \frac{1}{4} z^{-1} + \mathcal{O}(z^{-5/4}) \\
W_{(1)}(z)_8 =& t_3 z^2 + t_2 z + \frac{1}{\sqrt{2} t_0^{1/2}} z^{1/2} + \frac{1}{2t_0} - \frac{i}{2^{7/4} t_0^{3/4} t_3^{1/2}} z^{-1/4} + \frac{(t_3 - 5t_0 t_2)}{4\sqrt{2} t_0^{3/2} t_3} z^{-1/2} \\
& + \frac{i(t_0 t_2^2 - 2t_3)}{2^{17/4} t_0^{5/4} t_3^{3/2}} z^{-3/4} - \frac{1}{4} z^{-1} + \mathcal{O}(z^{-5/4})
\end{aligned}
$$

Appendix C

Negative Boltzmann Weights and the New Boundary Condition

In this appendix we study the New boundary condition of Affleck, Oshikawa and Saluer in the classical 3-state Potts model. We consider the 2D square lattice with a spin attached to each vertex, which we express as phases $\theta_i \in \{0, \frac{2\pi}{3}, \frac{4\pi}{3}\}$, and a nearest neighbour interaction governed by the Hamiltonian

$$H = -J \sum_{\langle i,j \rangle} \cos(\theta_i - \theta_j). \tag{C.1}$$

To study the boundary physics we introduce a boundary in the lattice, which we may take to be along the x-axis. We can select for particular boundary conditions on the spins that reside there by introducing a field interaction term at the boundary

$$H_B = -h \sum_j \cos\theta_j, \tag{C.2}$$

where h represents a boundary magnetic field, and we sum over spins attached to the boundary.

For $h \to \infty$, only configurations with $\theta_j = 0$ generate non-negligible contributions to the partition function, and so we may regard this limit as selecting the fixed boundary condition, where all boundary spins are in the same orientation. One the other hand, for $h = 0$, the spins are unconstrained, and we recover free boundary conditions. Mixed boundary conditions may be achieved by taking $h \to -\infty$. In this case, the boundary spins $\theta_j \in \{\frac{2\pi}{3}, \frac{4\pi}{3}\}$ generate equal non-negligible contributions to the partition function, while $\theta_j = 0$ does not.

To study the New boundary condition, we first discuss the dual spin system. Following [85], it is convenient to introduce the discrete difference operator,

$$\Delta_\mu \theta_i \coloneqq \theta_i - \theta_{i-\hat{\mu}}, \tag{C.3}$$

where $\hat{\mu}$ represents either the $\hat{x}$ or $\hat{y}$ directions in the lattice. To derive the dual we expand each Boltzmann factor in the discrete Fourier series,

$$\exp\left[J\cos\left(\Delta_\mu\theta_i\right)\right] = A\sum_{k=0}^{2} C_k(J)\exp\left(ik\Delta_\mu\theta_i\right). \tag{C.4}$$

The coefficients $C_k(J)$ maybe obtained through the inverse discrete Fourier series,

$$C_k(J) = A\sum_{l=0}^{2}\exp\left(J\cos\left(\frac{2\pi}{3}l\right) + \frac{2\pi i}{3}lk\right), \tag{C.5}$$

where A is a constant of proportionality. To each link emanating from site i we may associate a new variable $\phi_{\mu;i} = \frac{2\pi}{3}k_{\mu;i} \in \{0, \frac{2\pi}{3}, \frac{4\pi}{3}\}$ called the bond variable. Defining the dual coupling $\hat{J}$ as

$$e^{\hat{J}(\phi)} \coloneqq C_{\frac{3}{2\pi}\phi}(J), \tag{C.6}$$

we may thus rewrite the partition function in terms of the bond variables as

$$\begin{aligned} Z \propto & \sum_{\{\theta\}}\sum_{\{\phi_\mu\}}\prod_{\langle\mu\rangle} C_{(\phi_\mu)}\exp\left(\frac{3i}{2\pi}\phi_{\mu;i}\Delta_\mu\theta_i\right), && \text{(C.7)}\\ = & \sum_{\{\theta\}}\sum_{\{\phi_\mu\}}\prod_{\langle\mu\rangle} e^{\hat{J}\cos(\phi_\mu)}\exp\left(-\frac{3i}{2\pi}\theta_i\Delta_\mu\phi_{\mu;i}\right), && \text{(C.8)}\\ = & \sum_{\{\phi\}}\prod_{\langle\mu\rangle} e^{\hat{J}\cos(\phi_\mu)}\delta\left(\Delta_\mu\phi_{\mu;i}\right)_{\mathrm{mod}\,2\pi}. && \text{(C.9)} \end{aligned}$$

To move between lines (C.7) and (C.8) we ignored boundary terms. Intuitively, the delta function constraint is required to prevent the overcounting of the bond variable. Explicitly, the constraint at the i^{th} site is

$$\Delta_\mu\phi_{\mu;i} = \phi_{\hat{x};i} - \phi_{\hat{x};i-\hat{x}} + \phi_{\hat{y};i} - \phi_{\hat{y};i-\hat{y}} = 0. \tag{C.10}$$

Using $\phi_{\hat{x};i-\hat{x}} = -\phi_{-\hat{x};i}$ this may also be expressed as

$$\phi_{\hat{x};i} + \phi_{-\hat{x};i} + \phi_{\hat{y};i} + \phi_{-\hat{y};i} = 0. \tag{C.11}$$

We may solve (C.10) by introducing new spin variables $\theta'_i \in \{0, \frac{2\pi}{3}, \frac{4\pi}{3}\}$ defined on the vertices of the dual lattice. The constraint is then solved by taking

$$\phi_{\mu;i} = \varepsilon_{\mu\nu}\Delta_\nu \theta'_i, \tag{C.12}$$

where the indices on the left hand side refer to the original lattice sites, and the indices on the right hand side refer to the dual lattice sites. The dual partition function is then given by

$$Z \propto \sum_{\{\theta'\}} e^{\sum_{\langle i,j\rangle} \hat{J}\cos\left(\theta'_i - \theta'_j\right)}. \tag{C.13}$$

We now consider a boundary running along the x-axis, with free boundary conditions on the spins, and an interaction term between the boundary spins of strength J_B. This translates into a boundary magnetic field acting on the Potts spins in the dual picture (C.13). The dual field h may be determined by taking the Fourier transform (C.4) of the boundary Boltzmann weight,

$$e^{J_B\cos\left(\Delta_\mu\theta_i\right)} = B\sum_{k=0}^{2} e^{\frac{2\pi i}{3}\Delta_\mu\theta_i} e^{h\cos\left(\frac{2\pi}{3}k\right)}, \tag{C.14}$$

where B is another constant of proportionality. Considering the two cases where the boundary spins are equal and unequal, this gives

$$e^{3J_B/2} = \frac{e^h + 2e^{-h/2}}{e^h - e^{-h/2}}. \tag{C.15}$$

As we previously discussed, the mixed boundary condition is selected by taking $h \to -\infty$. As the mixed boundary is dual to the New boundary condition, this implies that we obtain the New boundary condition by taking a boundary interaction term with negative Boltzmann weights

$$e^{3J_B/2} = -2. \tag{C.16}$$

Scaling the interaction, such that neighbouring spins with the same orientation have Boltzmann weight 1, this gives a Boltzmann weight $-1/2$ for neighbouring spins in distinct orientations.

References

[1] G. 't Hooft and M. J. G. Veltman. *One loop divergencies in the theory of gravitation*, *Ann. Inst. H. Poincare Phys. Theor. A* 20 (1974), 69–94.

[2] J. Ambjørn, B. Durhuus, and T. Jonsson. *Quantum Geometry: A Statistical Field Theory Approach*. Cambridge Monographs on Mathematical Physics. Cambridge University Press, 2005.

[3] T. Regge. *General Relativity Without Coordinates*, *Nuovo Cim.* 19 (1961), 558–571.

[4] E. Brezin et al. *Planar Diagrams*, *Commun. Math. Phys.* 59 (1978), 35.

[5] W. T. Tutte. *A Census of Planar Triangulations*, *Canad. J. Math.* 14 (1962), 21–38.

[6] S. M. Carroll, M. E. Ortiz, and W. Taylor. *A Geometric approach to free variable loop equations in discretized theories of 2D gravity*, *Nucl. Phys. B* 468 (1996), 383–419. arXiv: `hep-th/9510199`.

[7] B. Eynard. *Topological expansion for the 1-Hermitian matrix model correlation functions*, *JHEP* 11 (2004), 031. arXiv: `hep-th/0407261`.

[8] B. Eynard, T. Kimura, and S. Ribault. *Random matrices*, (2015). arXiv: `1510.04430 [math-ph]`.

[9] R. E. Behrend and P. A. Pearce. *Integrable and conformal boundary conditions for sl(2) A-D-E lattice models and unitary minimal conformal field theories*, *J. Statist. Phys.* 102 (2001), 577. arXiv: `hep-th/0006094`.

[10] B. Eynard. *Random Matrices, Lecture Course, Saclay*, (2000).

[11] M. Staudacher. *Combinatorial solution of the two matrix model*, *Phys. Lett. B* 305 (1993), 332–338. arXiv: `hep-th/9301038`.

[12] B. Eynard. *Large N expansion of the 2 matrix model*, *JHEP* 01 (2003), 051. arXiv: `hep-th/0210047`.

[13] V. A. Kazakov. *Ising model on a dynamical planar random lattice: Exact solution*, *Phys. Lett. A* 119 (1986), 140–144.

[14] J. M. Daul, V. A. Kazakov, and I. K. Kostov. *Rational theories of 2D gravity from the two matrix model*, *Nucl. Phys. B* 409 (1993), 311–338. arXiv: `hep-th/9303093`.

[15] P. Di Francesco, P. H. Ginsparg, and J. Zinn-Justin. *2D Gravity and random matrices*, *Phys. Rept.* 254 (1995), 1–133. arXiv: `hep-th/9306153`.

[16] P. Di Francesco, P. Mathieu, and D. Senechal. *Conformal Field Theory*. Graduate Texts in Contemporary Physics. Springer-Verlag, 1997.

[17] S. Ribault. *Conformal field theory on the plane*, (2014). arXiv: 1406.4290 [hep-th].

[18] J. L. Cardy. *Boundary Conditions, Fusion Rules and the Verlinde Formula*, *Nucl. Phys. B* 324 (1989), 581–596.

[19] N. F. Robertson, J. L. Jacobsen, and H. Saleur. *Conformally invariant boundary conditions in the antiferromagnetic Potts model and the $SL(2,\mathbb{R})/U(1)$ sigma model*, *JHEP* 10 (2019), 254. arXiv: 1906.07565 [cond-mat.stat-mech].

[20] V. S. Dotsenko and V. A. Fateev. *Conformal Algebra and Multipoint Correlation Functions in Two-Dimensional Statistical Models*, *Nucl. Phys. B* 240 (1984), 312.

[21] I. Affleck, M. Oshikawa, and H. Saleur. *Boundary critical phenomena in the three state Potts model*, *J. Phys. A* 31 (1998), 5827. arXiv: cond-mat/9804117.

[22] J. Fuchs and C. Schweigert. *Completeness of boundary conditions for the critical three state Potts model*, *Phys. Lett. B* 441 (1998), 141–146. arXiv: hep-th/9806121.

[23] A. F. Caldeira, S. Kawai, and J. F. Wheater. *Free boson formulation of boundary states in W(3) minimal models and the critical Potts model*, *JHEP* 08 (2003), 041. arXiv: hep-th/0306082.

[24] R. Dijkgraaf, E. P. Verlinde, and H. L. Verlinde. *$C = 1$ Conformal Field Theories on Riemann Surfaces*, *Commun. Math. Phys.* 115 (1988), 649–690.

[25] C. M. Fortuin and P. W. Kasteleyn. *On the random-cluster model: I. Introduction and relation to other models*, *Physica* 57 (1972), 536–564.

[26] C. Itzykson and J.M. Drouffe. *Statistical field theory. Vol. 2. Strong coupling, Monte Carlo methods, conformal field theory, and random systems*. Cambridge University Press, 1989.

[27] V. Gorbenko, S. Rychkov, and B. Zan. *Walking, Weak first-order transitions, and Complex CFTs II. Two-dimensional Potts model at $Q > 4$*, *SciPost Phys.* 5 (2018), 050. arXiv: 1808.04380 [hep-th].

[28] P. Di Francesco, H. Saleur, and J.B. Zuber. *Modular Invariance in Nonminimal Two-dimensional Conformal Theories*, *Nucl. Phys. B* 285 (1987), 454.

[29] P. di Francesco, H. Saleur, and J. B. Zuber. *Relations between the Coulomb gas picture and conformal invariance of two-dimensional critical models*, *J. Statist. Phys.* 49 (1987), 57–79.

[30] B. Nienhuis et al. *First and Second Order Phase Transitions in Potts Models: Renormalization - Group Solution*, *Phys. Rev. Lett.* 43 (1979), 737–740.

[31] L. Chim. *Boundary S matrix for the tricritical Ising model*, *Int. J. Mod. Phys. A* 11 (1996), 4491–4512. arXiv: hep-th/9510008.

[32] I. Affleck. *Edge critical behavior of the two-dimensional tricritical Ising model*, *J. Phys. A* 33 (2000), 6473–6480. arXiv: cond-mat/0005286.

[33] S. Iino. *Boundary CFT and tensor network approach to surface critical phenomena of the tricritical 3-state Potts model*, (2020). arXiv: 2007.03182 [cond-mat.stat-mech].

[34] V. Fateev, A. B. Zamolodchikov, and Al. B. Zamolodchikov. *Boundary Liouville field theory. 1. Boundary state and boundary two point function*, (2000). arXiv: hep-th/0001012.

[35] A. B. Zamolodchikov and Al. B. Zamolodchikov. *Liouville field theory on a pseudosphere*, (2001), 280–299. arXiv: hep-th/0101152.

[36] Y. Nakayama. *Liouville field theory: A Decade after the revolution*, Masters Thesis. 2004. arXiv: hep-th/0402009.

[37] P. H. Ginsparg and G. W. Moore. "Lectures on 2D gravity and 2D string theory". *Theoretical Advanced Study Institute (TASI 92): From Black Holes and Strings to Particles*. 1993, 277–469. arXiv: hep-th/9304011.

[38] J. A. Gesser. *Non-Compact Geometries in 2D Euclidean Quantum Gravity*, PhD thesis. 2010. arXiv: 1010.5006 [hep-th].

[39] J. Rolf. *Two-dimensional quantum gravity*, PhD Thesis. 1998. arXiv: hep-th/9810027.

[40] A. M. Polyakov. *Quantum Geometry of Bosonic Strings*, *Phys. Lett. B* 103 (1981), 207–210.

[41] J. Polchinski. *String theory. Vol. 1: An introduction to the bosonic string*. Cambridge Monographs on Mathematical Physics. Cambridge University Press, 2007.

[42] F. David. *Conformal Field Theories Coupled to 2D Gravity in the Conformal Gauge*, *Mod. Phys. Lett. A* 3 (1988), 1651.

[43] J. Distler and H. Kawai. *Conformal Field Theory and 2D Quantum Gravity*, *Nucl. Phys. B* 321 (1989), 509–527.

[44] B. H. Lian and G. J. Zuckerman. *New selection rules and physical states in 2D gravity: Conformal gauge*, *Phys. Lett. B* 254 (1991), 417–423.

[45] P. Bouwknegt, J. G. McCarthy, and K. Pilch. *BRST analysis of physical states for 2D gravity coupled to $c \leqslant 1$ matter*, *Commun. Math. Phys.* 145 (1992), 541–560.

[46] B. Niedner. *Random Matrices, Boundaries and Branes*, PhD thesis. Univ. Oxford, 2015. arXiv: 1603.01196 [math-ph].

[47] N. Seiberg and D. Shih. *Branes, rings and matrix models in minimal (super)string theory*, *JHEP* 02 (2004), 021. arXiv: hep-th/0312170.

[48] N. Seiberg and D. Shih. *Minimal string theory*, *Comp. Ren. Phys.* 6 (2005), 165–174. arXiv: hep-th/0409306.

[49] V. G. Knizhnik, A. M. Polyakov, and A. B. Zamolodchikov. *Fractal Structure of 2D Quantum Gravity*, *Mod. Phys. Lett. A* 3 (1988), 819.

[50] B. Eynard and N. Orantin. *Algebraic methods in random matrices and enumerative geometry*, (2008). arXiv: 0811.3531 [math-ph].

[51] C. Itzykson and J.B. Zuber. *The Planar Approximation. 2.*, *J. Math. Phys.* 21 (1980), 411.

[52] V. A. Kazakov. "Solvable matrix models". 2000. arXiv: hep-th/0003064.

[53] G. Akemann, J. Baik, and P. Di Francesco. *The Oxford Handbook of Random Matrix Theory*. Oxford Handbooks in Mathematics. Oxford University Press, 2011.

[54] B. Eynard. *Formal matrix integrals and combinatorics of maps*, (2006). arXiv: `math-ph/0611087`.

[55] V. A. Kazakov. *Exactly solvable Potts models, bond- and tree-like percolation on dynamical (random) planar lattice*, *Nucl. Phys. B - Proc. Supp.* 4 (1988), 93–97.

[56] D. V. Boulatov and V. A. Kazakov. *The Ising model on a random planar lattice: The structure of the phase transition and the exact critical exponents*, *Phys. Lett. B* 186 (1987), 379–384.

[57] J. M. Daul. *Q states Potts model on a random planar lattice*, (1994). arXiv: `hep-th/9502014`.

[58] P. Zinn-Justin. *The Dilute Potts model on random surfaces*, *J. Statist. Phys.* 98 (2001), 245–264. arXiv: `cond-mat/9903385`.

[59] B. Eynard and G. Bonnet. *The Potts-q random matrix model: Loop equations, critical exponents, and rational case*, *Phys. Lett. B* 463 (1999), 273–279. arXiv: `hep-th/9906130`.

[60] B. Niedner, M. R. Atkin, and J. F. Wheater. *Boundary States of the Potts Model on Random Planar Maps*, *Springer Proc. Phys.* 170 (2016), 387–393. arXiv: `1511.01525 [math-ph]`.

[61] M. R. Atkin, B. Niedner, and J. F. Wheater. *Sums of Random Matrices and the Potts Model on Random Planar Maps*, *J. Phys. A* 49 (2016), 185201. arXiv: `1511.03657 [math-ph]`.

[62] A. Kulanthaivelu and J. F. Wheater. *Boundary Conditions and the q-state Potts model on Random Planar Maps*, (2019). arXiv: `1911.00266 [math-ph]`.

[63] Harish-Chandra. *A Formula for Semisimple Lie Groups*, *Proc. Nat. Acad. Sci.* 42.8 (1956), 538–540.

[64] C. Itzykson and J. B. Zuber. *The planar approximation. II*, *J. Math. Phys.* 21 (1979), 411–421.

[65] P. Zinn-Justin. *Universality of Correlation Functions of Hermitian Random Matrices in an External Field*, *Commun. Math. Phys.* 194.3 (1998), 631–650.

[66] L. A. Dickey. *Soliton equations and Hamiltonian systems*. Vol. 12. 1991.

[67] O. Bernardi and M. Bousquet-Mélou. *Counting colored planar maps: Algebraicity results*, *J. Comb. Theo. B* 101 (2011), 315–377.

[68] A. Guionnet et al. *Loop Models, Random Matrices and Planar Algebras*, *Commun. Math. Phys.* 316.1 (2012), 45–97.

[69] M. R. Atkin and J. F. Wheater. *The Spectrum of FZZT Branes Beyond the Planar Limit*, *JHEP* 02 (2011), 084. arXiv: `1011.5989 [hep-th]`.

[70] G. Borot and B. Eynard. *Enumeration of maps with self avoiding loops and the O(n) model on random lattices of all topologies*, *J. Stat. Mech.* 1101 (2011), P01010. arXiv: `0910.5896 [math-ph]`.

[71] B. Durhuus and C. Kristjansen. *Phase structure of the O(n) model on a random lattice for $n > 2$*, *Nucl. Phys. B* 483 (1997), 535–551. arXiv: `hep-th/9609008`.

[72] B. Eynard and C. Kristjansen. *More on the exact solution of the O(n) model on a random lattice and an investigation of the case $|n| > 2$*, *Nucl. Phys. B* 466 (1996), 463–487. arXiv: `hep-th/9512052`.

[73] B. Eynard and J. Zinn-Justin. *The O(n) model on a random surface: Critical points and large order behavior*, *Nucl. Phys. B* 386 (1992), 558–591. arXiv: hep-th/9204082.

[74] J. B. Kogut. *An Introduction to Lattice Gauge Theory and Spin Systems*, *Rev. Mod. Phys.* 51 (1979), 659.

[75] S. M. Carroll, M. E. Ortiz, and W. Taylor. *Spin / disorder correlations and duality in the c = 1/2 string*, *Nucl. Phys. B* 468 (1996), 420–438. arXiv: hep-th/9510208.

[76] S. M. Carroll, M. E. Ortiz, and W. Taylor. *Boundary fields and renormalization group flow in the two matrix model*, *Phys. Rev. D* 58 (1998), 046006. arXiv: hep-th/9711008.

[77] G. Bonnet. *Solution of Potts-3 and Potts-infinity matrix models with the equations of motion method*, *Phys. Lett. B* 459 (1999), 575–581. arXiv: hep-th/9904058.

[78] M. R. Atkin and S. Zohren. *FZZT Brane Relations in the Presence of Boundary Magnetic Fields*, *JHEP* 11 (2012), 163. arXiv: 1204.4482 [hep-th].

[79] A. B. Zamolodchikov. *Irreversibility of the Flux of the Renormalization Group in a 2D Field Theory*, *JETP Lett.* 43 (1986), 730–732.

[80] I. Affleck and A. W. W. Ludwig. *Universal noninteger 'ground state degeneracy' in critical quantum systems*, *Phys. Rev. Lett.* 67 (1991), 161–164.

[81] D. Friedan and A. Konechny. *On the boundary entropy of one-dimensional quantum systems at low temperature*, *Phys. Rev. Lett.* 93 (2004), 030402. arXiv: hep-th/0312197.

[82] A. Kulanthaivelu. *Free Variable Loop Equations for the 3-State Potts Model Coupled to 2D Gravity*, (2019). arXiv: 1911.00032 [math-ph].

[83] M. R. Douglas and M. Li. *Free variables and the two matrix model*, *Phys. Lett. B* 348 (1995), 360–364. arXiv: hep-th/9412203.

[84] A. Kulanthaivelu. *Loop Equations GitHub Repository*. URL: https://github.com/johnfwheater/LoopEquations.git.

[85] R. Savit. *Duality in Field Theory and Statistical Systems*, *Rev. Mod. Phys.* 52 (1980), 453.